Spring 2000

Nitrated poly(4 -hydroxystyrene) microspheres for optical pH and potassium ion sensing based on turbidity changes accompanying polymer sweller

Hongming Wang
University of New Hampshire, Durham

INFORMATION TO USERS

This manuscript has been reproduced from the microfilm master. UMI films the text directly from the original or copy submitted. Thus, some thesis and dissertation copies are in typewriter face, while others may be from any type of computer printer.

The quality of this reproduction is dependent upon the quality of the copy submitted. Broken or indistinct print, colored or poor quality illustrations and photographs, print bleedthrough, substandard margins, and improper alignment can adversely affect reproduction.

In the unlikely event that the author did not send UMI a complete manuscript and there are missing pages, these will be noted. Also, if unauthorized copyright material had to be removed, a note will indicate the deletion.

Oversize materials (e.g., maps, drawings, charts) are reproduced by sectioning the original, beginning at the upper left-hand corner and continuing from left to right in equal sections with small overlaps.

Photographs included in the original manuscript have been reproduced xerographically in this copy. Higher quality 6" x 9" black and white photographic prints are available for any photographs or illustrations appearing in this copy for an additional charge. Contact UMI directly to order.

Bell & Howell Information and Learning
300 North Zeeb Road, Ann Arbor, MI 48106-1346 USA
800-521-0600

NITRATED POLY(4-HYDROXYSTYRENE) MICROSPHERES FOR OPTICAL pH AND POTASSIUM ION SENSING BASED ON TURBIDITY CHANGES ACCOMPANYING POLYMER SWELLING

BY

HONGMING WANG

B.S., South China Normal University, 1982
M.S., University of Minnesota, 1994

DISSERTATION

Submitted to the University of New Hampshire
in Partial Fulfillment of
the Requirements for the Degree of

Doctor of Philosophy

in

Chemistry

May, 2000

This dissertation has been examined and approved.

Dissertation Director, Dr. W. Rudolf Seitz
Professor of Chemistry

Dr. N. Dennis Chasteen
Professor of Chemistry

Dr. Todd S. Gross
Professor of Mechanical Engineering

Dr. Sterling A. Tomellini
Associate Professor of Chemistry

Dr. Charles K. Zercher
Associate Professor of Chemistry

12/21/99
Date

DEDICATION

To my parents for their love, support, and encouragement.
And to Jin, who brought happiness in my life.

ACKNOWLEDGEMENTS

First I thank my adviser, W. Rudolf Seitz, for his support, encouragement, and guidance throughout the five years of my stay at UNH. I appreciated and enjoyed the opportunity to work for you and I have benefited from your encouragement to develop and explore ideas.

I also thank the other members of my committee and the other professors who have contributed to my education as a scientist. Your efforts and example in research and teaching have been an inspiration to me.

I thank the UNH Instrumentation Center, especially Nancy and Mark for electron microscopy and CHN.

I thank Dr. Todd S. Gross for his help on the use of Atomic Force Microscopy at the Department of Mechanical Engineering.

Finally, I thank my colleagues in the chemistry department, past and present, who made my stay at UNH enjoyable.

TABLE OF CONTENTS

LIST OF TABLES

LIST OF FIGURES

ABSTRACT

NITRATED POLY(4-HYDROXYSTYRENE) MICROSPHERES FOR OPTICAL pH AND POTASSIUM ION SENSING BASED ON TURBIDITY CHANGES ACCOMPANYING POLYMER SWELLING

By

Hongming Wang

University of New Hampshire, May, 2000

Porous poly(4-acetoxystyrene) swellable microspheres with diameters approximately 1 ~ 2 μm were prepared by seeded emulsion polymerization. Toluene was used as the porogenic solvent and divinylbenzene was used as the crosslinker. The seed particles with diameters approximately 0.5 ~ 1 μm were prepared by dispersion polymerization without adding porogenic solvent and crosslinker. Functionality was introduced by two derivatization reactions, hydrolysis and nitration, to form nitrated poly(4-hydroxystyrene). These polymer microspheres swell at high pH due to the deprotonation of the hydroxyl group on the polymer backbone. Swelling is accompanied by an increase in water content which causes the polymer refractive index to decrease. These microspheres were embedded in a hydrogel for pH sensing. When either dibenzo-18-crown-6 or valinomycin was co-immobilized on the polymer, they were then used to sense potassium ion.

Poly(2-hydroxyethylmethacrylate) or poly(vinylalcohol) hydrogel membranes with embedded nitrated poly(4-hydroxystyrene) microspheres were prepared by photopolymerization. These membranes possess desirable optical properties for pH sensing. The refractive index of the hydrated hydrogel is constant and not affected by pH,

but the refractive index of the microspheres does vary with pH. When the membrane is in contact with a buffer at high pH, the membrane turbidity decreases because the refractive index difference between the microspheres and the hydrogel decreases. The apparent pK_a values can be adjusted by varying the nitrogen percentage of the microspheres by controlling the conditions of the nitration reaction. The observed pK_a value can be as low as 5.6 or as high as 10.2. The response time of the membrane with microspheres prepared by seeded emulsion polymerization utilizing PVA as the membrane matrix was 10 ~ 15 seconds. Response times were longer for the poly(HEMA) matrix with embedded microspheres synthesized by dispersion polymerization. A very small amount of particles, 0.1 wt %, in a 127 μm thickness membrane was needed to obtain significant changes in turbidity. Stability tests showed that the poly(HEMA) hydrogel membranes were mechanically stable when they were stored in pH 4, pH 10, deionized water, and dry under room temperature, 80 ^{0}C, or in sunlight for about a month.

Membranes consisting of ionophore modified nitrated poly(4-hydroxystyrene) microspheres in a hydrogel were prepared for potassium ion sensing. The sensing concept can be modeled as a cation-exchange system. When the membrane is immersed in a solution of potassium ions, the neutral ionophore, DB18C6 or valinomycin, in the polymer will selectively bind the potassium ion to form the cation complex. The ion binding is accompanied by release of a proton to maintain electroneutrality. This introduces charged sites into the polymer causing it to swell. The observed detection limit was as low as 10^{-4} M potassium ion. The response time of the PVA membrane with microspheres prepared by seeded emulsion polymerization was ~ 2 minutes.

CHAPTER I

INTRODUCTION

1.1 Fiber Optic Sensors for Chemical Sensing

1.1.1 Introduction

On-line, real-time identification and remote monitoring of chemical substances utilizing high-quality, inexpensive optical fibers has been, and will be, an exciting direction for chemical sensors especially in the areas of health care and environmental analyses. A report for the next 20 years prepared by the major American chemistry and chemical engineering professional organizations identified chemical sensors as one of the important areas of development in the chemical industry.[1] According to the report: "Robust measurement techniques for real-time, highly reliable analysis in practical environments... requires sensitive, selective, distributed, multiplexed, and integrated instruments for on-line process and environmental analysis. The needs include multifunction chemical sensors, fiber-optic probes..." Fiber optic sensors are becoming the technology of choice in many scientific and industrial fields. As reported in Design News[2]: "Nearly every designer in the 21st Century will be working in some way with light... It predicts major increase in the use of light-related technologies in fields of communication, medicine, defense, research, energy, and manufacturing... The entire world will be linked with high-speed fiber-optic communications. People will have personal monitors that will keep tabs

of their health non-invasively by evaluating the optical properties of their blood and tissue... Factories will be crammed with optical sensors."

Optical spectroscopy with optical fibers can provide rapid, nondestructive, and remote online monitoring analysis of many important compounds. The concept of optical fiber-chemical sensing using direct spectroscopy is to obtain quantitative information from a spectroscopic measurement performed directly in the sample. An optical fiber is used to transmit electromagnetic radiation to and from a sensing element which is in contact with the analyte. One approach for chemical recognition is the direct optical interaction with the analyte. In this design, a spectroscopically detectable optical property of the analyte can be detected directly through the fiber optic sensing phase without a specific recognition reaction. Alternatively, an indirect analysis using an immobilized reagent, e.g., a chemical indicator or complexing reagent, can be designed for the chemical recognition phase. Chemical changes caused by the interaction between the analyte and immobilized reagent lead to a measurable optical property change that can be determined by analyzing the radiation that returns from the sensing region through the fiber. The advantages are that no "reference electrode" is needed - however, a reference source is useful; there is no electrical interference; they have desirable physical properties (small size, ruggedness, strength, elasticity, durability); a replaceable immobilized reagent is used which does not have to be in contact with the optical fibers; there are no electrical safety hazards; they are highly stable with respect to calibration; they can respond simultaneously to more than one analyte using multiple immobilized reagents with different wavelengths for response; and they have the potential for a higher information content than electrical transducers.

1.1.2 Optical Techniques

Optical spectroscopy is one of the most valuable tools for analytical chemists and has played a key role for optical fiber sensor techniques. As shown in Figure 1.1, the electromagnetic spectrum indicates the wavelengths of important types of radiation such as visible, ultraviolet and infrared.

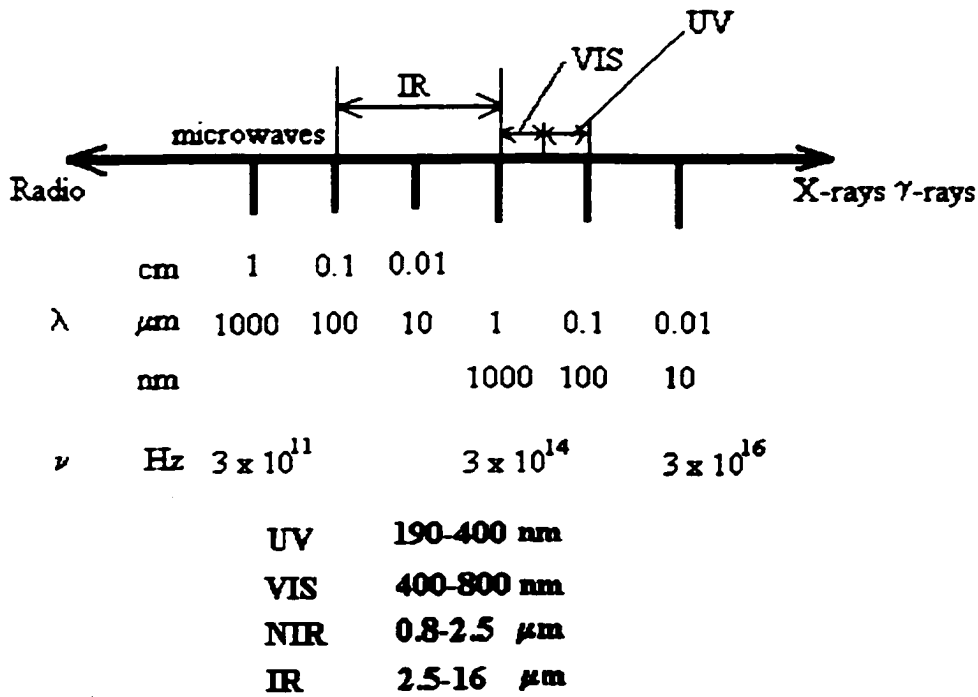

Figure 1.1 The electromagnetic spectrum

The development of fiber optic devices that respond to the presence of a chemical species by a change in their optical properties has played an important role in chemical, biological, and environmental monitoring and process control. The main types of conventional spectrometric methods, absorption, reflection, or fluorescence /

luminescence, can be the detection techniques for fiber optic sensors that use appropriate indicator dyes, polymers, and other additives fabricated on the end of the fiber. Figure 1.2 shows three techniques which can be used as fiber optical probes for chemical sensing.

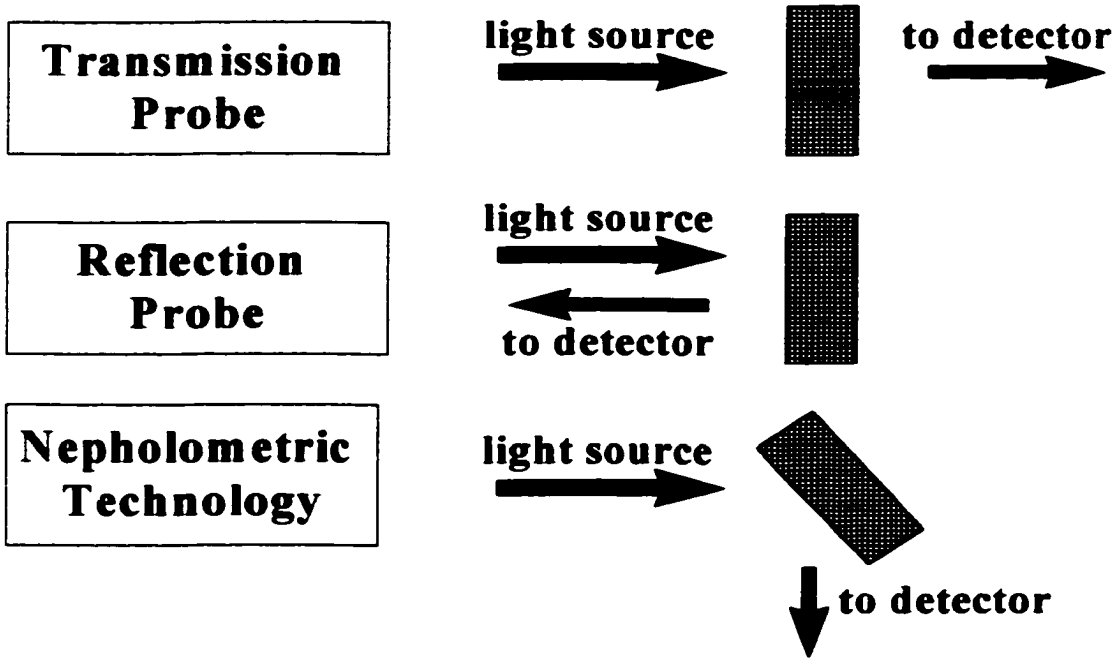

Figure 1.2 Three techniques which can be used as fiber optical probes for chemical sensing based on swellable polymer sensing elements.

1.1.3 Examples of Fiber Optic Sensors Using Spectroscopy

Fiber-optic chemical sensors have been actively investigated in the last decade. A variety of sensing elements, such as pH indicators and neutral ionophores, can be covalently or noncovalently immobilized on the end of optical fiber(s) for biomedical, environmental and other analytical applications. Most fiber optic chemical sensors

reported in the literature are based on dye chemistry. Either a change in absorbance or fluorescence is measured. This has two important limitations. One is that the measurement has to be made at a wavelength where the dye absorbs and/or emits. The other is the possibility of photodegradation.

1.1.3.1 Transmission / Absorbance Based Sensors

This is the most commonly used technique utilizing commercially available standard optical fibers for the wavelength region from approximately 400 to 1900 nm. Figure 1.3 shows a system of a transmission sensor using direct spectroscopy. A collimation lens is used to focus the light source from the outgoing fiber through the sample region and refocus the transmitted light into the return fiber. Samples with strong spectral absorption peaks can easily be monitored in short lengths with low-loss transmission through a fiber.[3] The device shown in Figure 1.2, using two fibers, was designed by Freeman to monitor copper-sulphate concentration in an electroplating bath.[4]. A light source consisting of a 820-nm LED was connected to one of the fibers and the transmitted light was collected by the other one. The intensity was measured by a photomultiplier with excellent correlation between the analyte concentration and the absorbance of the light transmitted through the fibers over the range of 0.2 to 0.4 M.

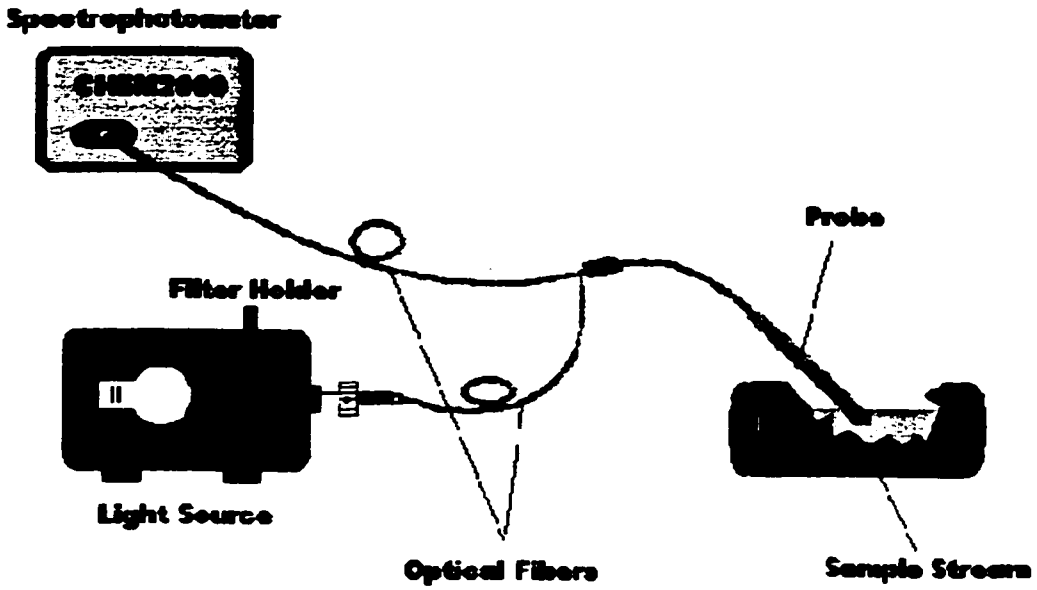

Figure 1.3 A transmission sensor using direct spectroscopy

Fiber optic sensors based on indirect methods using optical indicators and polymers are the most common. Indicators with the desired analytical wavelength, high photostability, and low molar absorbance can only be used for sensing purposes in the preferred operating region, say 350 to 900 nm, of the fiber optic sensor system. Upon interaction with the analyte, most of the indicators undergo a color or fluorescence change which can be detected by inexpensive photodetectors such as photodiodes. The first absorption-based pH sensor was developed by Peterson in 1980.[5] Phenol red with a pK_a value of 7.92 was used as the pH indicator incorporated into polyacrylamide beads. The response time was 0.7 minutes for the signal to drop to 63% of its initial value. Figure 1.4 shows a schematic of this sensor. Another pH sensor was reported by immobilizing phenol red on XAD-type ion exchangers.[6] The dry bead of the resin was soaked in a 0.1

% methanolic indicator solution for four hours. The biggest advantage was the ease of fabrication. However, there was a slow leaching of the indicator with time which caused long-term drift. Moreover, due to the pH-dependent swelling an interference response was observed.

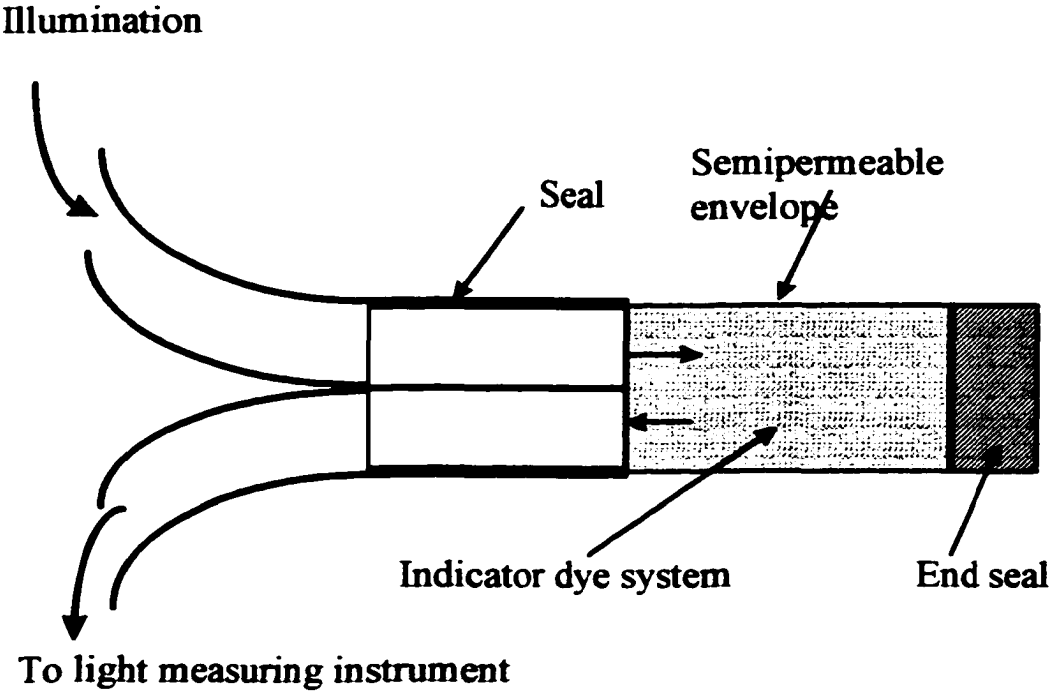

Figure 1.4 Fiber-optic pH sensor with reflective pH indicator chemistry contained in a semipermeable envelope at the tip

1.1.3.2 Fluorescence Based Sensors

This type of sensor is based on immobilized reagents whose fluorescence characteristics change with pH and / or metal ion concentration. A pH sensor based on immobilized fluoresceinamine was contributed by this research group in 1982.[7] The

active amino compound, fluoresceinamine, was immobilized on cellulose. The system consisted of a tungsten halogen lamp, a bifurcated fiber connected to the other components, a photomultiplier, and a photometer / power supply. The excitation wavelength was 480 nm and the emission wavelength was 520 nm. Fluorescence measurements were made as the pH was varied by adding 4.0 M KOH. Hydroxypyrene trisulfonate (HPTS) has been used for pH fluorosensors.[8] HPTS was electrostatically immobilized on an anion-exchange membrane. The excitation was 405 nm for the acid form and 470 nm for the base form and the emission wavelength was 510 nm. The pH sensing range was from 6 to 8. The measurement was related to the ratio of emission intensities excited at 405 and 470 nm, a parameter which is not affected by source fluctuations and slow loss of reagent. However, the loading of indicator affected the sensor response and shifted the pKa to lower values when the amount of indicator was increased. In several alternative approaches, HPTS was immobilized on surface-modified controlled porous glass (CPG) for measurement of near-neutral pH values with a pK_a which was distinctly lower than that determined in solution.[9,10] HPTS was also covalently bound to a hydrophilic cellulose matrix and then was deposited at the end of a single optical fiber.[11] An intensity ratio was related to pH in all cases to avoid drift due to source intensity changes and indicator loss.

1.1.4 Ion Sensors

Fiber optic chemical sensors for the detection of ions other than hydrogen ions have been the subject of much research. Ion-selective fiber optic sensors have been actively pursued in the last decade. A variety of sensing elements, such as pH indicators

and neutral ionophores, can be covalently or noncovalently immobilized on the end of optical fiber(s) for biomedical, environmental and other analytical applications. Natural and synthetic ionophores, especially neutral carriers, are among the most selective chemical recognition agents used for analytical chemical measurements.[12]

1.1.4.1 Sensors Based on Ion Exchange

Organic host-guest chemistry is based on the interaction between the guest ion and the cavity inside the cyclic structure of the host molecule.[13] The organic host molecule is capable of binding and extracting ions from an aqueous phase when it is incorporated into a polymeric matrix such as plasticized PVC membrane. Among a variety of host molecules, the neutral antibiotic, valinomycin, and synthetic carriers, such as crown ethers, have been used in ion sensors.

Ion exchange occurs between two phases when a lipid carrier is used. Usually the counterion cannot be extracted into the lipid phase. Because of the electroneutrality effect, the process would end quickly due to the establishment of equilibrium at the phase boundary. However, if a proton donor incorporated in the lipid phase can release a proton at the same time, then complete ion exchange may take place. One typical approach has been reported based on an ion exchange mechanism.[14-16] The sensitive membrane consists of PVC, plasticizer, an ion carrier such as valinomycin, and a deprotonable dye. Potassium ion extraction onto the membrane is accompanied by loss of a proton from the dye incorporated in the membrane to the external solution. Upon deprotonation, the dye undergoes a color change which can be detected spectrometrically. What is actually measured is the cation / hydrogen ion ratio.

The most promising advantage of the ion exchange approach is that the selectivity to certain ions is exclusively governed by the carrier. Moreover, there is some control over the equilibrium constant which is what determines the range of concentrations that can be sensed.

1.1.4.2 Sensors Based on Coextraction

Coextraction is an alternative approach for ion sensors. Charlton and co-workers reported a membrane which involved the use of a plasticized PVC film with valinomycin as the ion carrier.[17,18] The important aspect was that a lipophilic and highly colored anion was added to the sample solution. Ion binding with the ion carrier extracts the potassium ion onto the membrane which is accompanied by co-extraction of the counterion. As a result, a colored membrane was obtained. The reflectivity was measured at 550 nm and the linear region covered potassium ion concentrations from 2 to 10 mM.

1.1.4.3 Sensors Based on Chromoionophores

Chromoionophores have attracted particular attention with respect to sensing alkali ions.[19, 20] There are normally two functions in one chromoionophore molecule, usually a crown ether dye. One is that the crown ether is capable of binding ions; and the other is that the chromophore part is designed to bring about specific color changes. The chromophoric group can bear one or more dissociable protons or can be nonionic. In the first case, ion exchange between the metal ion and the proton causes a color change and in the second case, ion binding induces a change of the charge transfer band of the dye. Because the chromophore has been covalently linked to a crown ether, the ion-binding

oxygen atom or nitrogen atom is part of the π-electron system of the dye. Ion-binding results in the donation of the lone pair electrons of the crown ether to the metal ion so they can not then fully participate in the π-electron system of the chromophore. Among the chromoionophore based sensors, the biggest disadvantage is the limitation of the detection to the ultraviolet or visible region.

1.2 pH Sensing Based on Swellable Polymer Microspheres

1.2.1 General Idea

Optic chemical sensors based on swellable polymer materials have been developed in this research group since 1982. The original idea was to use dimensional changes accompanying polymer swelling for sensing.[21-24] However, because the size of the polymer used for the optical measurement was fairly large, e. g., the whole piece of the sensing polymer is a membrane, response was slow and the swelling force was a problem. Besides, there was also a cracking problem. To solve the cracking problem, Kraton G1652 was added to the formulations to toughen the polymer. In the course of making Kraton toughened polymers for sensing, it was noticed that these materials became clearer when they swelled. This led to the idea of using bulk Kraton toughened materials for sensing and to measure the change in reflected intensity accompanying swelling. After some time, it was realized that the reason that these materials became clearer was because the refractive index of the polymer decreased upon swelling, bringing it closer to the refractive index of the pores which were filled with water. These materials had pores which were large enough relative to the incident wavelength that light would be scattered. This led to the idea of reversing the phases and formulating the swellable polymer as

microspheres in a hydrogel. The distinctive advantages of this technique are that the materials are rugged and free from photodecomposition; the polymer materials are quite stable and can reversibly undergo many cycles of swelling and shrinking without degradation; and the ease with which they can be combined with any conventional spectrophotometer or optical reflective device in the wide Vis-NIR wavelength region.

1.2.2 Study of Swellable Polymer Microspheres for pH sensing

1.2.2.1 Aminated Polystyrene Derivatives

Polymer microspheres were initially prepared by dispersion polymerization and then derivatized by a variety of amines to introduce the pH sensitive functional groups. However, it was found that the response time for diethanolamine modifed poly(vinylbenxylchloride-co-divinylbenzene), poly(VBC-co-DVB), microspheres embedded in the poly(2-hydroxyethylmethacrylate), poly(HEMA), hydrogel membrane was 53 minutes for shrinking and 73 minutes for swelling.[25] This indicated that porosity was the factor which limited the ion diffusion from the aqueous phase to the polymer phase. To solve the problem, a new approach, seeded emulsion polymerization was used to prepare microspheres with more and larger pores.[26] Aminated poly(VBC-co-DVB) microspheres embedded in a PVA hydrogel membrane showed greatly improved response and tremendously reduced response time. The response time to reach 90 % of the final signal was less than 10 seconds for both the shrinking and swelling processes. Other co-polymers such as poly(vinylbenxylchloride-co-2,4,5-trichlorophenylacrylate-co-divinylbenzene), poly(VBC-coTCPA-co-DVB), prepared by seeded emulsion polymerization were also studied and the results were very encouraging.[27]

1.2.2.2 Nitrated Poly(4-hydroxystyrne)

Aminated polystyrene derivatives with pK_a values between 6~7 were not suitable for other applications such as for pH sensing in seawater because the ocean pH varies from 7.4 to 8.7. In searching for a polymer with a higher pKa value, Zhang started using polynitrophenol as the sensing material.[28] Polymer microspheres were prepared by dispersion polymerization. The principal monomer was 4-acetoxystyrene and DVB was used as the crosslinker or co-monomer. Two derivatization reactions, hydrolysis and nitration, were carried out to form poly(3-nitro-4-hydroxystyrene). The final polymer microspheres have a yellowish color in their acidic form and a reddish color in their basic form. The observed pK_a value was about 8.4. Deprotonation of the polymer causes it to swell and this swelling leads to an increase in the volume of the polymer and a decrease in refractive index. The optical measurement was made by the Optical Reflectance Device and the response time was about 30~50 seconds.

1.2.2.3 Role of Hydrophilicity

Ionic polymer swelling is the main driving force for the change of polymer refractive indices for pH sensing . The higher the swelling ratio, the larger the response. The development of hydrophilic polymer microspheres with a high degree of porosity has been the priority focus of the polymer synthesis. Hydrophilicity can affect the interaction between hydrogen ions in solution and on the polymer active sites and can be adjusted by using different monomers and derivatizing reagents. TCPA has been used as a co-monomer for increasing polymer hydrophilicities with VBC because the acrylate group

on the TCPA can be easily replaced by most derivatizing reagents. [26,27] The polar amine reagent, diethanolamine, has been used for the purpose of preparing hydrophilic pH sensing polymers.

1.2.2.4 Role of Porosity

The other issue which can affect ionic polymer swelling is the porosity. High porosity in the polymer can enhance the diffusion of ions from the external solution into the polymer network and accelerate the exchange rate of ions and water thus increasing the rate of swelling. Porous polymers are reflective due to the difference in refractive indices between the pores and the polymer network. In aqueous solution the pores with ionizable sites on the surface are filled with water resulting in a refractive index different from the bulk polymer and light is reflected or scattered at the interface. It is obvious that the larger the number of pores, the higher the degree of swelling, and the higher the refractive index of the bulk polymer, the more reflected or scattered light.

Porosity in the polymer microspheres prepared by dispersion polymerization is introduced by adding diluent or a porogenic solvent to the polymer formulation and will be discussed in Chapters II and III. Observations have shown that polymer microspheres prepared by seeded emulsion polymerization give higher response for pH sensing than those prepared by dispersion polymerization.[29] One of the possible explanations is that these particles must have significant favorable features such as more and larger pores than particles prepared by dispersion polymerization.

1.2.3 Development of hydrogel membranes with embedded pH sensitive microspheres

As noted, in the earlier study aminated porous polystyrene membranes were coated on a glass substrate or on the tips of optical fibers which resulted in an adhesion problem as well as the limitation on the degree of swelling.[30-34] Hydrogel membranes were then used with embedded sensing microspheres and as a result the magnitude of the response was greatly improved. Because the microspheres are free to swell in all directions, the magnitude of the refractive index changes are increased.

The refractive index for the hydrated hydrogel is constant and is not affected by pH. In contrast, the refractive index of the nitrated poly(4-hydroxystyrene) microspheres is pH sensitive. Normally it is higher than that of the hydrogel matrix and decreases as the polymer swells. Deprotonation of the phenol group increases the water content of the porous particles causing the refractive index to decrease to a value closer to the refractive index of the hydrogel matrix. As a result, the amount of light scattered by the membrane decreases.[32,33] These membranes allow three-dimensional swelling and can undergo multiple swelling and shrinking cycles without degrading mechanically.

1.3 Potassium Sensing Utilizing Ion-Exchange Technology

The development of rugged, inexpensive ion-selective fiber optic chemical sensors based on polymer swelling has been an ultimate goal in this group, which has been accomplished for the first time by the work described in this dissertation. The principle of the sensing approach is actually that of a cation exchange system. Ionophores such as dibenzo-18-crown-6 (DB18C6) are incorporated onto lightly crosslinked nitrated poly(4-hydroxystyrene) microparticles. Potassium ion binding introduces a charge onto the polymer causing it to swell and this is accompanied by a loss of a proton to the external

solution. The overall process decreases the refractive index of the microparticles bringing it closer to the refractive index of the hydrogel. This change can be monitored as the membrane turbidity changes by a conventional spectrophotometer. The advantages are that there is no photoexcitation or possible photodegradation involved and, without using a dye or other indicator, measurements can be made at any wavelength including telecommunication wavelengths at which optical fibers have extremely low attenuation. Moreover, the use of hydrogels as the membrane matrix is suitable for biomedical applications because the hydrogel serves as a "filter" to block out larger molecules, such as proteins, that might otherwise foul the microspheres.

1.4 Goal of the Thesis Research

The development of polymer formulations and characterization of swellable polymer microspheres for chemical sensing has been the main focus of the research in this group. Previous work has explored pH sensitive polymer systems for use in optical sensors.[25-27] These studies have included aminated polystyrene, polyVBC, and poly(VBC-TCPA) co-polymer as well as nitrated poly(4-hydroxystyrene) systems. Polymer polarities and porosities have been studied extensively by variations in polymer compositions, formulations, and the techniques of polymerization including the optimization of the degree of crosslinking, effective diluents or porogenic solvents, and derivatization reagents.[26] Polymer formulations have been evaluated by measuring turbidity changes with microspheres embedded in a hydrogel. The thermal and mechanical stability of both polymer particles and hydrogel matrices have been studied.

1.4.1 Improved Synthesis of Microspheres with More and Larger Porous

This dissertation covers three major areas in the development of fiber optic chemical sensors. The first area is the synthesis of swellable polymer microspheres which will be discussed in Chapter III. Both dispersion and seeded emulsion polymerization techniques have been applied for the preparation of monodisperse poly(4-hydroxystyrene) spherical particles with diameters of 0.6 to 2.5 μm. For dispersion polymerization, particle size, size distribution, and particle shape are affected by the dispersion medium, concentration of monomer, concentration of stabilizer, degree of crosslinking and type of crosslinker while other parameters such as the amount of initiator, reaction temperature, stirring rate, and reaction time were kept constant. Poly(4-acetoxystyrene)-TCPA co-polymer was also studied for the synthesis of monodispersed microspheres. For seeded emulsion polymerization, particle size, size distribution, and particle shape are affected by the seeds, concentration of monomer, concentration of stabilizer, and degree of crosslinking while other parameters such as the amount of initiator, swelling time, reaction temperature, stirring rate, and reaction time were kept constant. It is believed that particles made from seeded emulsion polymerization have a larger number of pores and greater pore size which enhance the swelling process. The results showed that the response for pH sensing had been greatly improved by using particles prepared from seeded emulsion polymerization.

1.4.2 Evaluation of the Properties of the Polymer Materials for pH sensing

The second area is the continued investigation of swellable polymers for pH sensing which has been extensively studied in previous work.[25-28] Sensors utilizing an

Optical Reflective Device coupled to a pH sensing polymer membrane were investigated for the determination of pH in seawater by measuring changes in reflection.[28,30] The sensing pH range was from 7.4 to 8.7. Poly(4-hydroxy-3-nitrostyrene) microspheres embedded in a hydrogel were chosen for the sensing element due to the higher pK_a value than that of the amine-modified polystyrene. The improvement in both the pH sensing range and the sensor response based on nitrated poly(4-hydroxystyrene) as the sensing element is described in Chapter IV. This improvement was achieved by applying the seeded emulsion polymerization technique to the preparation of the porous polymer microspheres and by controlling the conditions of the nitration reaction. In this way the degree of nitration could be modified resulting in the formation of pH sensitive polymers having a wide range of pK_a values. The pH sensitive polymer was characterized by measuring the membrane turbidity change in a special membrane holder on the Cary 5 spectrophotometer. The pK_a values of the polymers can be tuned from 5 to 10 which will cover the pH sensing range from 4 to 11. Theoretically any pK_a value can be obtained by varying the degree of the nitration reaction and different nitration reagents may be used to get reproducible results. The response time, sensitivity, and stability of the membrane have been greatly enhanced by using polymer microspheres prepared from seeded emulsion polymerization.

1.4.3 Evaluation of the Possibility of Ion Sensing by Combining the pH sensitive Polymer with a Neutral Ionophore

It has been the goal of our research group to develop chemical sensors for other ions than hydrogen ion by utilizing the same concept of chemical sensing based on

polymer swelling. This is the third area of my dissertation. A new type of polymer material with desirable optical properties for potassium ion sensing will be discussed in Chapter V. The sensing element is a pH sensitive polymer, nitrated poly(4-hydroxystyrene), with an incorporated ionophore. As will be seen, the same pH sensitive polymer was used as described in Chapter IV and DB18C6 or valinomycin was used as the potassium ionophore. Ion binding by the ionophore is accompanied by deprotonation of the hydroxy group and causes the polymer to swell as a function of analyte concentration at a pH which is below the designed pK_a of the polymer. The ionopheres were immobilized either by incorporating them into the polymer formulation before polymerization or by soaking the polymer beads or membrane with embedded beads in an ionophere saturated solution. The modified beads were suspended in a hydrogel with the same procedure described in Chapter IV. Membrane response was evaluated by measuring the turbidity change as a function of potassium ion concentration. The successful potassium ion-selective sensing approach may lead to a variety of ion-selective sensors based on polymer swelling.

CHAPTER II

THEORY

2.1 Polymers and Polymer Synthesis

2.1.1 Free-Radical Polymerization

Polymers are large molecules that are made up of many repeating subunits. Many polymerization reactions can be initiated by free radicals. Free-radical polymerization processes can be carried out in bulk, solution, suspension, dispersion, emulsion or by other precipitation techniques.[35,36] The polymer studied in this project, poly(4-acetoxystyrene), is prepared by free-radical polymerization.

As shown in Figure 2.1, there are three distinct stages in the free-radical polymerization of poly(4-acetoxystyrene). The first stage is the activation of a free-radical center from an initiator to form free radicals. Then the free radicals subsequently add to the vinyl double bond of the monomer to produce a new chain radical. Initiators can be activated either by thermolysis or photolysis. The most important initiators that can undergo thermolysis or photolysis are those that contain peroxide (-O-O-) or azo (-N=N-) groups, such as benzoyl peroxide and azo-bis-isobutyronitrile (AIBN). The second stage of polymerization is called propagation. Chain radicals formed from the first stage rapidly attack other monomers at the active center, the vinyl group. The propagation stage takes place so fast that several thousand additions can occur within a few seconds. The polymer chain stops growing when it is terminated. Two growing chains, each with a radical en

1. Initiation

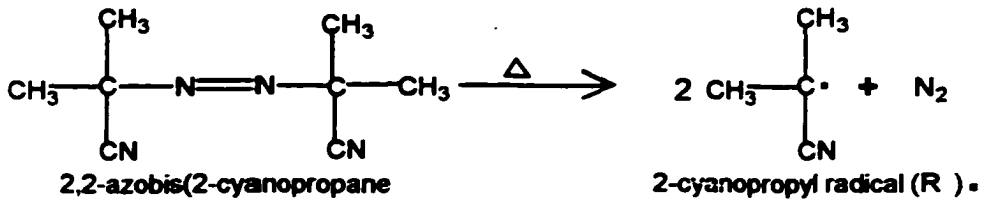

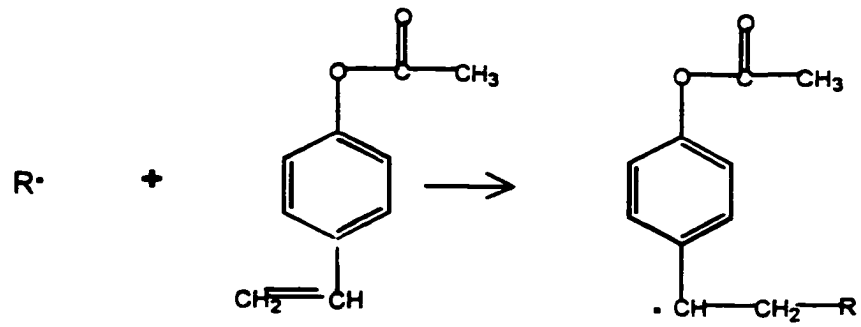

2. Propogation

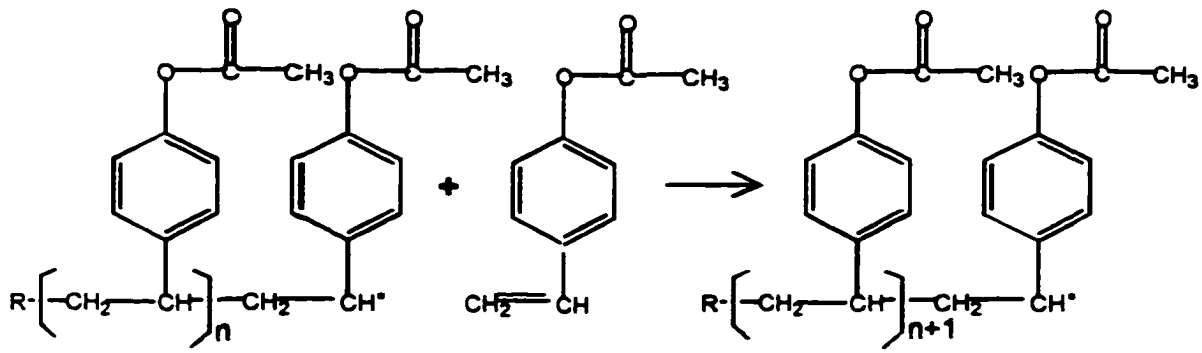

3. Termination

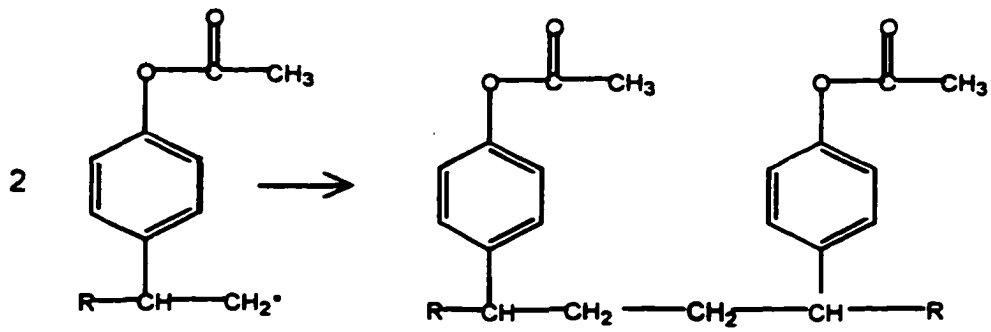

Figure 2.1 The addition polymerization of 4-acetoxystyrene

can react to form a single polymer molecule. This is called combination. The other mechanism of termination is disproportionation. In this reaction, a hydrogen atom is abstracted from one chain by another. As a result, two polymer molecules are formed, one with a saturated end

and the other with an unsaturated end. Different monomer systems under different polymerization reaction conditions have different termination reactions. For example, in the styrene system the chain radicals terminate predominantly by combination.

2.1.2 Suspension Polymerization

The suspension polymerization system consists of an aqueous media with dispersed droplets of monomer in an immiscible liquid phase. A dispersing agent is added to stabilize the resulting suspension, and the initiator is dissolved in the monomer phase. The polymerization reaction takes place as the monomer-soluble initiator is thermally activated. The particle sizes of the resulting polymer typically are in the100 μm ~ 1000 μm range.[35,36] The use of suspension stabilizers and stirring techniques is necessary to protect the droplets of monomer swollen particles from coalescing during the "tacky" period.

Stirring technique plays a major role in controlling the collisions of the beads as well as in determining the bead size distribution during the polymerization process. A suitable stirring rod with an efficiently angled paddle is essential. The droplet size is affected by variety of parameters and can be controlled by changing the surface tension between the droplet and the aqueous media, the stirring rate, and the ratio of monomer to

aqueous phase. Bead size decreases with increasing surface tension between the beads.[36,37]

2.1.3 Dispersion Polymerization

Dispersion polymerization is a logical extension of emulsion polymerization and is widely used for the preparation of polymer particles with diameters from 1 to 20 μm. The reaction process is rapid, and conversion is high.[37] The distinct character of the technique is that the dispersion is a continuous phase. A solvent is chosen which is a good solvent for monomer but not for polymer. The minimum requirements for a dispersion polymerization are monomer, solvent, initiator and steric stablizer. Figure 2.2 shows the schematic of particle growth in dispersion polymerization.

Since the monomer must be soluble in the reaction mixture and its polymer insoluble, the choice of monomer / solvent pair is critical. In practice, both polar and non-polar solvents can be used for dispersion polymerization. Most free radical dispersion polymerizations use alcohol as the solvent. Water is added to adjust the solvency in order to control the particle size and size distribution. In this study a water / ethanol solvent mixture is used for styrene based monomers, such as vinylbenzyl chloride (VBC) and 4-acetoxystyrene (AS). Similar to suspension polymerization, a steric stabilizer is used to produce a colloidally stable dispersion as well as to keep the final polymer particles from coagulating. Polyvinyl pyrrolidone (PVP) has been used as the steric stabilizer in this work.

Stirring is required for dispersion polymerization so that product particles rapidly re-disperse rather than clumping together. There are many factors affecting the particle

size, size distribution, and mono-dispersity. These include such variables as the type of stabilizer, its molar mass and concentration, percentages of monomer and solvent, reaction temperature, and initiator concentration. These will be discussed in the following sections.

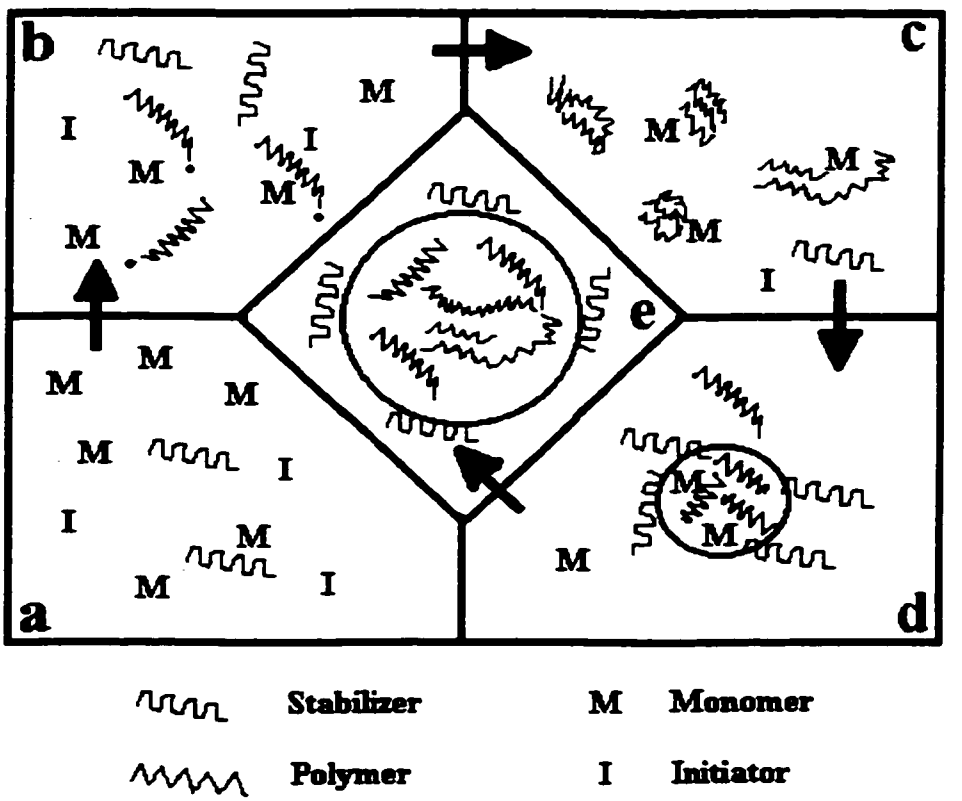

Figure 2.2 Schematic of particle growth in dispersion polymerization. (a) homogeneous polymer solution, (b) oligomeric radicals, (c) self-nucleation, (d) particle growth, and (e) continued growth. [37]

2.1.4 Seeded Emulsion Polymerization

Traditional emulsion polymerization is a free-radical chain polymerization. As in suspension polymerization, water is a chief ingredient.[37] The distinctive feature of

emulsion polymerization is its heterogeneity over the entire process. The main ingredients for emulsion polymerization are the monomer, water, surfactants, initiators and transfer agents. Water plays an important role in the system because it is used to maintain a low viscosity and provides for good heat transfer as well as to isolate polymerization loci. All ingredients are added at the beginning of the polymerization. As soon as the temperature reaches the point at which reaction begins, latex particles start to form and grow simultaneously.

The overall process of emulsion polymerization is rather complex due to its heterogeneous nature. Upon mixing the monomer(s), water and surfactant(s), phase separation starts. The surfactant(s) molecules cluster into micelles with hydrophobic cores that are swollen with monomer to form the micellar phase. The monomer droplet phase consists of the bulk of the monomer existing in the form of large-size droplets with surfactant molecules adsorbed on their surfaces. The particle phase is formed upon heating the mixture in which radicals are formed in the aqueous phase followed by propagation, nucleation, particle formation, and particle growth. In the propagation stage, radicals may propagate in the aqueous phase to form oligoradicals by adding monomers that are dissolved in the aqueous phase. Particle nucleation then begins to form polymer particles which swell with monomer by diffusion of monomer from the monomer droplets. In the final stage, the monomer-swollen polymer particles propagate to form particles. The monomer required for this reaction is supplied from the monomer droplets suspended in the water phase. The growing polymer particles are protected by adsorbing surfactant molecules on their surface to maintain colloidal stability. The termination of the polymerization occurs when all the monomer is converted to polymer. Emulsion

polymerization usually produces very small particles (< 1 μm) because little control over the particle numbers and size distribution can be exerted during the polymerization process.

Seeded emulsion polymerization is used to prepare porous, larger monodisperse polymer particles.[38-45] It is an alternative approach to emulsion polymerization in which the particle nucleation stage is replaced with the use of a pre-formed seed particle as one of the reactants. This technology has important advantages since the preparation of seed particles is sufficient to provide polymerizations with control of particle numbers and size distribution. Monodisperse polymer seeds can be prepared by conventional dispersion polymerization as described previously.

Seeded emulsion polymerization may be described as a standard suspension polymerization that uses an aqueous dispersion of swollen seed particles, instead of droplets. The swollen polymer seeds are preformed by swelling seed particles in an emulsion of a mixed monomer. Unlike suspension polymerization, the size of the starting droplets is not determined by the stirring conditions but is controlled by the size of the seed particles. Emulsifier is added to prevent formation of coagulum or small secondary particles during polymerization. The swollen particles with saturated monomer mixture behave as individual bulk polymerization sites that are polymerized in an aqueous medium. The spherical shape of the original seed particle is maintained. Macroporosity in the final beads may be introduced by adding porogens and crosslinking the polymerization mixture. The swelling of seed particles plays an important role in the size of the final products. The properties of the seeded polymerized particles depend on the amount of monomer added,

the type and amount of porogen and crosslinking, as well as the features of the polymer seed particles.

Seeded emulsion polymerization has been used for the preparation of monodisperse porous particles. A variety of methods have been developed to produce polymer particles with different sizes and different porosities which are useful for different applications. Depending on the desired polymer properties, seed particles can be prepared by emulsifier-free emulsion polymerization, dispersion polymerization, or perhaps suspension polymerization. Smigol has developed a method in which the seed particles are produced by emulsifier-free emulsion polymerization.[46] It was reported that the seeds can swell up to 70 times their volume or 4 times their diameter to produce 10 μm beads in diameter with an average pore size about 500 Å in diameter. A method called multi-step swelling seeded emulsion polymerization was reported in 1992 [44]. The seed particles for this method were also prepared by emulsifier-free emulsion polymerization. There are two swelling steps involved. In the first step, the seed particles are "activated" by a low molecular weight organic hydrophobic compound, such as 1-chlorodecane, which partitions into the seed particles. Then the swelling was continued by the addition of emulsified monomer mixture before polymerization. The swelling ratio was 100-5000 times in volume and the size of the final particles was >100 μm in diameter. Other methods using seed particles prepared by dispersion polymerization with one step swelling have been developed with a large degree of swelling, 200 times or more in volume. These methods can produce monodisperse porous particles in the size range 4~10 μm. [41-43, 47-51] In these methods a small amount of polymeric surfactant is used to stabilize the swollen particles by a steric stabilization mechanism and to increase the viscosity of the medium

which reduces the tendency of the particles to coalesce. It is believed that the absorption capacity increases by using the surfactant without pre-swelling to activate the seed particles.

2.2 Nature of Polymer Swelling

When a crosslinked polymer is in contact with a compatible solvent it swells and its physical dimensions increase. Polymer swelling is a phenomenon which has both advantages and disadvantages for the use of polymer materials in different areas. For example, polymer particles have been used as the stationary phase for column chromatography. The efficiency of the column can be greatly reduced due to unwanted polymer swelling. However, for sensors based on refractive index changes, a large degree of swelling accompanying analyte concentration changes is necessary for good sensing response. Porous, lightly crosslinked polymers can swell a great deal more in good solvents than polymers that are nonporous and highly crosslinked. Charged polymers swell in aqueous solutions, while uncharged, hydrophobic polymers do not swell or only have a very low degree of swelling in water. In this work, the main purpose was to develop opticcal chemical sensors based on swelling of ionic polymer microspheres.

2.2.1 Nonionic Polymer Swelling

According to Flory's theory,[52] the polymer swelling can be defined as either nonionic or ionic depending on the polymer backbone and the type of interaction between the polymer and the medium surrounding it.

For polymers with a nonionic network the swelling process is mainly affected by 1) the degree of crosslinking and 2) the interaction between the polymer and the solvent. Nonionic polymer swelling results from the absorption of solvent into the polymer network with a resulting increase in volume. The degree of swelling depends on the parameters shown in the equation:

$$q_m^{5/3} \cong (vM_C)\,(1 - 2M_C / M)\,(1/2 - \chi_1) / V_1 \qquad (1)$$

where,

$q_m \equiv$ equilibrium swelling ratio

$v \equiv$ specific volume of the polymer

$M_C \equiv$ molecular weight per crosslinked unit

$M \equiv$ molecular weight of the polymer network

$\chi_1 \equiv$ a parameter of interaction which represents the interaction free energy per solvent molecule divided by kT (the affinity of the polymer for solvent)

$V_1 \equiv$ molecular volume of the solvent

It can be seen that the swelling ratio depends on the degree of crosslinking and the compatibility of the solvent as expressed by χ_1 in the equation. When in contact with a pure good solvent the polymer swelling ratio at equilibrium increases with a decrease in crosslinking due to the increase in the average molecular weight of a crosslinked unit, M_C. The second term, $(1 - 2M_C / M)$, is the network imperfection factor. The higher the

polymer molecular weight (larger M) and the lower the crosslinking (smaller M_C), the higher the swelling ratio.

2.2.2 Ionic Polymer Swelling

Polymers with ionizible functional groups may be used for ion sensors based on ionic polymer swelling. Polymers which have been used for this dissertation are ionic polymers which selectively interact with analytes. The parameters that describe the swelling ratio of ionic polymers are given in the following equation:

$$q_m^{5/3} \cong [\,(i/2V_u S^{1/2})^2 + (1/2 - \chi_1)/V_1\,]/(\nu_e/V_0) \qquad (2)$$

where,

$i \equiv$ number of electronic charges per polymer unit

$V_u \equiv$ molecular volume of a repeating polymer unit

$S \equiv$ molar ionic strength

$\chi_1 \equiv$ interaction parameter

$V_1 \equiv$ molecular volume of solvent

$\nu_e \equiv$ effective number of chains in network

$V_0 \equiv$ volume of unswollen polymer network

The equilibrium swelling ratio depends on both the electrostatic repulsion between like charges on the polymer backbone, as shown in the first term, and the interaction between the polymer and the solvent, as shown in the second term. Increasing the charge density (i/V_u) of the polymer network or decreasing the ionic strength (S) in the solution

results in an increase in the swelling ratio. High ionic strength decreases swelling due to shielding of the charges and the reduction in the force of repulsion.

Ionic swelling can also be explained by osmotic pressure. As the charge density of the polymer increases, the local ionic strength on the polymer backbone becomes higher than its surroundings. Thus, due to the osmotic pressure, the higher ionic strength is balanced by solvent entering the network causing the polymer to swell.

For ionic polymers the first term in equation (2) is usually more significant. The overall swelling degree of ionic polymers depends on the charge density, the nature of the solvent, and the level of crosslinking. Figure 2.3 illustrates ionic polymer swelling in an electrolyte solution.

2.3 Light Scattering and Membrane Turbidity

Membranes that are optically sensitive to analytes have been used to develop fiber optic chemical sensors. These membranes consist of hydrogels as a matrix with suspended polymer particles as the selective sensing element. In an aqueous solution the hydrogel has a constant refractive index and is not sensitive to analytes. In contrast, the polymer particles are designed to sense analytes by swelling with changes in analyte concentration. This increases the water content of the polymer causing its refractive index to decrease. As the membrane is exposed to a sample solution, the refractive index of the suspended particle decreases as a function of analyte concentration while the refractive index of the

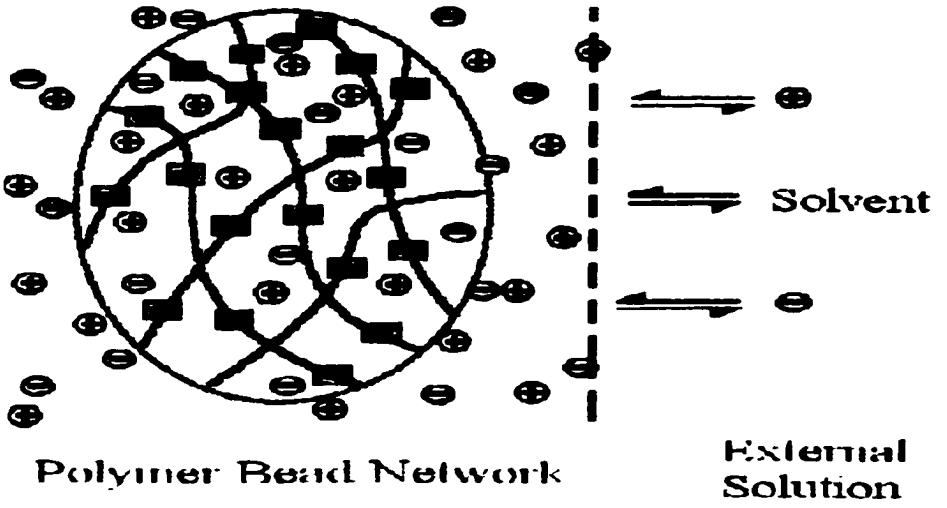

(a)

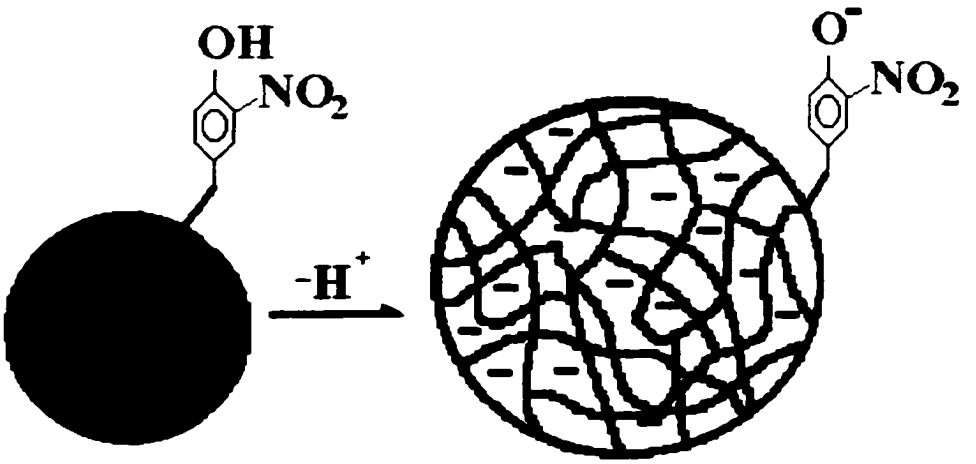

(b)

Figure 2.3 Illustration of ionic polymer swelling. (a) shows the polymer bead with charged sites in contact with the external electrolyte solution (squares represent fixed charges on the backbone, circles represent mobile charges, the dash line indicates the phase bondary), (b) shows the polymer bead with functional group swelling when the deprotonation occurs

hydrogel remains the same. Therefore, the overall optical property changes of the membranes can be determined by measuring the reflected or scattered light or the intensity of the membrane turbidity.

2.3.1 Light Scattering

Figure 2.4 illustrates the effect of a medium with suspended particles on the intensity of a transmitted light beam. Reflection takes place at the phase boundaries as a result of refractive index differences between the medium and its surroundings. Scattering is caused by suspended particles and occurs only if the major dimension of the scattering particle is comparable to the wavelength or larger and its refractive index is different from the medium. Each scattering center can be characterized by a complex refractive index ratio n_s / n_m , where s identifies the scattering center and m the medium. The amount of light reflected at the interface between two dissimilar phases depends on the difference in the refractive indices of the two phases. For normal incidence:

$$R = (n_2 - n_1)^2 / (n_2 + n_1)^2 \qquad (3)$$

It is clear that the reflectance increases as the difference in refractive index between n_1 and n_2 increases.[53]

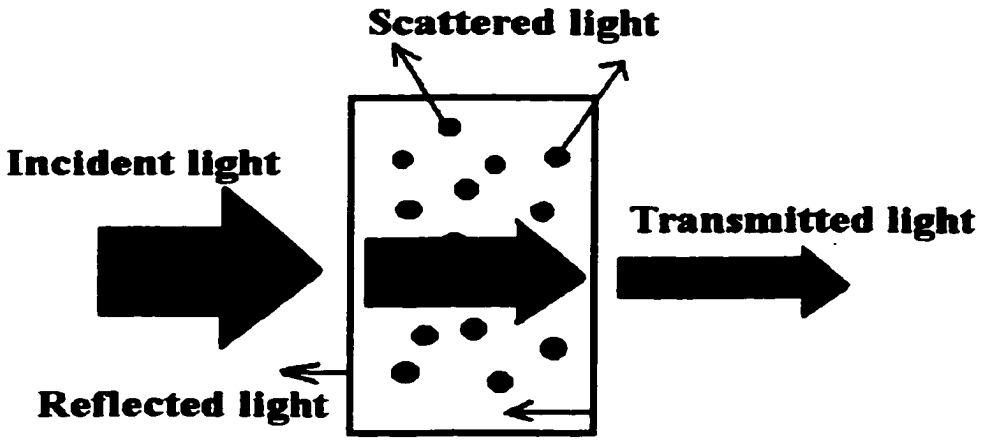

Figure 2.4 The effect of a medium with suspended particles on the intensity of a transmitted light beam

2.3.2 Membrane Turbidity

There are two factors involved in polymer swelling. One is the increase in the size of polymer microspheres and the other is the decrease in the refractive index by which the refractive index of the polymer becomes closer to the refractive index of the membrane matrix. This leads to a decrease in the amount of light reflected/scattered by the particles. The change in refractive index is the dominant effect for most of our systems. This can be measured as a change in membrane turbidity. Turbidity can be defined as the intensity change of light as it passes through the sample and obeys the relationship:

$$I = I_o e^{-\tau b} \qquad (4)$$

where,

$I \equiv$ intensity of light passing through the sample

$I_0 \equiv$ intensity of incident light

$\tau \equiv$ turbidity coefficient or turbidity

$b \equiv$ pathlength (cm)

This equation defines the turbidity of suspended particles in a medium. It is analogous to Beer's law.

2.4 Theory of Optical Sensing Based on Swellable Polymer Embedded in a Hydrogel

Unlike Beer's law, there is no theory or model that can be used for the calculation of membrane response based on the light scattering by microspheres embedded in a hydrogel. Since the microspheres have diameters that are similar in magnitude to the scattered wavelength, it is not easy to develop a simple equation to describe such a complicated system. Rooney and Seitz have reported a simplistic model in which a modified Fresnel equation is used:[54]

$$R \propto (d_p/\lambda)^m \times (n_p - n_h)^2 / (n_p + n_h)^2 \qquad (5)$$

where,

$R \equiv$ the reflectance

$d_p \equiv$ diameter of the polymer microspheres

$\lambda \equiv$ wavelength of light

$n_p \equiv$ refractive index of the polymer microspheres

$n_h \equiv$ refractive index of the hydrogel

The $(d_p/\lambda)^m$ term indicates that the reflectance decreases as the wavelength increases relative to the size of the microspheres. It is also shown that there is an increase in reflectance accompanying an increase in particle size when the wavelength is fixed. If the refractive indices for swollen and unswollen particles are n_{ps} and n_{pu} respectively, the ratio of the reflectances will be:

$$\frac{(d_{ps}/\lambda)^m \times (n_{ps} - n_h)^2 / (n_{ps} + n_h)^2}{(d_{pu}/\lambda)^m \times (n_{pu} - n_h)^2 / (n_{pu} + n_h)^2} \qquad (6)$$

by assuming $(n_{pu} + n_h)^2 / (n_{ps} + n_h)^2 = 1$, equation (6) becomes:

$$R_r = (d_{ps}/ d_{pu})^m \times (n_{ps} - n_h)^2 / (n_{pu} - n_h)^2 \qquad (7)$$

where,

$R_r \equiv$ reflectance ratio

The refractive index of the swollen particles decreases due to an increase in water content and can be defined as:

$$n_{ps} = n_{pu} \times (1 - f_{H20}) + n_{H20} \times f_{H20} \qquad (8)$$

where,

$f_{H20} \equiv$ fraction of swollen polymers with water

Equation (8) can be expressed in terms of volume changes:

$$f_{H20} = (V_{ps} - V_{pu}) / V_{ps} = [(d_{ps}/d_{pu})^3 - 1] / (d_{ps}/d_{pu})^3$$

$$= (d_r^3 - 1) / d_r^3 \qquad (9)$$

where,

$V \equiv$ volume of particles

and $d_r = d_{ps}/d_{pu}$

Substituting equations (8) and (9) into (7) leads to the following:

$$R_r = d_r^m \times [(n_{pu} \times 1/ d_r^3) + n_{H20} \times (d_r^3 - 1) / d^3 - n_h]^2 / (n_{pu} - n_h)^2 \qquad (10)$$

Equation (10) shows the relationship between the reflectance ratio, the particle diameter ratio, and the refractive indices of the unswollen polymer particles and the hydrogel. From this equation we can estimate the relative reflectance membrane by membrane with various assumptions.

CHAPTER III

SYNTHESIS OF FUNCTIONAL POLYMER MICROSPHERES

3.1 Introduction

The use of styrene-based functionalized monomers to make crosslinked polymers has found numerous applications, such as in polymer-supported reactions,[55] polymer resins, [56-58] and as the stationary phase for chromatography.[59-61] A large variety of functional groups may be attached to crosslinked poly(styrene) and related polymers.[62] The synthesis and study of polymer materials utilizing 4-acetoxystyrene as a functional monomer has become widespread. [63-66] The monomer of 4-acetoxystyrene is commercially available from Aldrich Chemical Company. Its availability makes the synthesis of polyphenols more attractive. Poly(4-acetoxystyrene) can be synthesized by free radical initiation and has been well studied.[67-69] The use of derivatized poly(4-acetoxystyrene) for the chemically sensitive element of sensors was first established in this research group in 1996.[70] The main purpose of this chapter is to present a comprehensive study of recent work on the development of swellable poly(4-acetoxystyrene) microspheres by dispersion, and seeded emulsion polymerization, and to indicate how the main parameters which determine the behaviour of chemical sensing can be controlled and improved. The chapter also presents experiments on suspension polymerization of lightly crosslinked 2,4,5-trichlorophenylacrylate (TCPA)-styrene copolymers.

3.2 Preparation of TCPA-Styrene Copolymer Particles by Suspension Polymerization

The copolymer of 2,4,5-trichlorophenylacrylate (TCPA), styrene, and divinylbenzene (DVB) with incorporated dibenzo-18-crown-6 was prepared by suspension polymerization. The purpose of this experiment was to prepare a material for the preliminary testing of the sensing chemistry to be used for a potassium ion-selective sensor. Dibenzo-18-crown-6 was used as the potassium ion complexing agent.

3.2.1 Reagents

Styrene, dodecane, o-xylene, hydroxybutyl methyl cellulose, xanthan gum and dibenzo-18-crown-6 (DB18C6) were purchased from Aldrich Chemical Company, Inc., Milwaukee, WI. 2,4,5-Trichlorophenylacrylate was synthesized in this laboratory as described in the literature.[27] Divinylbenzene (45-55 % active, 2:3 meta/para) and benzoyl peroxide (water wet, 77 %) were both purchased from Polysciences, Inc., Warrington, PA. Kraton G1652, styrene triblock copolymer (styrene - ethylene / butylene), was donated by Shell Chemical Co. Acetone and toluene were purchased from Fisher Scientific, Fair Lawn, NJ. Double deionized water was obtained by using a Corning Megapure water distillation apparatus. All other chemicals (reagent grade) were directly used without further purification.

3.2.2 Apparatus

The reaction apparatus for suspension polymerization is illustrated in Figure 3.1. It consists of a 750 mL, indented cylindrical, 3-necked reaction flask, and a mechanical stirrer with a stirring rod equipped with 90^0 paddles. The reaction was carried out at

constant temperature in a water bath. A hot plate was used to control temperature. Particle diameters were analyzed by a Fisher Scientific Stereomaster Microscope, magnification 30X or 60X.

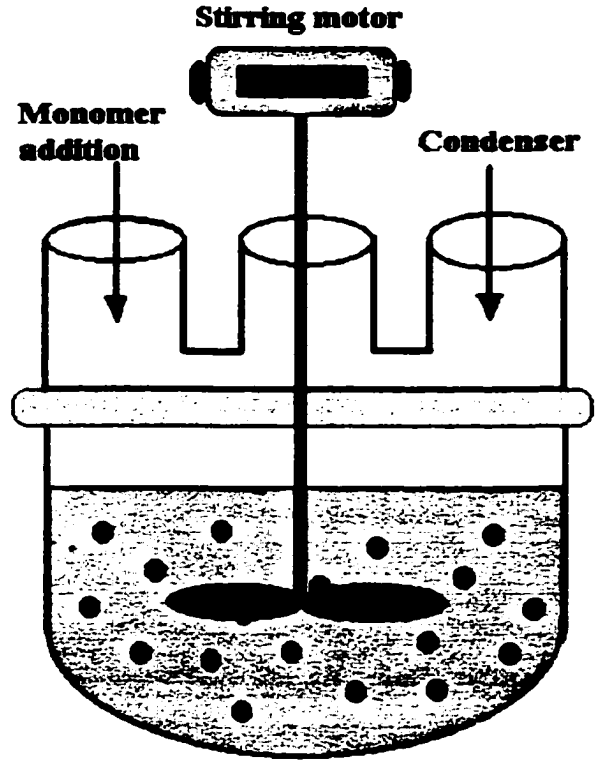

Figure 3.1 Schematic of suspension polymerization apparatus

3.2.3 Procedure

3.2.3.1 Preparation of Aqueous Suspension System

In suspension polymerization two phases are prepared independently.[70] The aqueous suspension phase was prepared by dissolving a mixture of Xanthan gum and hydroxybutyl methyl cellulose in 500 mL of distilled water. For efficient dissolution, 0.04g Xanthan gum and 0.28g hydroxybutyl methyl cellulose were gradually dispersed on the surface of distilled water before stirring to allow the solid to swell. The whole process

took approximately one hour. Then the mixture was constantly stirred with minimal heat until a homogeneous suspension was obtained.

3.2.3.2 Preparation of Organic Monomer System

The monomer phase consisted of 2,4,5-trichlorophenylacrylate (monomer), styrene (monomer), divinylbenzene (crosslinker), Kraton G1625 (elastomer), benzoyl peroxide (initiator), and DB18C6 (see Figure 3.2 for the structures) dissolved in a mixture of dodecane and o-xylene. A known amount of DB18C6 was dissolved in xylene at 70 ^{0}C before it was combined with the other reagents. Different polymer formulations are listed in Table 3-1. The percentage of crosslinker was calculated based on a mole / mole ratio to monomer. All other calculations including the amounts of initiator, Kraton G1625, and DB18C6 were based on the wt % of the co-monomers. The total volume refers to the volume of monomer, crosslinker, dodecane, and o-xylene in the monomer mixture. The total volume contains 60 % (v/v) 2 : 1 (by volume) xylene : dodecane as a porogenic solvent.[70] For example, one recipe with 25% TCPA, 2% Kraton G1625, 6% divinylbezene, 33% dodecane, and 60% total diluent is: 0.044 moles TCPA (11.1 g), 0.132 moles styrene (15.12 mL), 0.021 moles divinylbenzene (3.0 mL), 0.496g Kraton G1652, 3.60 mL dodecane, 7.28 mL xylene, 0.496 g benzoyl peroxide, and 1.24g DB18C6.

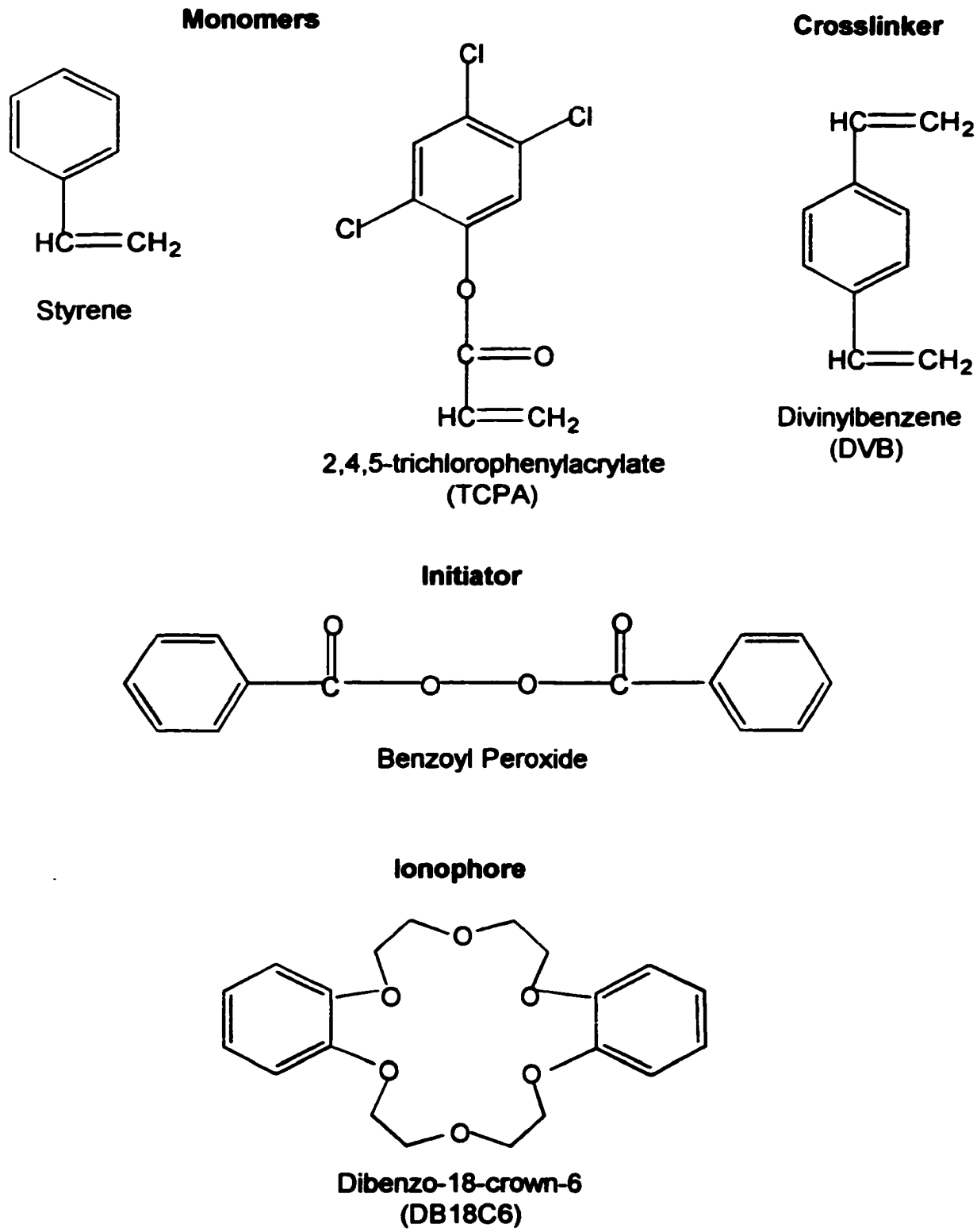

Figure 3.2 Structures of the reagents used in the preparation of DB18C6 modified TCPA-styrene co-polymer

Table 3-1 Formulations for the suspension polymerization of DB18C6 modified copolymers

Polymer	TCPA (Mole%)	Styrene (mole%)	DVB (wt%)	Initiator (wt%)	DB18C6 (wt%)	Kraton (wt%)	Dodecane (%)
#1	25	75	6	2	5	2	33
#2	50	50	6	2	5	2	33
#3	50	50	6	2	0	2	33

3.2.3.3 Suspension Polymerization

Suspension polymerization was carried out in the reaction vessel where the suspension aqueous phase and monomer organic phase were mixed. Initially, two separate layers were observed. Upon stirring, small droplets formed with a stirring rate of approximately 200 rpm. The reaction took about 8 hours at a temperature of 84 ^{0}C.

After polymerization, the beads were filtered using a Buchner funnel, washed with distilled water to remove the excess aqueous phase, and then washed with acetone to remove the excess xylene and dodecane. The final beads were air dried overnight.

3.2.4 Amination of TCPA-Styrene Co-polymer Beads

For the purpose of introducing hydrophilicity and microporosity into the polymer beads, derivatization was necessary after polymerization. The beads were aminated at room temperature with diethanolamine according to the procedure of Hassen.[71] A known amount of beads was swollen in 1,4-dioxane for 1 hour and after removal of the excess 1,4-dioxane, enough diethanolamine was added to cover the beads. The amination reaction (Figure 3.3) took about 48 hours with constant stirring to allow a good yield at room temperature.

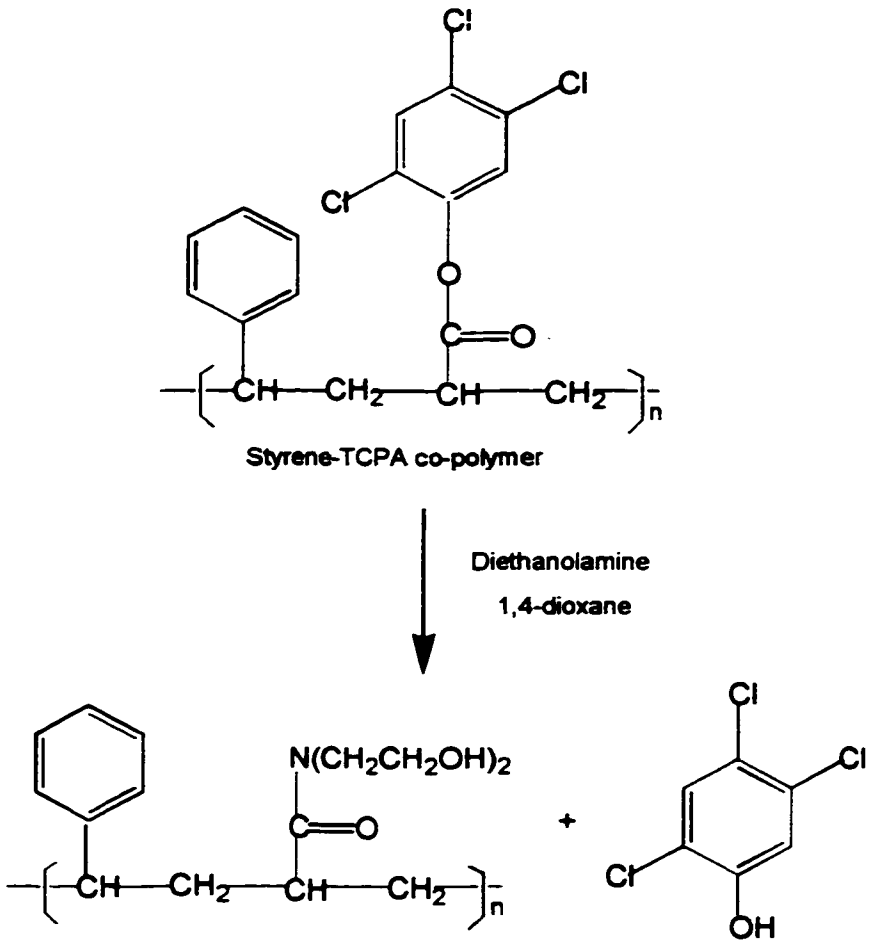

Figure 3.3 Amination reaction for the preparation of amine modified TCPA-styrene co-polymer

3.3 Preparation of Polymer Microspheres by Dispersion Polymerization

The optimum size of swellable polymer microspheres suspended in hydrogel is slightly larger than the wavelength of light used to interrogate the membrane. Since we use wavelengths in the visible and near infrared, we want particle diameters on the order of 1 to 2 micrometers. Particles in this size range were prepared by dispersion

polymerization. Most experiments were performed with lightly crosslinked poly(4-acetoxystyrene). However, selected experiments were performed with other monomer system.

3.3.1 Reagents

Toluene, 1,4-dioxane, 4-acetoxystyrene (AS), styrene, vinyl benzyl chloride (VBC), poly(vinyl alcohol) (PVA), 2,2'- azobisisobutyronitrile (AIBN), glutaraldehyde , and polyvinyl pyrrolidone (PVP) were purchased from Aldrich Chemical Company, Inc., Milwaukee, WI. 2,4,5-Trichlorophenylacrylate (TCPA) was synthesized in this laboratory as described in the literature. Divinylbenzene (45-55 % active, 2:3 meta/para) was purchased from Polysciences, Inc., Warrington, PA. Acetone, methanol, ethanol, and toluene were purchased from Fisher Scientific, Fair Lawn, NJ. Doubly deionized water was obtained by using a Corning Megapure water distillation apparatus. All other chemicals (reagent grade) such as bases, acids, and salts were directly used without further purification.

3.3.2 Apparatus

The reaction apparatus for dispersion polymerization is illustrated in Figure 3.4. It consists of a 500 mL, three-necked round-bottom reaction flask and a water bath on the hot plate with magnetic stirrer. The reaction was carried out at constant temperature under a nitrogen atmosphere. A Branson 1210 Sonicator was used before and after polymerization for the purpose of preparing homogeneous monomer solutions and breaking agglomerated microspheres to re-suspend them in the reaction solution, as well

as in other solvents, during the washing stage. A Fisher Scientific Centrifuge Model 228 was used to separate particles from the reaction medium. Particle diameters and size distribution were analyzed by an Amray Model 3300FE Scanning Electron Microscope (SEM). A Perkin-Elmer Model 2400 was used for the CHN analysis in order to determine the extent of formation of poly mono- and di- nitrophenol and a Nicolet 205 FT-IR Spectrometer was used to confirm complete introduction of functional groups to form poly(3-nitro-4-hydroxystyrene).

3.3.3 Polymer Synthesis

Polymer microspheres were synthesized by dispersion polymerization in an ethanol / water / toluene solvent system. Polymerizations were carried out in a reaction vessel with a homogeneous monomer solution. The monomer solution was prepared by dissolving solid stabilizer and initiator in the water-ethanol mixed solvent with sonication, then adding monomer, crosslinker, and porogenic solvent respectively. The mixture was sonicated for ~10 minutes and then stirred for ~20 minutes until a homogeneous clear solution formed. A nitrogen blanket was applied before and during the reaction. The flask was suspended in a water bath maintained at 70^0C with a magnetic stirrer at a constant stirring rate. The requisite amounts of solvents (ethanol and water), porogenic

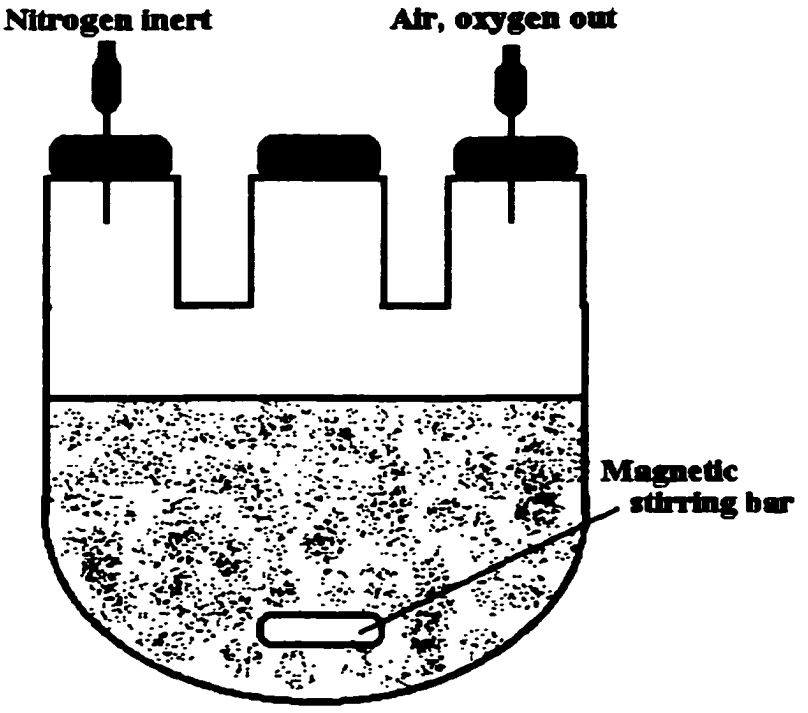

Figure 3.4 Schematic of dispersion polymerization apparatus

solvent (toluene), monomer (4-acetoxystyrene or TCPA-Styrene), crosslinker or co-monomer (DVB), stabilizer (PVP) and initiator (AIBN) were placed into the reaction flask and magnetically stirred. Nitrogen was bubbled for ~ 10 minutes before the temperature was increased and then the bubbling was continued for 20 minutes to exclude air. Polymerizations were allowed to run for about 20 hours. The average size of the microspheres that formed was from 0.5 μm to 0.8 μm. Table 3-2 gives the basic recipe for the formation of micro-porous polymer microspheres.[28]

Table 3-2. A basic recipe for polymer microspheres based on dispersion polymerization

Ingredient	Name	Amounts
Monomer	4-acetoxystyrene	10 mL
Crosslinker	Divinylbenzene	2 wt % to monomer
Stabilizer or Surfactant	Polyvinylpyrrolidone	22 wt% to monomer
Initiator	2,2'- azobisisobutyronitrile	2 wt% to monomer
Solvent I	Ethanol	140 mL[a]
Solvent II	Water	50 mL[a]
Porogenic Solvent	Toluene	10 mL[a]

[a] The amount of solvent is subject to variation from formulation to formulation

After polymerization the beads were separated from the reaction by centrifugation at 3400 rpm for 5-10 minutes, then washed with 95% ethanol to remove the excess aqueous phase, toluene, and other residual materials. A small portion of the beads was air dried overnight for SEM analysis and the remainder were kept in 95% ethanol for further derivatization reactions.

3.3.4 Derivatization

3.3.4.1 Hydrolysis of Poly(4-acetoxystyrene)

The cross-linked polymer of 4-acetoxystyrene can be derivatized in alkaline aqueous 1,4-dioxane to introduce the hydroxy functional group to give cross-linked poly(4-hydroxystyrene). Hydrolysis was carried out in a reaction flask with stirring at room temperature for 48 hours. Pure white polymer beads (~0.1g) were separated from the storage solvent by centrifugation and then transferred to the reaction vessel containing 0.5M sodium hydroxide in 50% aqueous 1,4-dioxane (30 mL). Care had to be taken since the microspheres were very soft and easy to break in the completely swollen stage in the solution. The reaction was visually observed to be complete when the beads became light white-pink. At this point the beads were strengthened by neutralizing the deprotonated

hydroxy group with 2M sulfuric acid. The products were alternately separated from the solution by centrifugation and then re-suspended and washed in distilled water four times at 3400 rpm for 5~10 minutes to yield poly(4-hydroxystyrene) microspheres.

Poly(4-hydroxystyrene) was characterized by its infrared spectrum. The FT-IR spectrum of the hydrolyzed polymer is shown in Figures 3.5,3.6,3.7. There is essentially complete loss of the sharp carbonyl (C=O) absorption band at 1758 cm^{-1} accompanied by an increase in the O-H absorption band at 3440 cm^{-1}. This shows that the hydrolysis procedure is very efficient.

3.3.4.2 Nitration of Poly(4-hydroxystyrene)

Poly(4-hydroxystyrene), a polar vinyl polymer, exhibits important characteristic properties. Many derivatization reactions can be carried out on this polymer.[72] Electrophilic substitution reactions on the aromatic ring in poly(4-hydroxystyrene) are restricted to the position *ortho* to the hydroxyl group. Since there are two *ortho* positions on the aromatic ring, theoretically both mono- and di- nitrophenol derivatives are possible. The calculated nitrogen content for mono-nitrophenol, poly(3-nitro-4-hydroxystyrene) is 8.46 % and for di-nitrophenol, poly(3,5-dinitro-4-hydroxystyrene) is 13.3 %.

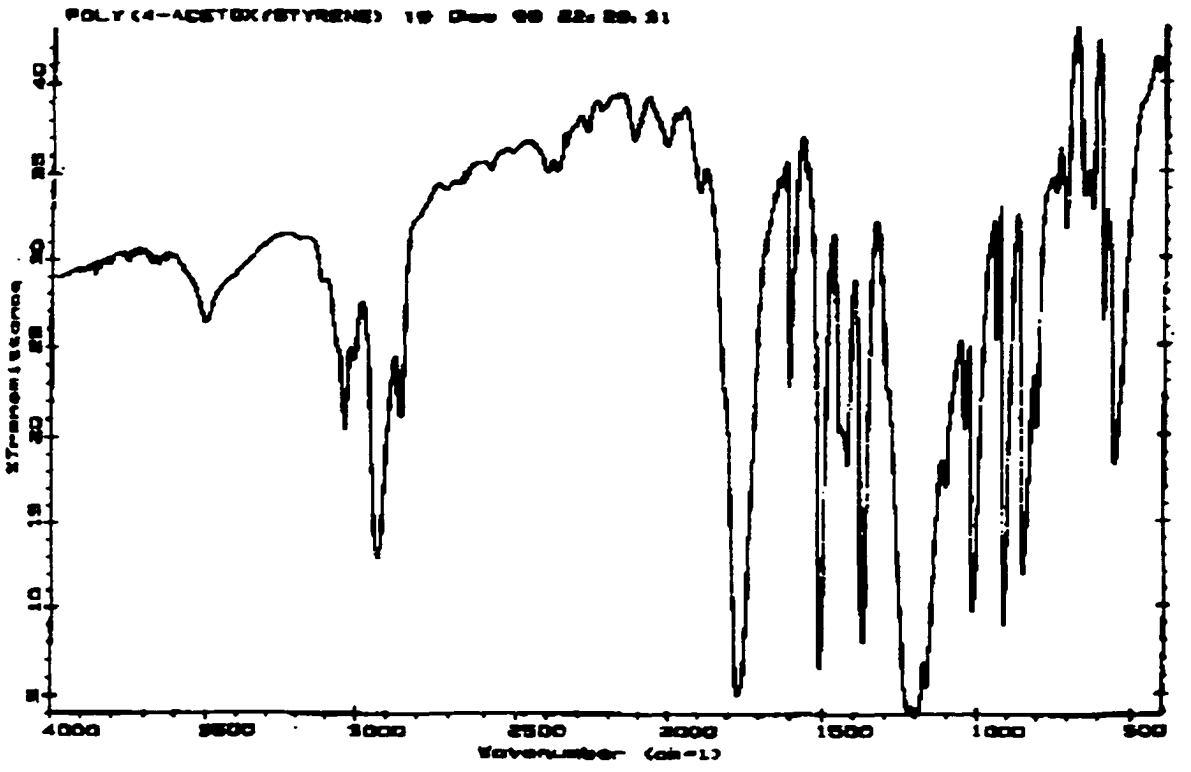

Figure 3.5 FT-IR spectrum of poly(4-acetoxystyrene) microspheres prepared by dispersion polymerization

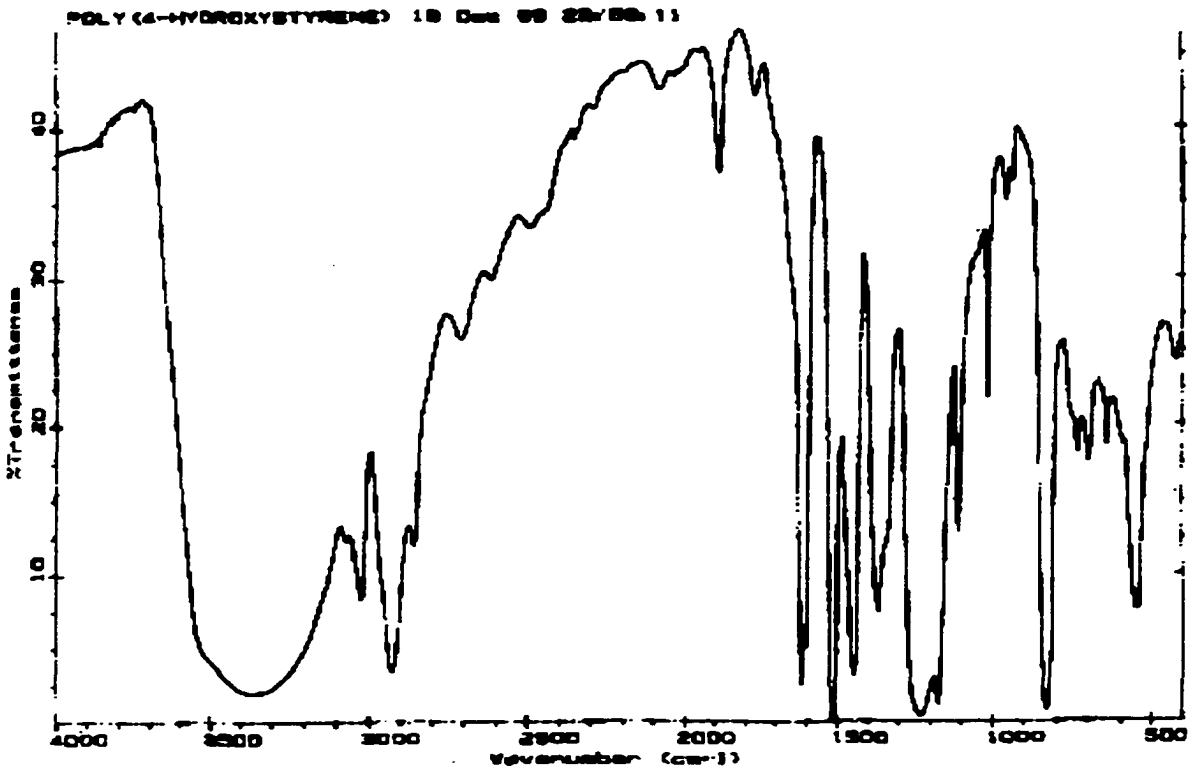

Figure 3.6 FT-IR spectrum of poly(4-hydroxystyrene) microspheres hydrolyzed from poly(4-acetoxystyrene)

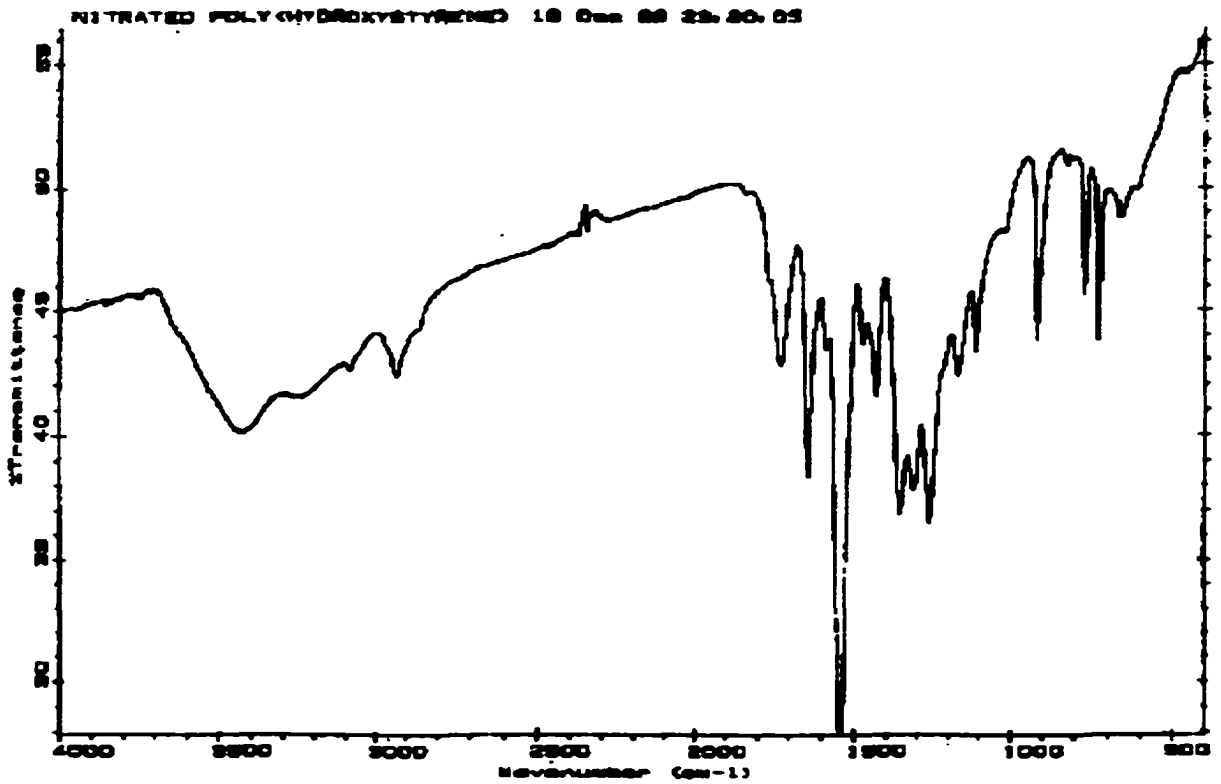

Figure 3.7 FT-IR spectrum of nitrated poly(4-hydroxystyrene) microspheres derivatized from nitration of poly(4-hydroxystyrene)

The nitration reaction was carried out by adding the poly(4-hydroxystyrene) microspheres (~0.1g) to differing concentrations of nitric acid (30 mL), with stirring, at various temperatures depending on the degree of nitration desired. The beads were separated from the reaction solution by centrifugation and then washed repeatedly with distilled water and ethanol. The final polymer beads were bright yellow. They swell in basic media and shrink in acidic media. Figure 3.8a and Figure 3.8b shows the schematic bead pictures with functional groups and the derivatization reactions.

Nitrated poly(4-hydroxystyrene) was characterized by CHN analysis and by determining the pK_a value, which will be discussed in the following chapter. The results showed that at room temperature in concentrated nitric acid, the highest N % was 8.98. It was clear that mono-nitrophenol was predominantly obtained although there was some di-nitrophenol present. With controlled temperature pure mono-nitrophenol can be obtained at 0°C. The percentage of CHN vs. the time of the nitration reaction is shown in Figure 3.9.

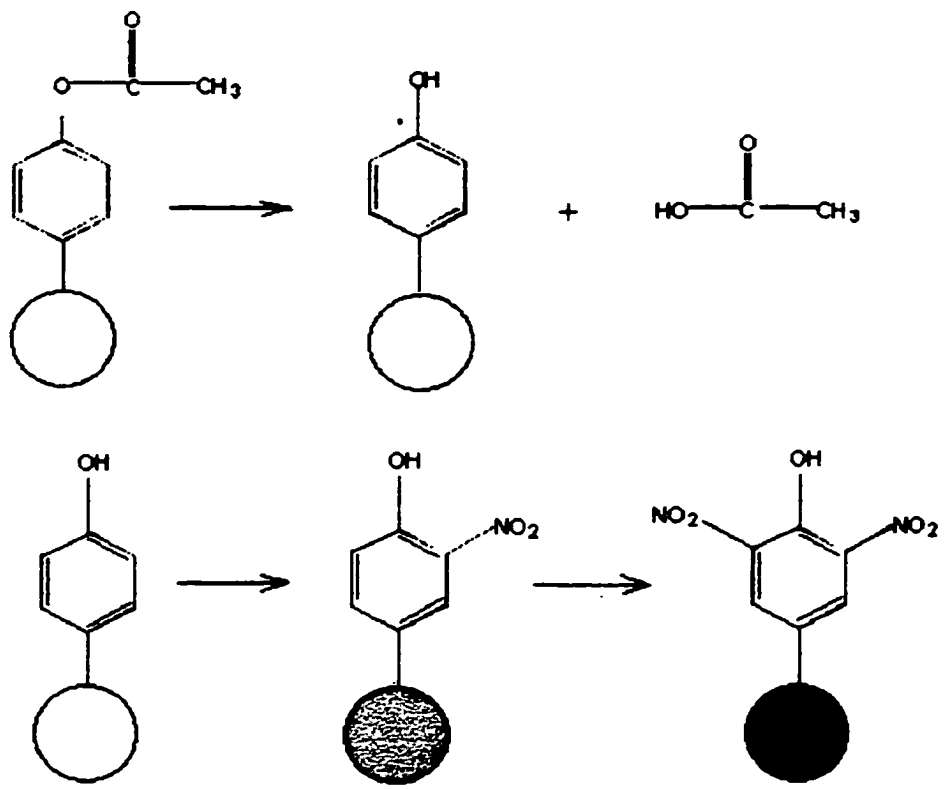

Figure 3.8 a Schematic PNHS and PDNHS bead pictures with functional groups

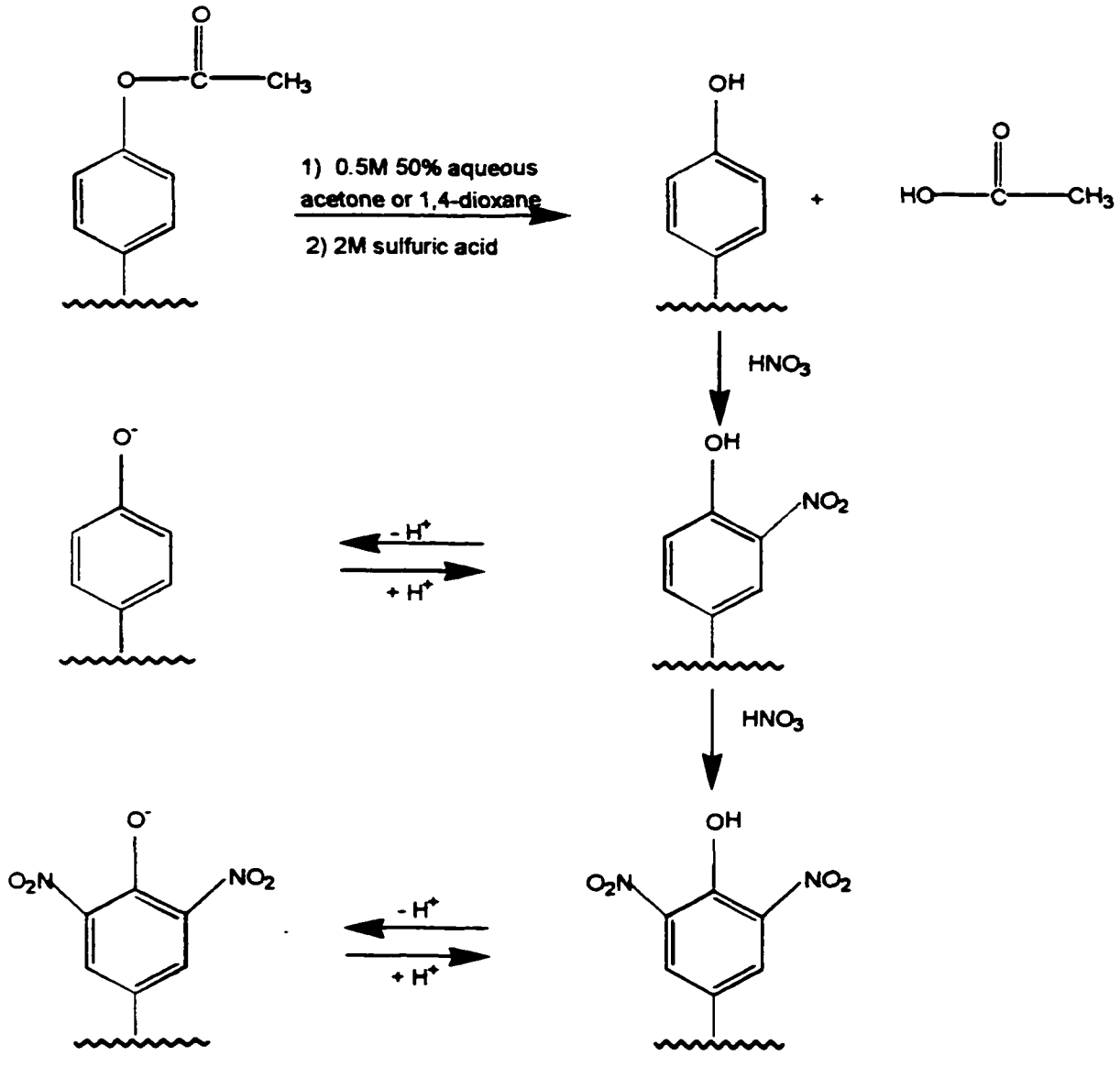

Figure 3.8 b The derivatization reactions of poly(4-acetoxystyrene)

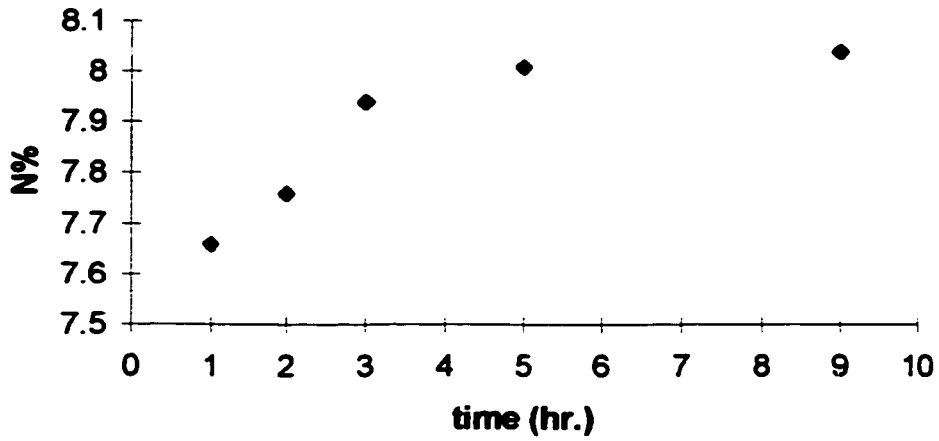

Figure 3.9 N% vs. time during the nitration reaction at 0^0C for nitrated poly(4-hydroxystyrene) microspheres prepared by dispersion polymerization

3.3.5 Results and Discussion

The ability to control microsphere size and size distribution has been one of the most distinctive features of dispersion polymerization. The type of stabilizer, the molar mass and concentration of the stabilizer, the concentration of monomer, the polarity of the solvent, the temperature, and the initiator concentration can affect the size and monodispersity of microspheres. This part of the work was to optimize the particle size and size distribution.

Polymer microspheres with and without crosslinking have been synthesized. Lightly crosslinked polymers, with 0.5 ~ 2 % DVB were used for the sensing study. Polymers without crosslinking were served as the seeds for the emulsion polymerization.

3.3.5.1 Effect of Solvent

The polarity of the solvent can affect both particle nucleation and the efficiency of the stabilizer. Tables 3-3 and Table 3-4 show the effect of solvent polarity on the size and monodispersity of microspheres. As can be seen from Table 3-4, with the water / ethanol / toluene solvent system, the optimum formulation is 5 vol % AS, 2 wt% DVB (monomer), 22 wt% PVP (monomer), 2 wt% AIBN (monomer) and 1:5:14 toluene / water / ethanol solvent system when ~1 wt% of DB18C6 was incorporated in the formulation. Without DVB and toluene, as shown in Table 3-5, the formula of 5 vol % AS, 22 wt% PVP (monomer), 2 wt% AIBN (monomer) and 1:3 water / ethanol solvent system shows the best results for monodispersed microspheres with sizes of 0.6 and 0.7 μm.

Table 3-3 Dispersion polymerization of 4-acetoxystyrene and DVB with a change of solvent polarity

Batch[a]	Water (%)	Toluene (%)	Average diameter (μm)	Results of polymer
A-1	15	5	0.5 ~ 3.6	Low yield, polydisperse particles
A-D-3	25	5	0.6	Low yield, monodisperse microspheres
AS-D-4	30	5	-	No products, reaction failed
AS-D-5	25	0	0.5 ~ 1.3	low yield, polydisperse microspheres

[a]5 Vol % 4-acetoxystyrene, 2 wt% (monomer) DVB, 22 wt% (monomer) PVP, 2 wt% (monomer) AIBN, ~1 wt% DB18C6, remainder ethanol

Table 3-4 Dispersion polymerization of 4-acetoxystyrene as a change of solvent polarity

Batch[a]	Water (%)	Toluene (%)	Average diameter (μm)	Results of polymer
SP#AS-2	0	0	-	Reaction failed, no products
SP#AS-4	15	5	0.4 ~ 2	Very low yield, aggregated particles
SP#AS-6	15	0	0.3 ~ 2	Low yield, polydisperse microspheres
SP#AS-7	35	0	0.2 ~ 3	Very low yield, coagulated particles
SP#AS-8	20	0	0.4 ~ 0.6	Low yield microspheres
SP#AS-1	25	0	0.6	monodisperse microspheres
SP#AS-9	25	0	0.7	monodisperse microspheres

[a]5 Vol % 4-acetoxystyrene, 0 wt% DVB, 22 wt % (monomer) PVP, 2 wt% AIBN, remainder ethanol

3.3.5.2 Effect of Monomer Concentration

The size of the microspheres prepared in a dispersion polymerization increases with increasing monomer concentration. Normally the monomer is also a solvent for its polymer. The higher the monomer concentration, the higher the solubility of the polymer. However, the role of monomer is complicated during the process of polymerization because monomer consumption changes the character of the solvent. Table 3-5 shows the effect of monomer concentration on the size and monodispersity of microspheres. Figures 3.10~3.13 shows the SEM of the resulting particles. It can be seen that with the 1:3 water / ethanol solvent system, the size of the microspheres increases as the monomer concentration increases (from 5 vol % to 35 vol %). However, only the formulas with 5, 10, 15, and 25 vol% monomer give monodisperse microspheres. At the higher monomer level nucleation occurs over a longer period of time resulting in wider diameter variations.

Table 3-5. Dispersion polymerization of 4-acetoxystyrene as a function of monomer concentrations

Batch[a]	AS[b] Vol%	Water (%)	Toluene (%)	Average diameter (μm)	Results of polymer
SP#AS-1	5	25	0	0.6	Monodisperse microspheres
SP#AS-2	5	0	0	-	Reaction failed, no products
SP#AS-12R	10	25	0	0.75	Monodisperse microspheres
SP#AS-13	15	25	0	1.0	Monodisperse microspheres
AS-M25	20	6	0	-	Aggregated particles
SP#AS-14	20	25	0	0.6 ~ 3	Polydisperse microspheres
SP#AS-15	25	25	0	2.3	Monodispers microspheres
SP#AS-16	30	25	0	1.0 ~ 7.6	Polydisperse microspheres
SP#AS-17	35	25	0	1.0 ~ 6.8	Polydisperse microspheres

[a]0 wt% (monomer) DVB, 22 wt% (monomer) PVP, 2 wt% (monomer) AIBN, remainder ethanol; [b]4-acetoxystyrene

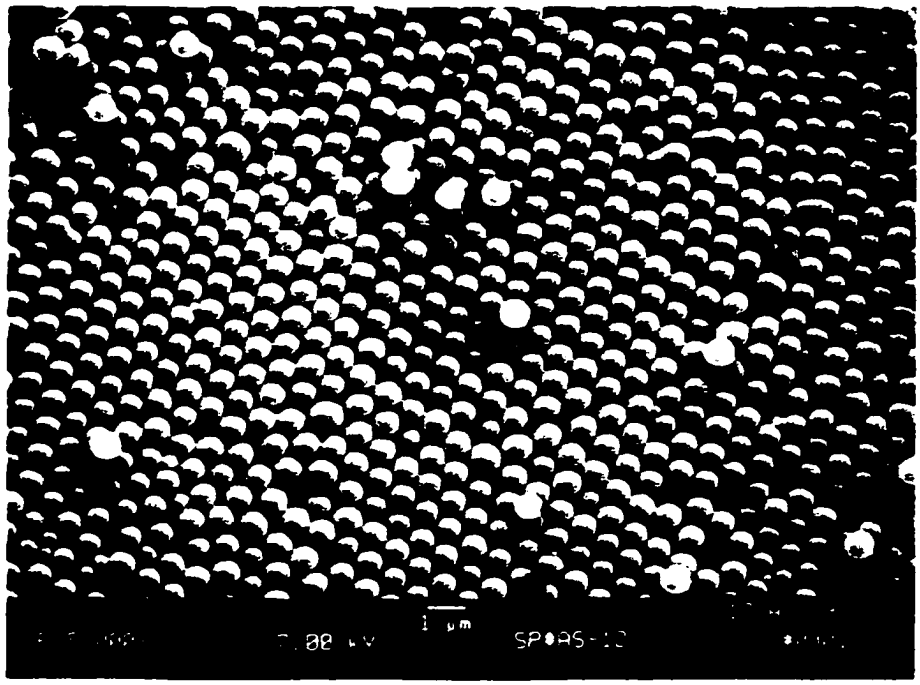

Figure 3.10 Scanning electron micrograph of poly(4-acetoxystyrene) microspheres prepared by dispersion polymerization with 10 mL monomer as listed in Table 3-5

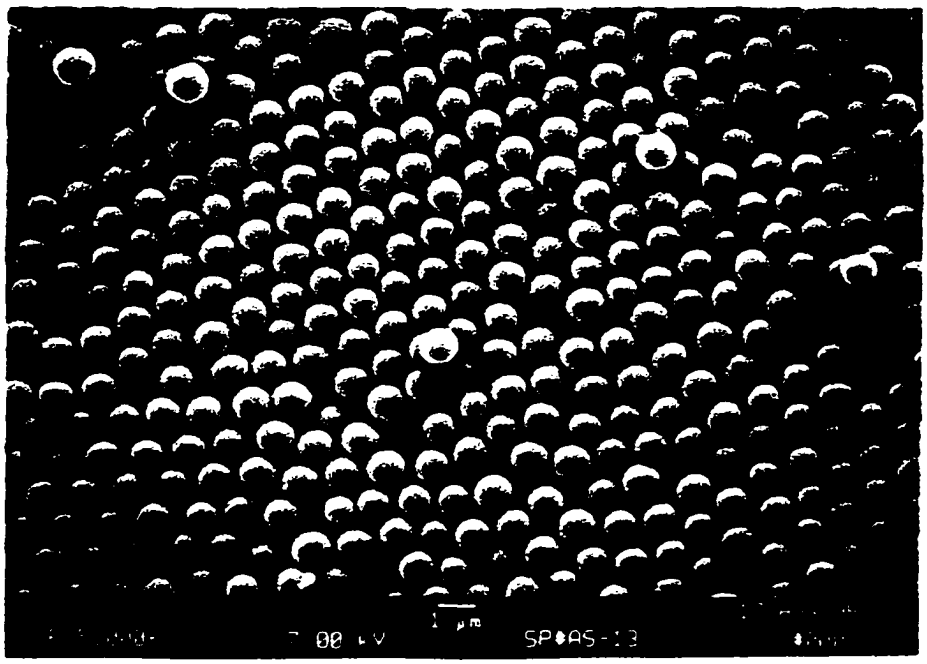

Figure 3.11 Scanning electron micrograph of poly(4-acetoxystyrene) microspheres prepared by dispersion polymerization with 15 mL monomer as listed in Table 3-5

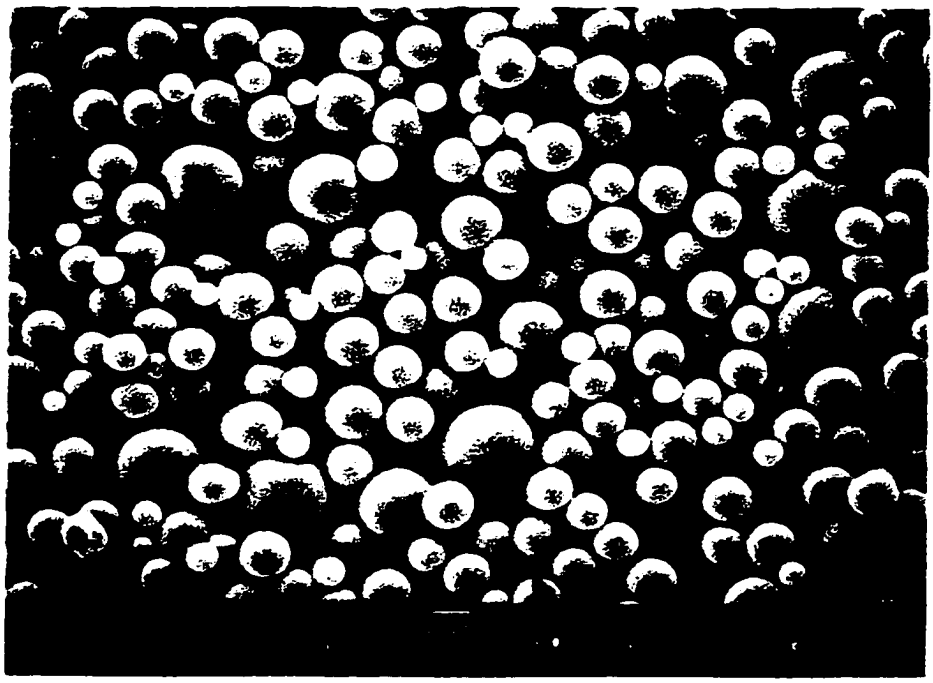

Figure 3.12 Scanning electron micrograph of poly(4-hydroxystyrene) microspheres prepared by dispersion polymerization with 20 mL monomer as listed in Table 3-5

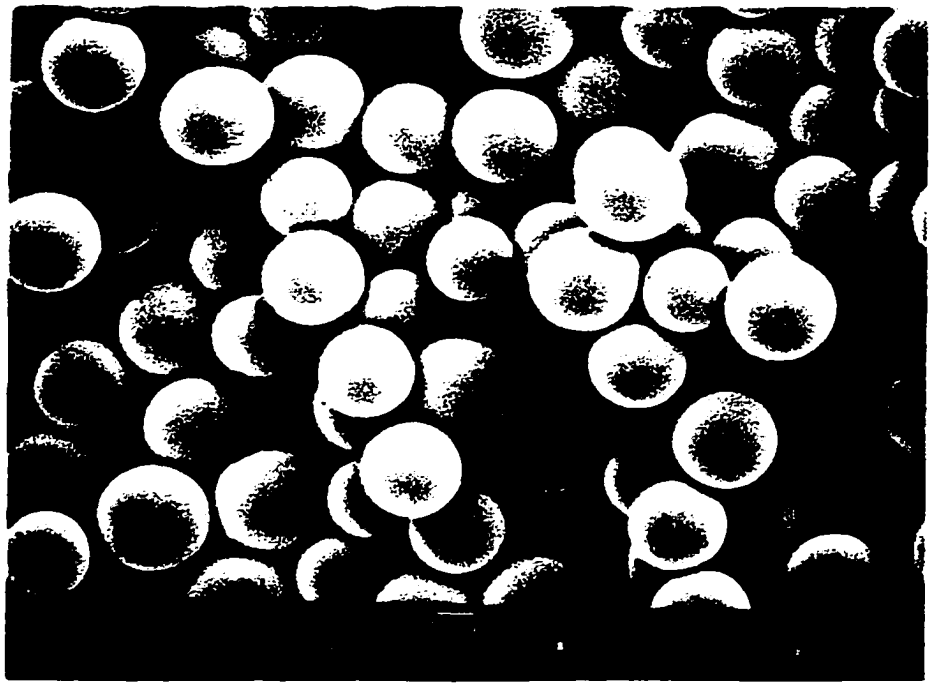

Figure 3.13 Scanning electron micrograph of poly(4-acetoxystyrene) microspheres prepared by dispersion polymerization with 25 mL monomer as listed in Table 3-5

3.3.5.3 Effect of Stabilizer Concentration

A high concentration of stabilizer will stabilize a large surface area. Normally this leads to smaller particles. Ideally larger particles could be obtained by reducing the level of the stabilizer. In practice this was not so simple due to particle aggregation. Table 3-6 shows the effect of PVP stabilizer concentration on the formation of microspheres. The formula with 22 wt% stabilizer was the only one that gave monodisperse particles. Lower levels led to aggregation.

Table 3-6. Dispersion polymerization of 4-acetoxystyrene as a function of stabilizer concentrations

Batch[a]	Water (%)	stabilizer (wt%)	Average diameter (μm)	Results of polymer
SP#AS-1	25	22	0.6	monodisperse microspheres
AS-M15-75	25	8	-	low yield, Aggregated particles
AS-M20-75	25	6	-	high yield, Aggregated particles
AS-M25-75	25	5	-	high yield, Aggregated particles

[a]5 vol % 4-acetoxystyrene, 0 wt% (monomer) DVB, 2 wt% (monomer) AIBN, remainder ethanol

3.3.5.4 Use of 1,2-Bis(p-vinylphenyl)ethane as a Crosslinker

DVB has been the most commonly used crosslinker for styrene based polymers. However, there are two drawbacks with the use of DVB as a crosslinker.[73] One is that commercial DVB consists of four main isomers (*para*- and *meta*-DVB, 50~60 %, and *para*- and *meta*-ethylvinylbenzene, EVB, 35~45 %) for which the reactivities are quite different. The second one is that the activity of the second double bond of DVB is different from that of the first one after it has reacted with the polymer due to the conjugation of the two vinyl groups through the benzene ring. This would lead to

inhomogeneous crosslink distributions. The nonconjugated crosslinker, 1,2-bis(p-vinylphenyl)ethane (p,p-BVPE), [74] is a more desirable crosslinking monomer which can give the same degree of crosslinking as DVB utilizing only half the number of moles. In this work p,p-BVPE was used to prepare polymer microspheres for the purpose of sensing materials and Table 3-7 shows the preliminary results for microspheres prepared using p,p-BVPE. Figures 3.14~3.17 show the SEM of the four batches of beads.

Table 3-7. Dispersion polymerization of 4-acetoxystyrene using p,p-BVPE as a crosslinker

Batch[a]	AS[b] (mL)	BVPE[c] (wt%)	Water (%)	Toluene (%)	Average diameter (μm)	Results of polymer
AS-DS-1	5	0.9	25	0	0.5 ~ 3	low yield, polydisperse microspheres
AS-DS-2	5	0.9	10	0	2 ~ 3	low yield, polydisperse microspheres
AS-DS-3	10	1.8	5	0	3 ~ 4	good yield, polydisperse microspheres
AS-DS-4	7.5	2.4	25	0	0.6	good yield, monodisperse particles
AS-DS-10	10	1.0	25	0	~ 0.2	very low yield, Aggregated particles
AS-DS-15	15	1.0	25	0	~ 0.5	low yield, polydisperse particles
AS-DS-20	20	1.0	25	0	-	no products, soluble polymer?
AS-DS-T-10	10	1.0	25	5	0.7 ~ 0.8	high yield, monodispers particles
AS-DS-T-15	15	1.0	25	5	~ 0.8	good yield, microspheres
AS-DS-T-20	20	1.0	25	5	0.9 ~ 1.0	good yield, microspheres

[a]22 wt% (monomer) PVP, 2 wt% (monomer) AIBN, remainder ethanol; [b]4-acetoxystyrene; [c]p,p-BVPE wt %

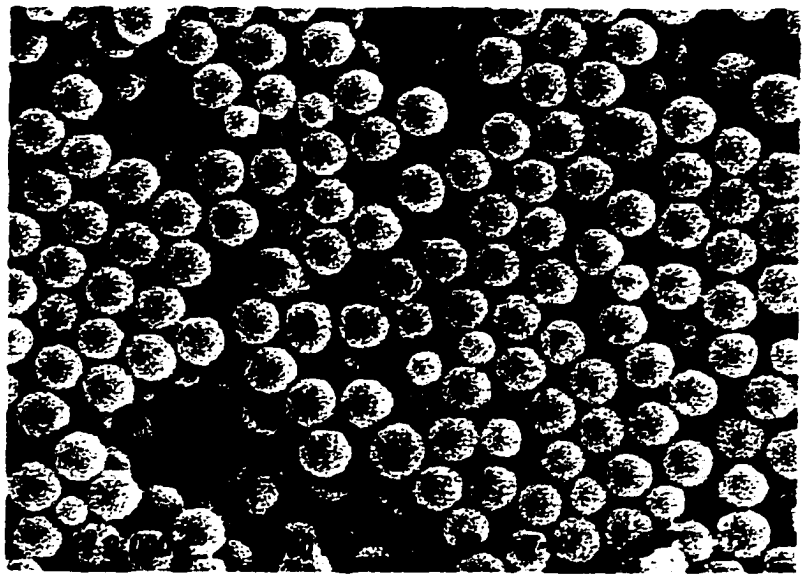

Figure 3.14 Scanning electron micrograoh for AS-DS-T-20 microspheres listed in Table 3-7

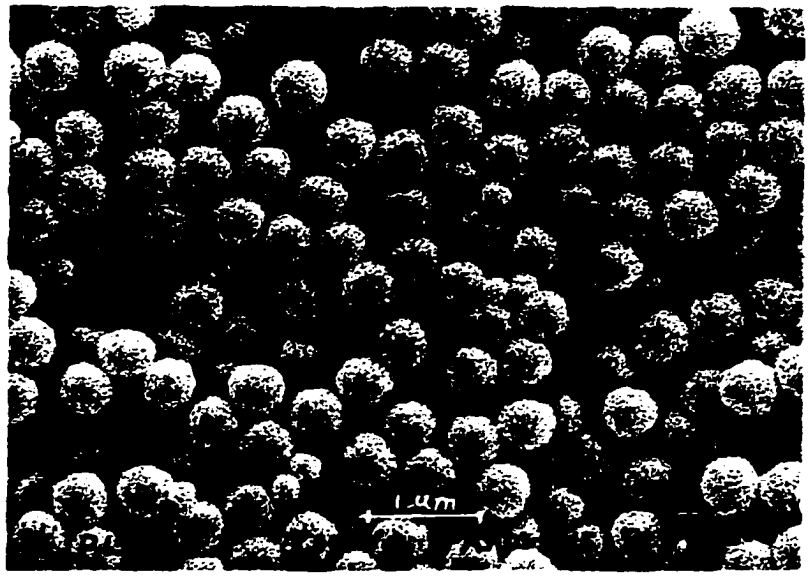

Figure 3.15 Scanning electron micrograoh for AS-DS-T-15 microspheres listed in Table 3-7

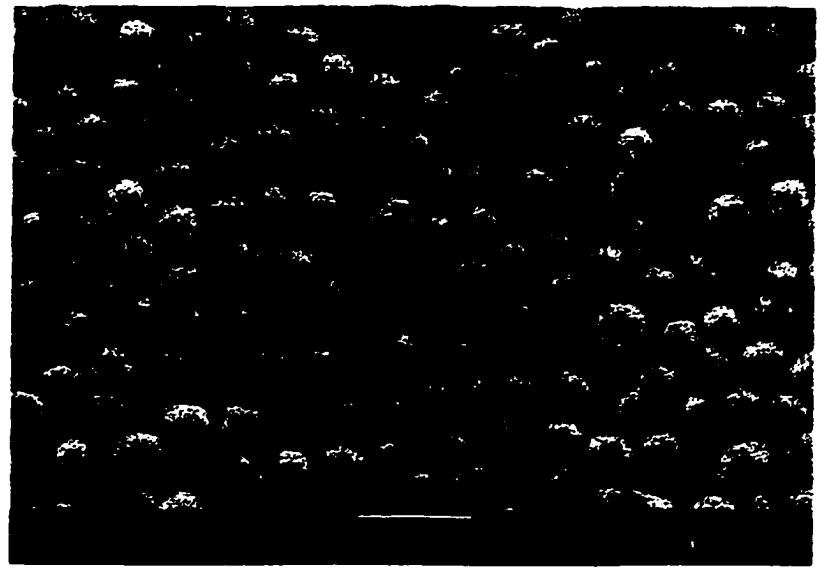

Figure 3.16 Scanning electron micrograoh for AS-DS-15 microspheres listed in Table 3-7

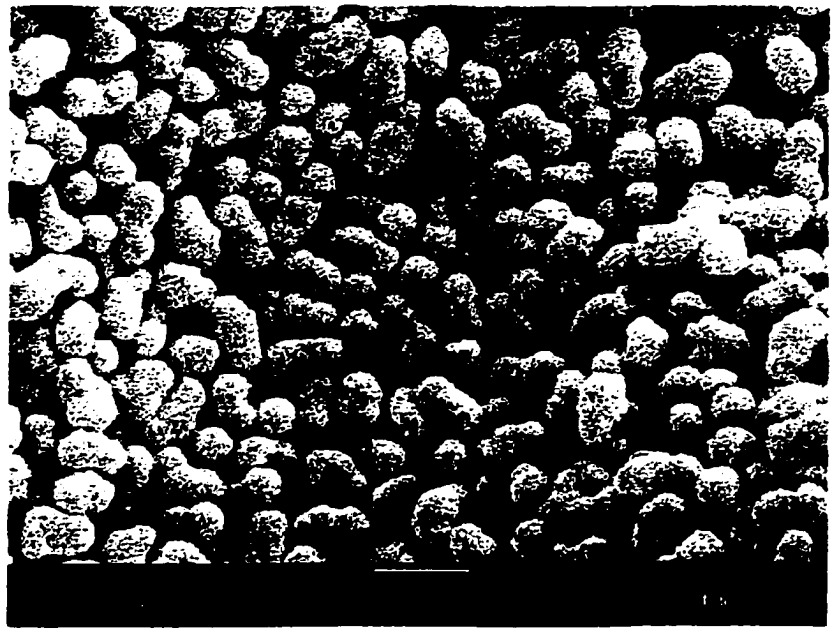

Figure 3.17 Scanning electron micrograoh for AS-DS-4 microspheres listed in Table 3-7

As can be seen, Figures 3.14 and 3.15, the formulation with 1 wt % p,p-BVPE and 5 % toluene, gave better results than those without toluene. Without toluene most of the batches did not produce satisfactory particles as a result of solvent polarity effect on the crosslinker. The microspheres obtained with 1 wt % p,p-BVPE and 5 % toluene are larger than those obtained with DVB as the crossliker. Figures 3.16 and 3.17 show that nonspherical particles formed without adding toluene.

3.3.5.5 Study of Acetoxystyrene and 2,4,5-Trichlorophenylacrylate Copolymer System

The copolymer of acetoxystyrene (AS) and 2,4,5-trichlorophenylacrylate (TCPA) opens the possibility of increasing the hydrophilicity of the polymer backbone. Table 3-8 shows the preliminary work.

Table 3-8. Dispersion polymerization of 4-acetoxystyrene- 2,4,5-trichlorophenylacrylate copolymer

Batch[a]	AS[b] mol%	TCPA[c] mol %	Water (%)	Toluene (%)	Average diameter (μm)	Results of polymer
AST-1	50	50	15	5	-	high yield, Aggregated particles
AST-2	50	50	20	5	~ 0.5	Aggregated particles
AST-3	50	50	25	0	~ 0.5	high yield, Aggregated particles

[a]1:1 4-acetoxystyrene : 2,4,5-trichlorophenylacrylate, 2 wt% (monomer) DVB, 22 wt% (monomer) PVP, 2 wt% (monomer) AIBN, remainder ethanol; [b]4-acetoxystyrene; [c]2,4,5-trichlorophenylacrylate

It is obvious that these two monomers are not really compatible. Perhaps this is due to the difference in the reactivity between the two monomers. Further investigation will be needed if the use of TCPA to increase the hydrophilicity is desired.

3.4 Preparation of Particles by Seeded Emulsion Polymerization

Results have shown that polymer microspheres prepared by dispersion polymerization for pH sensing have the disadvantages of low response and a long response time. In addition, particle diameters less than 1 μm are smaller than desired for remote sensors especially for use in the near IR region. Therefore, it was necessary to find a new method to prepare larger particles with more and larger pores to enhance response and decrease the response time. Therefore, a new approach with the use of monodisperse seed particles for the preparation of monodisperse acetoxystyrene-divinylbenzene copolymer particles via seeded emulsion polymerization was investigated.

3.4.1 Reagents

Sodium dodecyl sulfate (SDS) and poly(vinyl alcohol) (PVA, MW 14,000 and 85,000 - 146,000) were purchased from Aldrich Chemical Company. Other chemicals such as toluene, 1,4-dioxane, 4-acetoxystyrene (AS), styrene, vinyl benzyl chloride (VBC), 2,2'- azobisisobutyronitrile (AIBN), glutaraldehyde, divinylbenzene (45-55 % active, 2:3 meta/para) were purchased from the same sources as described from the previous section. Acetone, methanol, ethanol, and all other chemicals (reagent grade) such as salts, bases and acids were directly used without further purification. Doubly deionized water was used for all the preparation of aqueous solutions.

3.4.2 Apparatus

The reaction apparatus for seeded emulsion polymerization is similar to that used for the dispersion polymerization except for the design of the stirrer. As shown in Figure 3.18, it consists of a 500 mL, three-necked round-bottom reaction flask, an overhead stirrer motor with a stirring rod equipped with 90^0 paddles, and a nitrogen inlet. The swelling process for the seed particles took about 48 hours with constant stirring at a rate of 400 rpm. The seeded polymerization reaction was initiated by raising the temperature to 70 ^{0}C and carried out at this temperature in a water bath. A Branson 1210 Sonicator was used before and after polymerization for the purpose of preparing homogeneous monomer solutions and breaking agglomerated microspheres to re-suspend them in the reaction solution as well as in the solvents used for washing stage. A Fisher Scientific Model 228 Centrifuge was used to separate particles from reaction solutions or solvents. Particle diameters and size distribution were analyzed by an Amray Model 3300FE Scanning Electron Microscope (SEM). A Perkin-Elmer Model 2400 was used for CHN analysis in order to determine the relative amounts of poly mono- and di- nitrophenol and a Nicolet 205 FT-IR spectrometer was used to confirm that the polymer had been derivatized.

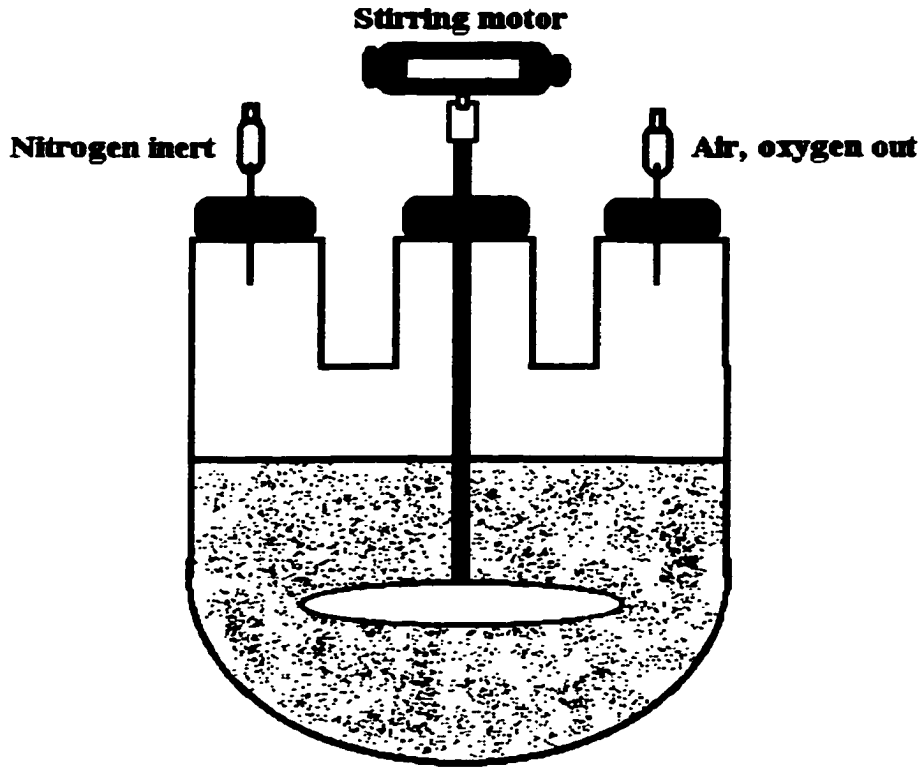

Figure 3.18 Schematic of seeded emulsion polymerization apparatus

3.4.3 Polymer Synthesis

3.4.3.1 Preparation of Seed Particles

Seed particles were synthesized by dispersion polymerization in an ethanol / water / toluene solvent system which is similar to the one described previously except that no crosslinker or a very low crosslinker concentration was included in the monomer solution. Polymerizations were carried out in a reaction vessel containing the homogeneous monomer solution with stabilizer, initiator, water-ethanol mixed solvent, and monomer respectively. The mixture was sonicated for ~10 minutes and then stirred for ~20 minutes until a clear homogeneous solution formed. A nitrogen blanket was applied before the reaction began and continued for 30 minutes after the reaction started to exclude air. The

flask was suspended in a water bath maintained at 70°C with a magnetic stirrer at a constant stirring rate. The desired amounts of solvents (ethanol and water), monomer (4-acetoxystyrene), stabilizer (PVP) and initiator (AIBN) were placed into the reaction flask and magnetically stirred. Polymerization was allowed to continue for about 5 hours. The average size of the microspheres that formed was from 0.5 to 2.5 μm. Table 3-9 gives the basic recipe for the formation of polymer seed microspheres. This is similar to the dispersion polymerization described earlier except that no crosslinker or toluene is included.

Table 3-9. A basic recipe for polymer microspheres based on dispersion polymerization

Ingredient[a]	Name	Amounts
Monomer	4-acetoxystyrene	10 mL
Stabilizer or Surfactant	Polyvinylpyrrolidone	22 wt% to monomer
Initiator	2,2'- azobisisobutyronitrile	2 wt% to monomer
Solvent I	Ethanol	140 mL
Solvent II	Water	50 mL

[a]The amount of solvent and monomer are subject to variation from formulation to formulation for the purpose of producing different size seed particles.

After polymerization the seeds were separated and washed with the same procedure as indicated previously for dispersion polymerization. Again a small portion of the beads was air dried overnight for SEM analysis and the remainder were kept in 95% ethanol or methanol for seeded emulsion polymerization reactions.

3.4.3.2 Preparation of Microspheres by Seeded Emulsion Polymerization

3.4.3.2.1 Pre-Swelling of Seed Particles

Normally there is one swelling step with seeded emulsion polymerization. Seed particles are directly swollen in their emulsified monomer mixture before polymerization. In this work pre-swelling of seed particles was used to enhance the swelling process. The uncrosslinked or very lightly crosslinked seed particles (0.7 μm in diameter or less) from the dispersion polymerization were activated before swelling in their monomers. Seed dispersions were preswollen by constantly stirring the suspension with an overhead stirrer at room temperature for 48 hours. The seed dispersion solution included known amounts of poly(4-acetoxystyrene) seed particles, 1.5:1 water /acetone mixed solvent, and emulsifier, SDS, (0.25% wt/vol). Acetone was used as the pre-swelling solvent. The "activated" seed particles were then used in the next step without separation.

3.4.3.2.2 Swelling of Seed Particles in an Emulsified Monomer Mixture

A mixture of 5 mL 4-acetoxystyrene, DVB (2 wt % of monomer), 2 mL toluene, and AIBN (1 wt % of monomer) (Table 3-10) was emulsified in 5 mL of 0.25 wt % aqueous SDS, 20 ml of 5 wt % PVA (MW 85,000-146,000, 88% hydrolyzed) solution by sonicating for 20 minutes to ensure that the emulsified droplets were small enough to be easily transferred to the seed particles. Poly(vinyl alcohol) prevented particle coagulation during the polymerization process. The emulsified droplet suspension was then carefully added to the aqueous dispersion of the pre-swollen seed particles and stirred continuously for another 24 hours at room temperature in order for the emulsified ingredients to transfer into the seed particles by the absorption of the emulsified monomer mixture. Toluene was added as a porogenic solvent to produce microporosity in the polymer beads.

Table 3-10. Typical polymerization recipes for 1.1 μm-diameter monodisperse porous polymer particles by seeded emulsion polymerization

Ingredient	Amounts
Poly(4-acetoxystyrene) seed particles (0.6 μm-Diameter)	0.4 g
Acetone	10 mL
SDS (0.25 wt%)	30 mL
DI water	25 mL
4-acetoxystyrene	5 mL
DVB	222 μL
Toluene	2 mL
PVA (5 wt%)	20 mL
AIBN	0.106 g

3.4.3.2.3 Synthesis of Monodisperse Porous Poly(4-acetoxystyrene) Microspheres

Nitrogen was bubbled through the dispersion of the swollen particles in the aqueous phase for 20 minutes at room temperature. The reaction was initiated by increasing the temperature to 70 ^{0}C and was completed in 24 hours. The reaction solution was transferred into a large beaker, and the beads were decanted repeatedly with deionized water and then with 95% ethanol until the supernatant became clear. The beads were washed repeatedly with methanol by centrifugation at 3400 rpm for 5-10 minutes and then kept in methanol for at least 48 hours to remove the porogenic solvent and other residual organic materials. This process was expected to result in the formation of a microporous structure on the polymer particles. A small portion of the beads was air dried overnight for SEM analysis and the remainder were used for further derivatization. Table 3-11 and Figure 3.19~3.24 (SEM) show the results from six experiments. It can be seen that the growth of particles was approximately equal to or less than a factor of two in diameter for all six experiments.

Table 3-11 Results for the preparation of monodispersed polymer microspheres by seeded emulsion polymerization

Ingredient[a]	AS-1	AS-1R	AS-11R	AS-12R	AS-13R	AS-14
Seed particles[b](μm)	0.66	0.44	0.50	0.734	0.634	1.14
r.s.d. (%)	(3.97)	(4.8)	(5.94)	(2.47)	(2.6)	(27.6)
AS (mL)	5.0	5.0	5.0	5.0	5.0	5.0
DVB (μL)	111	222	222	222	222	222
Toluene (mL)	0	2	2	3	3	5
AIBN, g	0.253	0.106	0.106	0.106	0.106	0.106
Bead particles[b](μm)	1.25	0.913	0.929	1.32	0.958	1.96
r.s.d. (%)	(19.4)	(8.6)	(10.84)	(4.64)	(36.9)	(47.2)
Growth factor	1.94	2.08	1.86	1.80	1.51	1.72

[a]Pre-swelling was in a mixture of 10 mL acetone, 15 mL water, 25 mL SDS with seed particles; [b]average size with the standard deviation as indicated.

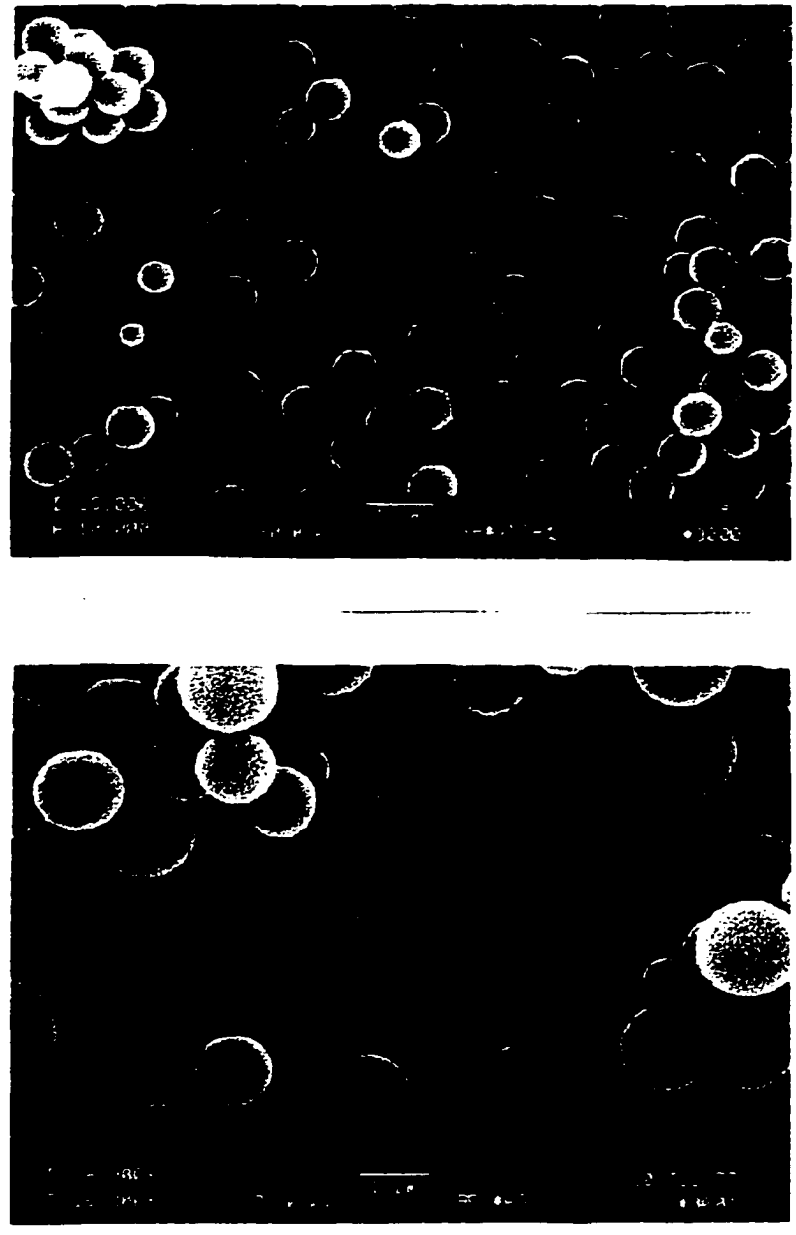

Figure 3.19 Scanning electron micrograph of the seed microspheres (SP#AS-1) (top) and the final microspheres (BP#AS-1) (bottom) listed in Table3-11

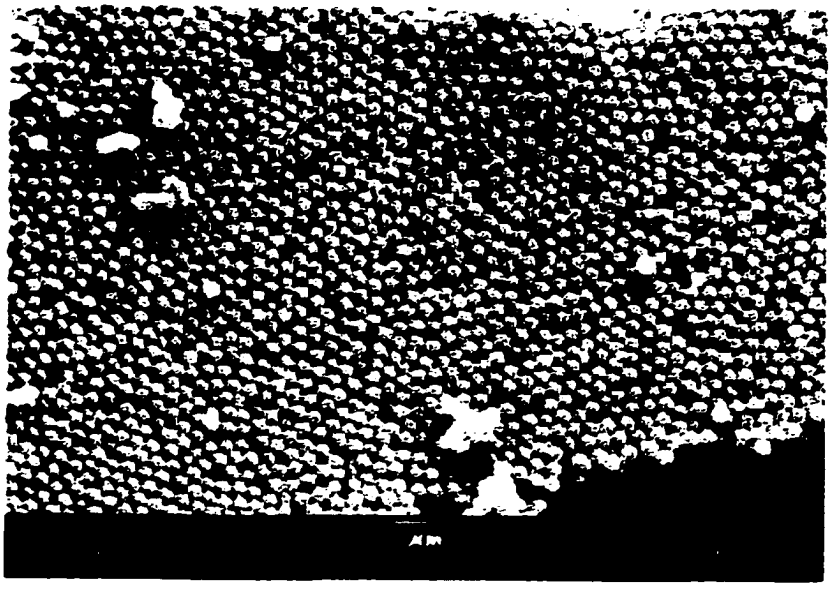

(a)

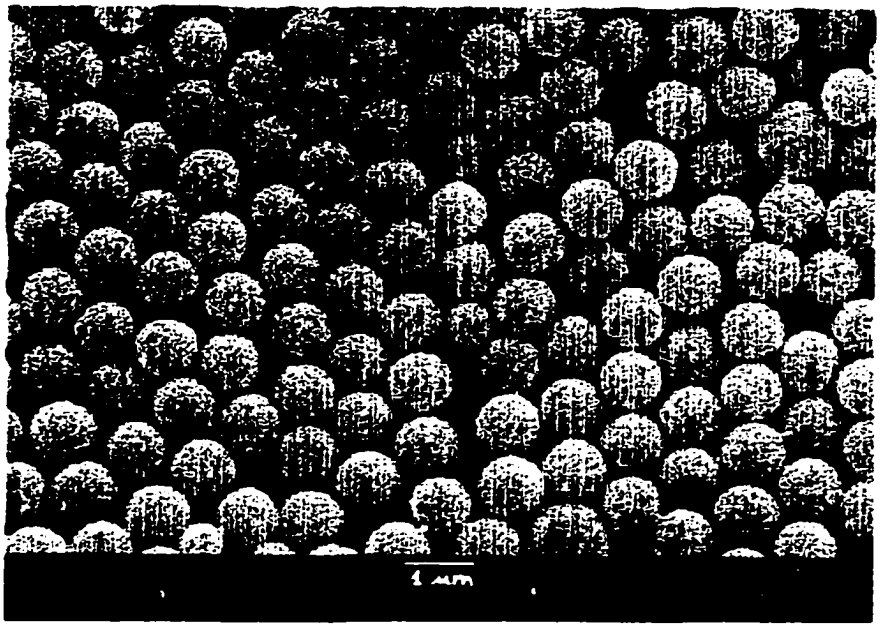

(b)

Figure 3.20 Scanning electron micrographes, (a) the seed microspheres (SP#AS-1R); (b) the final microspheres (BP#AS-1R) listed in Table3-11

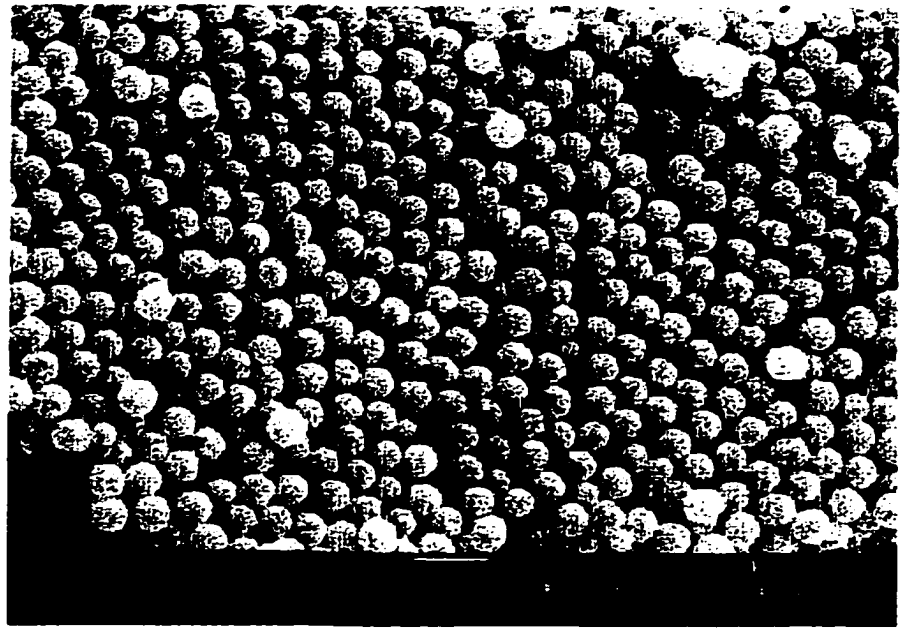

(a)

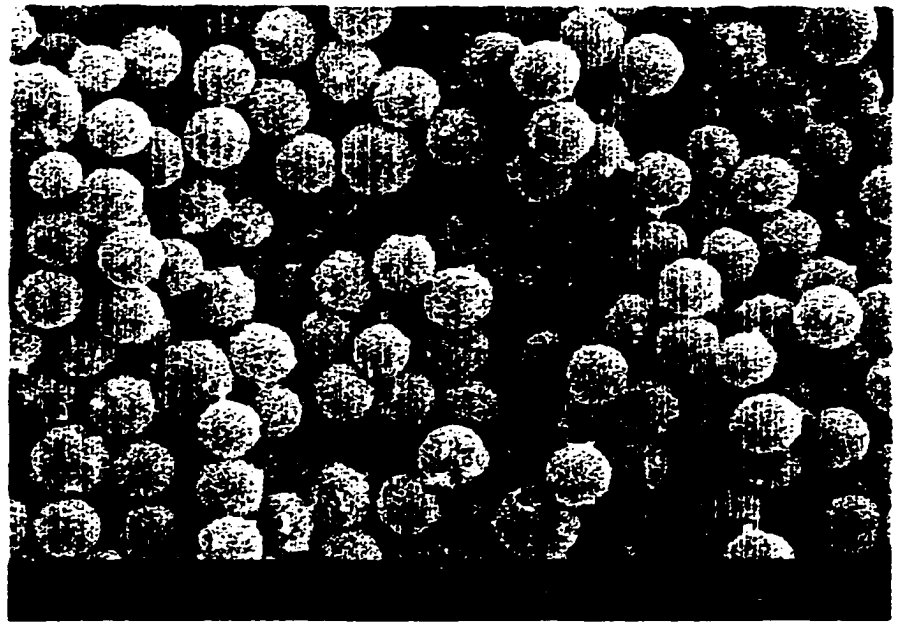

(b)

Figure 3.21 Scanning electron micrographes, (a) the seed microspheres (SP#AS-11R); (b) the final microspheres (BP#AS-11R) listed in Table3-11

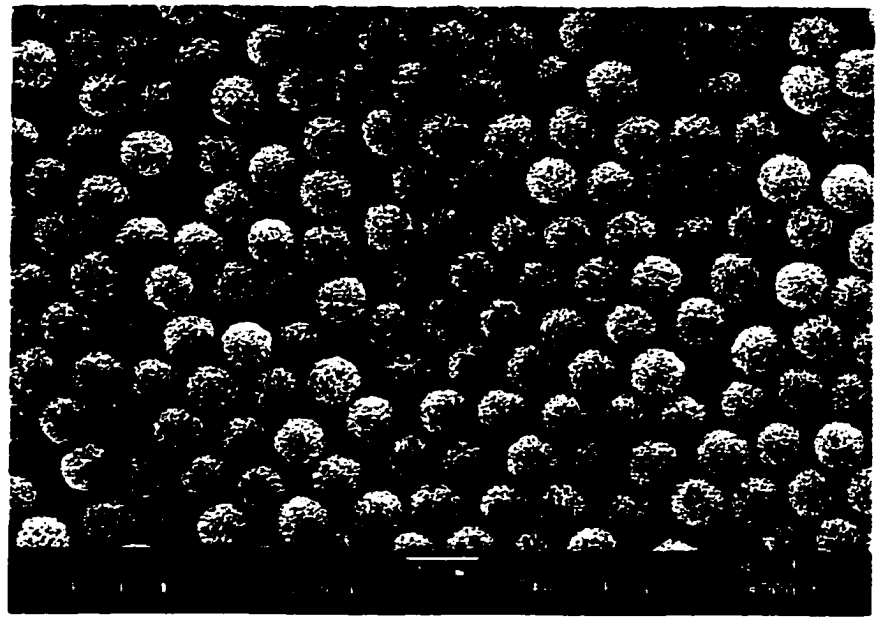

(a)

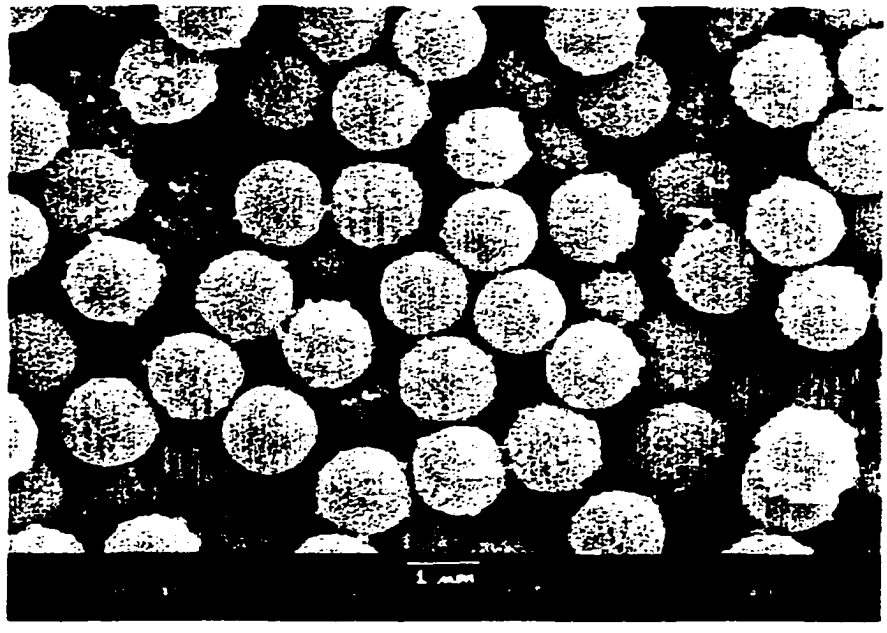

(b)

Figure 3.22 Scanning electron micrographes, (a) the seed microspheres (SP#AS-12R); (b) the final microspheres (BP#AS-12R) listed in Table3-11

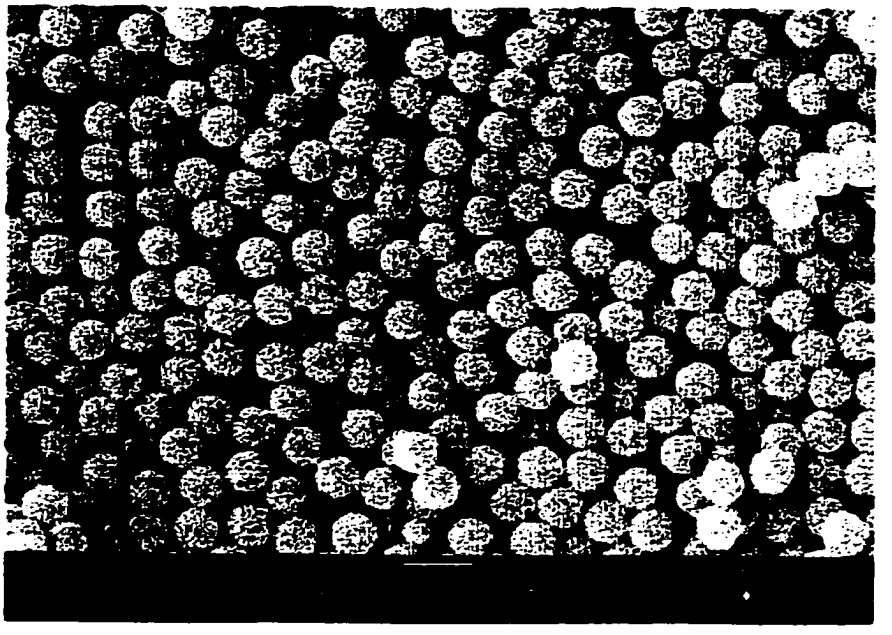

(a)

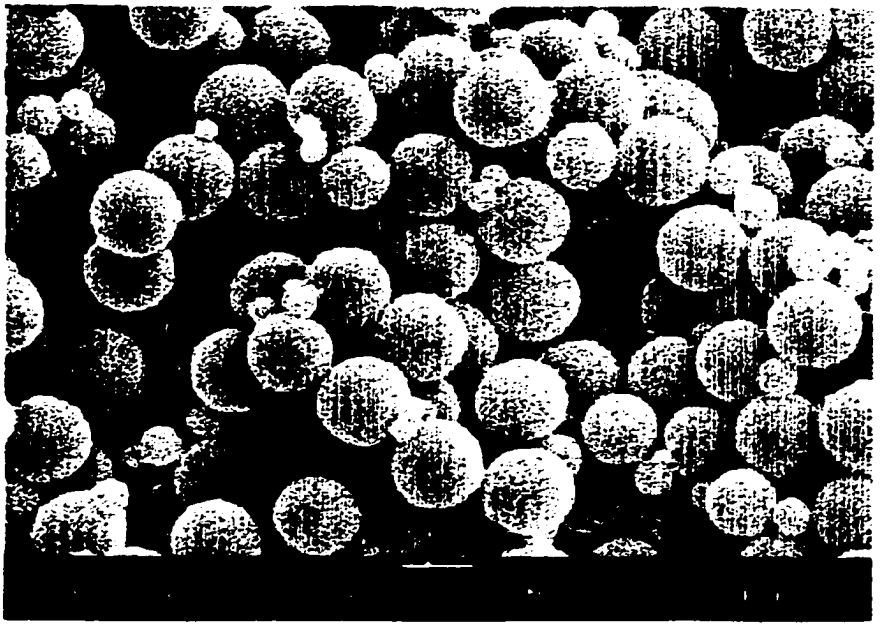

(b)

Figure 3.23 Scanning electron micrographes, (a) the seed microspheres (SP#AS-13R); (b) the final microspheres (BP#AS-13R) listed in Table3-11

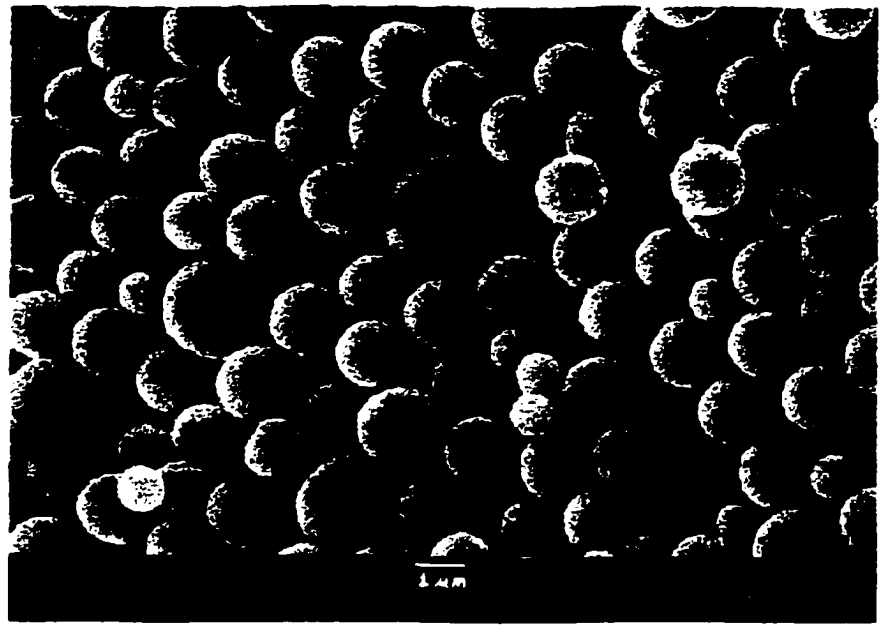

(a)

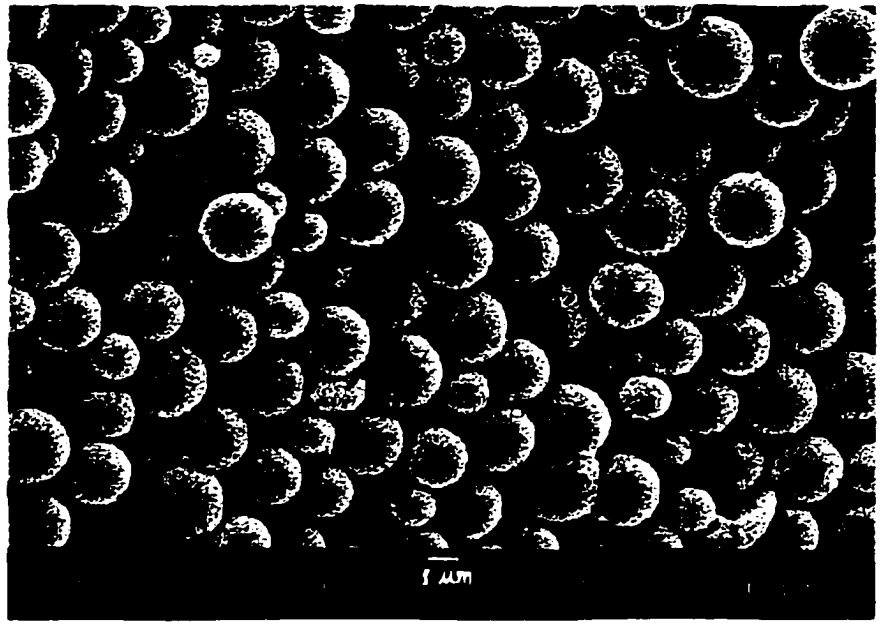

(b)

Figure 3.24 Scanning electron micrographes, (a) the seed microspheres (SP#AS-14); (b) the final microspheres (BP#AS-14) listed in Table3-11

3.4.4 Derivatization

3.4.4.1 Hydrolysis of Poly(4-acetoxystyrene)

The derivatization of 4-acetoxystyrene in alkaline aqueous 1,4-dioxane to form poly(4-hydroxystyrene) was done in the same way as described in the previous section for the dispersion polymerization.

3.4.4.2 Nitration of Poly(4-hydroxystyrene)

It is believed that microspheres synthesized by seeded emulsion polymerization are more porous. The nitration reaction can take place more easily than with the less porous particles prepared by dispersion polymerization. The nitration reaction can go further to introduce the second nitro group to form the di- nitrophenol if the concentration of the nitric acid and temperature for the reaction are properly adjusted. When the reaction was run for three hours at 0^0C with 50 wt % nitric acid, the nitrogen content of the polymer was found to be 7.01 %. This is lower than the theoretical value of 8.48 % expected for the mono-nitro derivative.

Figure 3.25 shows the percentage of nitrogen versus time for one batch of beads. When the reaction was run at room temperature, using concentrated nitric acid for a period of 24 hours, the nitrogen content was found to be 10.44 % which is much higher than that of the mono-nitrophenol but lower than the calculated value of 13.27 % for the di-nitrophenol polymer. This suggests that a mixture of mono- and di- nitrophenol was obtained.

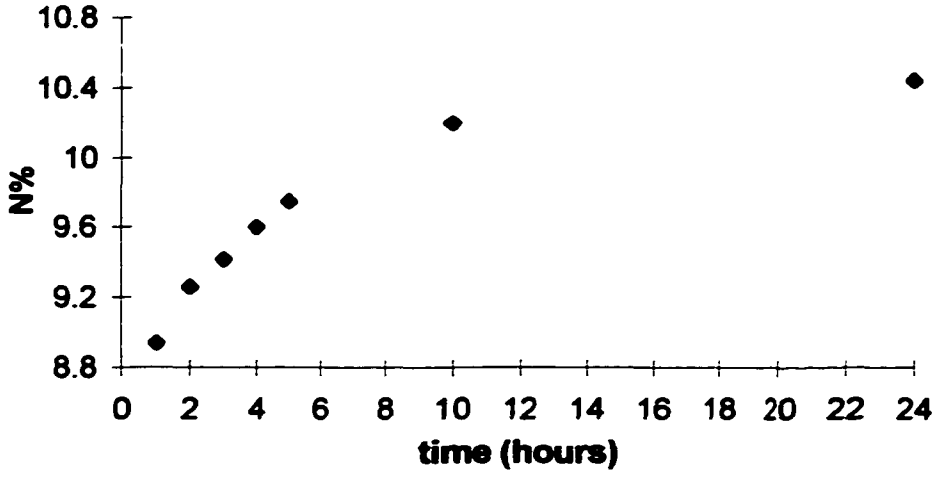

Figure 3.25 Nitrogen content vs. time with the nitration reaction for one batch of beads in concentrated nitric acid at room temperature for 24 hours

3.4.5 Results and Discussion

Seeded Emulsion Polymerization is a technique which has been used for the preparation of monodisperse porous particles. Depending on the application, seed particles can be prepared by emulsifier-free emulsion polymerization, dispersion polymerization, and perhaps by suspension polymerization methods. In this work, seed particles with no crosslinking were prepared by dispersion polymerization. The results, as listed in Table 3-11, showed that the growth of particles was approximately equal to a factor of two in diameter. As will be discussed in Chapter IV and V, these particles showed greatly improved sensing response and response time. Seed particles with light crosslinking and seed particles with a co-monomer were also studied for the purpose of comparison and the results showed that they are not as good as the seeds without the co-monomer and crosslinking.

3.4.5.1 Effect of Crosslinking Seed Particles

Table 3-12 shows the results of experiments in which seed particles with 1 wt % (for BP#AS-1X) and 1.5 wt % (BP#AS-2X) crosslinker were used. Figure 3.26 shows the SEM of one batch of the final particles. As can be seen, polydisperse particles were observed.

Table 3-12. Preparation of bead particles by using crosslinked seed particles

Ingredient	BP#AS-1X[a]	BP#AS-X2[b]
Seed dispersion, mL	AS-X1, 20	AS-X2, 50
AS, mL	9.6	5
DVB (wt %)	2	2
Toluene, mL	0	0
PVA (5 % wt / vol.), mL	20	20
SDS (0.25%, wt / vol.), mL	10	10
AIBN (wt%)	2	2
Deionized water, mL	10	10
Particle feature, diameter μm	polydp. 0.5~6.5	Aggregated particles

[a] First pre-swollen in 20 mL seed dispersion along with 10 mL acetone, and 20 mL deionized water; [b] first pre-swollen in 50 mL seed dispersion along with 10 mL acetone, and 20 mL DI water.

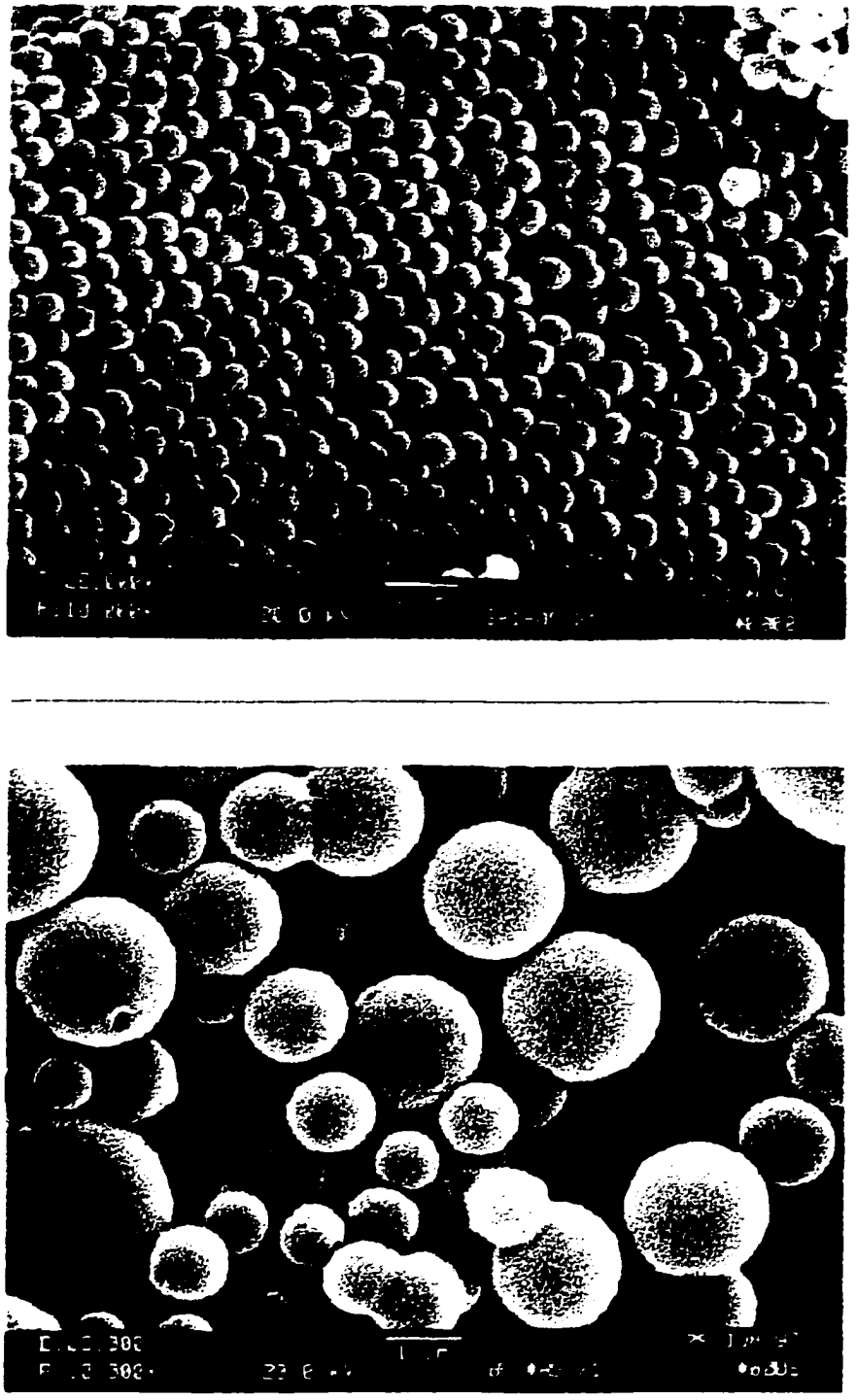

Figure 3.26 Scanning electron micrographes, (a) the seed microspheres (SP#AS-1X) with 2 % DVB (top); (b) the final microspheres (BP#AS-1X) (bottom) listed in Table3-12

3.4.5.2 Effect of Co-Polymer Seed Particles

Table 3-13 shows the results of experiments in which seed particles with 50 mole % of styrene was used as a co-monomer with 4-acetoxystyrene. Figure 3.27 shows the SEM of one batch of the final particles. Again, polydisperse particles were observed due to the polydisperse seed particles.

Table 3-13. Preparation of bead particles using co-polymer seeds

Ingredient	BP#AS-S-0[a]	BP#AS-S-1[b]
Seed dispersion, mL	AS-S-0, 10	AS-S-1, 10
AS, mL	5	10
DVB (%, wt), μm	2	2
Toluene, mL	2.5	3
$NaNO_2$, g	0.06	0.12
PVA (5 % wt / vol.), mL	20	20
SDS (0.25%, wt / vol.), mL	7.5	7
AIBN (wt %)	2	2
deionized water, mL	15	15
Particle feature, diameter μm	two avg. sizes: 2.1, 6.2	partial dissolved shelf and some huge particles

[a,b] Pre-swollen in 10 mL seed dispersion along with 10 mL SDS, 10 mL acetone, and 20 mL deionized water.

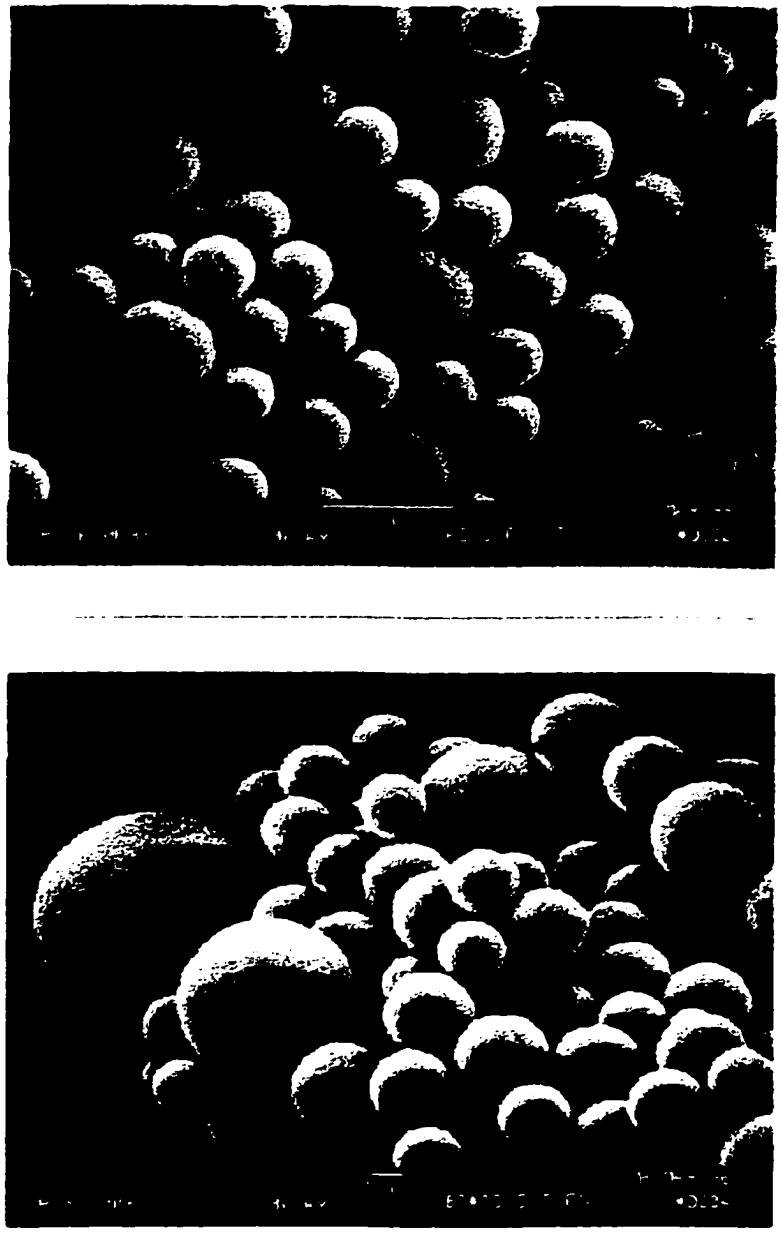

Figure 3.27 Scanning electron micrographes, (a) the seed microspheres (SP#AS-S-0) with 50 mol % of styrene (top); (b) the final microspheres (BP#AS-S(T)-0) (bottom) listed in Table3-14

3.5 Potential Methods for The Characterization of Polymer Microspheres

The concept of optic chemical sensing described in this work is based on polymer swelling. It would be very helpful if the size change before and after polymer swelling could be determined. If the maximum size of the swollen microspheres could be determined, then the magnitude of the response could be predicted. Porosity is also an important issue. Knowing the morphology of the particles can also help in optimizing and controlling the preparation of polymer microspheres. In this section, the feasibility of evaluation particle properties by atomic force microscopy is considered.

Atomic force microscopy (AFM) has become an increasingly common research tool for many applications in the fields of semiconductors, data storage and magnetic materials, biotechnology and life sciences, plastics and polymers, electrochemistry, and materials and surface characterization.[75]

The ability of AFM to create three-dimentional micrographs with resolution down to the nanometer and Angstrom scales has made it an essential tool for imaging surfaces of different materials. Polymers and organic films are often ideal samples for AFM force studies since they are usually soft enough to be easily indented by the AFM tip forces. The characterization includes the surface morphology, nanostructure, chain packing and conformation, as well as studies of nanomechanical properties, crystallization, surface stiffness and forces.

Figure 3.28 AFM image of the poly(4-acetoxystyrene) dry microspheres

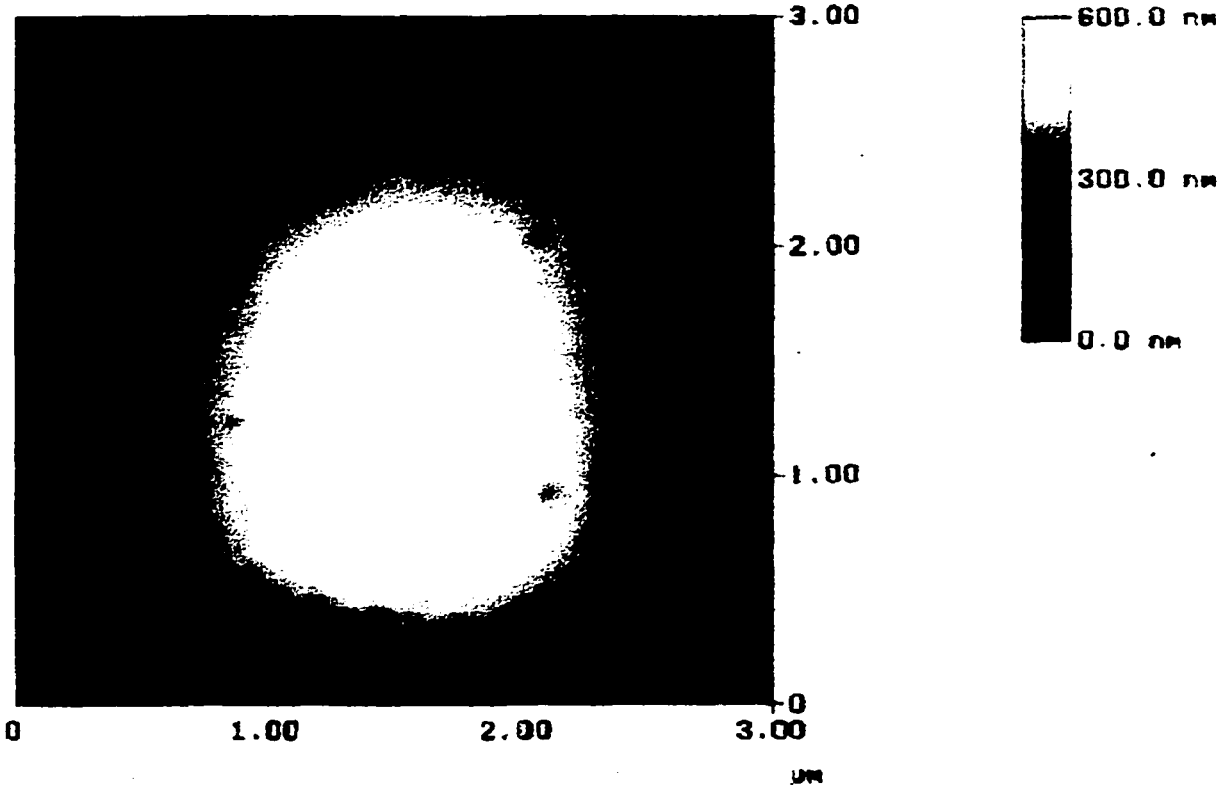

Figure 3.29 AFM image of a single dry poly(4-acetoxystyrene) bead

In this work, preliminary experiments were carried out for size and surface analysis for polymer microspheres. Figure 3.28 shows the image of the poly(4-acetoxystyrene) beads and Figure 3.29 shows the image of a single bead. These images were obtained on dry samples. Images of nitrated poly(4-hydroxystyrene) microspheres in a pH buffer solution were desired, however, due to adhesion problems between the particle and the surface of the slide, this experiment was unsuccessful.

3.6 Conclusions

The results of this chapter indicate that polymer particles can be prepared by suspension, dispersion, and seeded emulsion polymerization methods depending on the purpose of the desired application. Larger particles prepared by suspension polymerization can be used for the preliminary study of the sensing concept due to their ease of handling. Polymer microspheres prepared by dispersion polymerization have been used for chemical sensing purposes. Their main advantage is that there is only a one step polymerization involved. Seeded emulsion polymerization was introduced in this work because of the improvement in the response and response time. As will be discussed in Chapters IV and V, these polymer microspheres showed greatly enhanced response and reduced response times. For the seeded emulsion polymerization method, the seed particles were prepared by dispersion polymerization.

CHAPTER IV

pH SENSING MEMBRANES CONTAINING NITRATED POLY(4-HYDROXYSTYRENE) MICROSPHERES EMBEDDED IN HYDROGELS FOR OPTICAL SENSORS

4.1 Introduction

The potential of polymer swelling as a transduction mechanism for pH sensing has been explored in this research group since 1984.[21-28,30,31,34,76-82] (For more details see chapter I.) Polymer materials were designed to swell and shrink as a function of hydrogen ion concentration. Hydrogen ion binding introduces a positive charge onto the polymer backbone and increases the affinity of the polymer for the external aqueous solution. This results in swelling which leads to an increase in the water content of the polymer and a change in refractive index. In an earlier study we have shown that aminated poly(vinylbenzyl chloride) (poly-VBC) membranes coated on a glass substrate or on the tip of optical fibers respond to pH.[28,30,31,78] At low pH the polymer swells due to the protonation of the amino group causing its refractive index to decrease so that it is closer to the refractive index of the water in the pore space. As a result, the membrane turbidity decreases. However, polymer membranes adhering to a substrate are limited to swelling and shrinking in only one dimension when they are exposed to a solution. Since the

sensing process strongly depends on the swelling of the polymer membrane, the magnitude of the response would be improved if the polymer could swell and shrink in three dimensions. This has been accomplished by formulating the swellable polymer in the form of microspheres and embedding them in a hydrogel.[26, 28,78] The microspheres are free to swell in all directions. This is expected to increase the magnitude of the response and to decrease the response time. Derivatized poly(VBC) microparticles suspended in poly(HEMA) membranes have been studied in this research group.[78] pH sensitive polymer microspheres are embedded in the hydrogel. The use of the hydrogel has several advantages over the previous bulk polymer membrane. First, the membrane acts like a filter to protect the microspheres from direct contact with the sample. Second, the hydrogel is a biocompatible material that can be used for biological applications. Third, the hydrogel is not pH sensitive itself and does not swell or shrink with changes in the hydrogen ion concentration. Last, the hydrogel is mechanically stable, especially the poly(2-hydroxyethyl methacrylate), poly(HEMA), membrane.

This chapter presents research on pH sensitive nitrated poly(4-hydroxystyrene) microspheres embedded in a PVA or poly(HEMA) hydrogel matrix. The goal was to improve the response and decrease the response time of the membranes. The microspheres are synthesized by dispersion or two-step seeded emulsion polymerization methods with light crosslinking and are derivatized to introduce functionality as discussed in the previous chapter. The microspheres are suspended in a hydrogel membrane which has a lower refractive index than the particles. The optical properties of the membrane with the embedded microspheres are affected by both the change in size of the particles and the change in refractive index that accompanies the swelling. For this work the refractive

index change is the dominant effect. The amount of light scattered by the membrane varies with the difference in refractive index between the microsphere and the hydrogel as a function of hydrogen concentration.[28, 78] These properties can be measured either as a change in membrane turbidity or reflectance. The sensor can be interrogated with a light beam of any desired wavelength in the visible or near infrared regions. These membranes allow three-dimension swelling which leads to significant improvement in the magnitude of the response compared to the bulk polymer membranes. The stability test showed that the membranes can undergo multiple swelling and shrinking cycles under high temperature and in sunlight for weeks without degrading mechanically.

4.2 Optical Properties of Polymer Particles Embedded in a Hydrogel

The nature of light scattering in a medium with suspended particles has been discussed in chapter I. As indicated in the Fresnel equation, for normal incidence, $R(\lambda) = (n_2 - n_1)^2 / (n_2 + n_1)^2$, the amount of scattered light is dependent on the squared difference of the refractive indices between the media and the particles. The refractive index is the cause of the intensity change of the reflected light. Scattering is caused by suspended particles and occurs only if the major dimension of the scattering particle is comparable to the wavelength (less than $3 / 2 \lambda$). Larger particles will reflect the light. Scattering is enhanced when the wavelength of the incident radiation is close to the particle size. The intensity of scattered light decreases rapidly when the size of the particle is smaller than the incident wavelength. Kaval showed that using ~ 0.5 μm particles, the membrane turbidity decreases by a factor of five when scanning from wavelengths of 400 to 1000 nm.[27] On the other hand, the scattered light is less affected by wavelength changes when

the particle diameters in a membrane are larger than the incident radiation. In order to develop membranes for remote sensing applications in the NIR region, relatively larger particles are needed for a measurable response. In this work both large and small microspheres have been studied.

Strobel defined the turbidimetry as "the measurement of suspended particulate matter of refractive index different from that of the fluid by transmitted or forward scattered light"[53] The use of turbidity as a measure of the opacity of the membrane was first accomplished in this group in 1996 by Rooney.[25] Optical measurements presented in this dissertation were made by measuring the turbidity of membranes with a Cary 5 spectrophotometer. This approach was more convenient than the reflectance based sensors, because the measurements can be easily made quantitatively using a conventional spectrophotometer with a special membrane holder. This enables comparisons from membrane to membrane.

4.3 Principle of pH Sensitive Membranes

The pH sensitive, lightly crosslinked, nitrated poly(4-hydroxystyrene) microparticles were synthesized and derivatized as described in Chapter III. The principle of polymer swelling can be described as follows: the lightly crosslinked microspheres with charged sites embedded in a hydrogel are designed to swell and shrink as a function of hydrogen ion concentration. The hydrogel matrix is not pH sensitive. The larger the difference of refractive index between the matrix and the polymer microspheres, the larger the membrane response. The refractive index of a completely dehydrated or dry polymer can be estimated based on group contributions (Appendix 1).[83] For a completely

hydrated polymer the refractive index is estimated based on the degree of hydration of the polymer using the value 1.33 as the refractive index of water. For example, the calculated refractive index of dry poly(HEMA) is 1.500. When completely hydrated, it adsorbs approximately 48% water by weight, and the refractive index becomes 1.420.

The degree of hydration of the polymer can be determined by subtracting the weight of a completely dry polymer from the weight of a completely hydrated polymer and then dividing by the weight of the dry polymer. Because the degree of hydration of a polymer is also related to the degree of crosslinking, the estimated refractive indices are very dependent on the percentage of crosslinking of the polymer. The calculated refractive indices of poly(3-nitro-4-hydroxystyrene) and poly(3,5-dinitro-4-hydroxystyrene) are 1.630 and 1.641. These refractive indices become 1.555 and 1.564 in acid if they take up approximately 25% water. In base, the refractive indices are 1.450 and 1.456 if they take up approximately 60% water, respectively.

Table 4-1 shows the estimated refractive indices of pH sensitive polymers and hydrogels and Figure 4.1 shows the model of the pH sensitive membrane. At high pH the polymer microspheres swell due to deprotonation of the hydroxyl group which introduces a negative charge onto the polymer backbone. Deprotonation increases the water content of the porous particles causing its refractive index to decrease so that it is closer to the refractive index of the hydrogel matrix. As a result, the scattered light of the membrane is reduced dramatically when deprotonation of the hydroxyl groups reaches equilibrium. This can be measured as a change in turbidity or reflectance of the membrane. The polymer microspheres also react as pH indicators with distinct color changes at different

pH values. They are reddish in the swollen stage at high pH and yellowish in the shrunken stage at low pH.

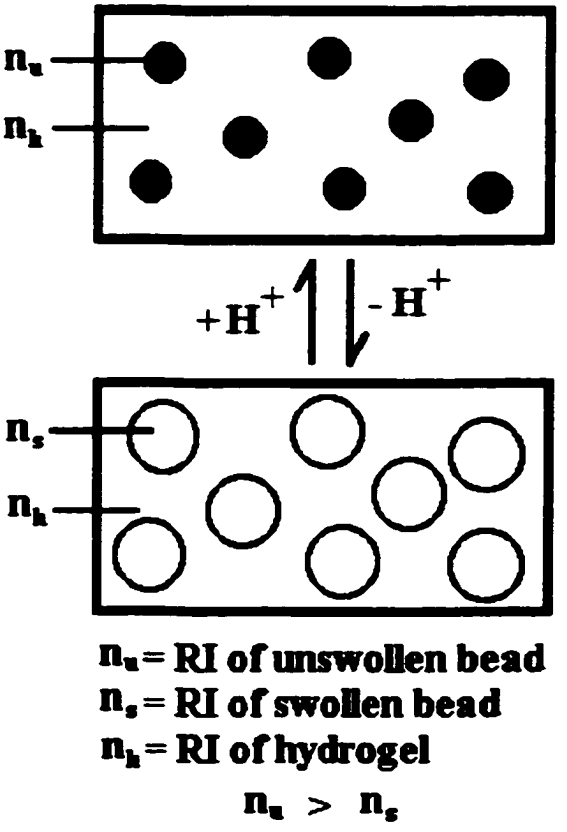

Figure 4.1 Model of pH sensitive nitrated poly(4-hydroxystyrene) microspheres embedded in a hydrogel membrane. The microparticles swell in basic and shrink in acidic solutions accompanied by a decrease or increase in refractive index.

Table 4-1. Estimated refractive indices of polymers [a]

Components	Refractive Index	Refractive Index in acid	Refractive Index in base
Water	1.330	-	-
poly(HEMA)	1.500(dry) / 1.428(wet) [b]	-	-
PVA	1.522(dry) / 1.340(wet) [c]	-	-
PNHS	1.630	1.555 [d]	1.450 [d]
PDNHS	1.641	1.564 [d]	1.456 [d]

[a] The number is calculated from the Lorenz and Lorentz equation[83]; [b] water content is on the order of 48%; [c] water content is on the order of 90%; [d] completely hydrated stage

4.4 Experimental

4.4.1 Reagents

Ethylene glycol dimethacrylate (EGDMA), 2-hydroxyethyl methacrylate (HEMA), and 2,2-dimethoxy-2-phenyl-acetophenone (DMPAP) were purchased from Aldrich Chemical Company. All other chemicals (reagent grade) such as sodium acetate, ammonium chloride, sodium phosphate monobasic, sodium phosphate dibasic, potassium chloride, sodium chloride, as well as bases and acids were purchased from Fisher Scientific and were directly used without further purification. The water used for all solutions was deionized and then distilled with a Corning Megapure distillation apparatus.

4.4.2 Apparatus

A Branson 1210 Sonicator was used for the purpose of preparing homogeneous membrane solutions and breaking agglomerated microspheres to re-suspend them in the hydrogel monomer solution. Glass microscope slides with Teflon spacers of different thicknesses were used to prepare membranes and to control their thickness. The uniformity of the membrane may be determined by microscopy. A 400-Watt UV lamp from UV Process Supply Inc. Chicago, Illinois, was used to photopolymerize the hydrogel

membrane. The membranes were characterized by measuring membrane turbidity. Two special Teflon membrane holders were used for these measurements which were carried out with a Cary 5 spectrophotometer at room temperature.

4.4.3 Preparation of Hydrogel Membranes

4.4.3.1 Poly(HEMA) membranes

The basic recipe for the poly(HEMA) membrane consists of the HEMA monomer, 1 mol % (based on monomer) ethylene glycol dimethacrylate (EGDMA) crosslinker and 1 wt % (based on monomer) 2,2-dimethoxy-2-phenylacetophenone (DMPAP) photoinitiator. The weight percentage of microspheres based on monomer varied from 1 to 6 wt %. Figure 4.2 shows the structure of the monomers, crosslinkers, and initiators used for this work. Table 4-2 shows the basic formula for the preparation of membranes. A monomer solution with total volume of 2 mL is usually prepared. The mixture was sonicated for 20 ~ 30 minutes until a completely homogenous suspension was obtained. Aggregated particles in the membrane would cause an undesired response. A small amount of the suspension was then transferred onto a glass slide that was covered with a Teflon strip around the edge, then covered with a second Teflon taped glass slide, and the two slides were carefully clamped together. The thickness of the Teflon tape ranged from 51 ~ 127 μm. The membrane solution was photopolymerized under a 400-Watt UV lamp for 10 minutes. The two slides were then separated and the membrane was conditioned in pH 4 and pH 10 buffers several times and stored in pH 4 buffer for further optical measurements.

Hydrogel Monomer

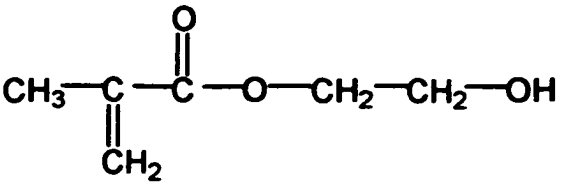

2-hydroxyethylmethacrylate

Hydrogel Crosslinker

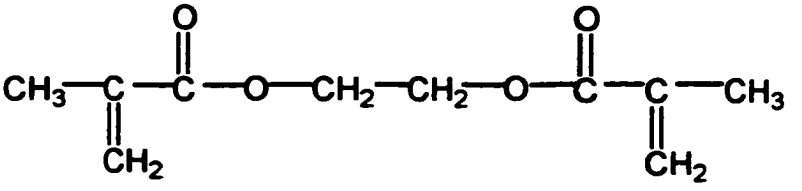

Ethylene glycol dimethacrylate

Photoinitiator

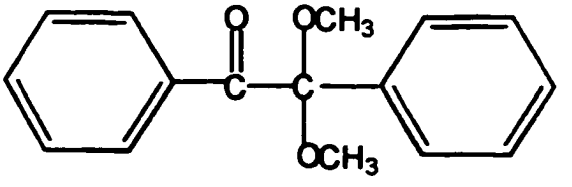

2,2-Dimethoxy-2-phenylacetophenone

Figure 4.2 Structured of reagents used for the preparation of poly(HEMA) hydrogel membrane

Table 4-2 The basic formula for the preparation of poly(HEMA) membranes

Ingredients	Name	Amount
Monomer	HEMA	2 mL
Crosslinker	EGDMA[a]	1 mole %
Initiator	DMPAP	1 wt %
Sensing element	Nitrated PHS beads[b]	2 wt % [b]

[a] EGDMA concentration varies from 0 ~2 %; [b] The percentage of beads varies from 1 to 6 wt % to the monomer.

4.4.3.2 Poly(vinyl alcohol) membranes

The high molecular weight, water soluble polymer, poly(vinyl alcohol) was crosslinked with glutaraldehyde for the PVA membrane. A 5% (wt/vol) solution of PVA (MW 14,000) was prepared by adding 5 grams of PVA to a 100 mL volumetric flask and diluting to the mark with dionized water. The solution was stirred with a stirring bar until a clear, homogeneous solution was obtained. A 10% aqueous solution of glutaraldehyde was used as the crosslinker. It was prepared from a stock solution by dilution. Both solutions are stable at room temperature.

Polymer microspheres were suspended in a solution of 2 mL PVA, 100 μL of glutaraldehyde, and various weight percentages of microspheres were mixed with sonication until a uniform suspension was obtained. Then 25 μL of 4M HCl was added to the mixture. Table 4-3 shows the basic formula for the preparation of PVA membranes. Polymerization was initiated at room temperature. In less then one minute the solution became more viscous under stirring with a glass rod. A portion of the solution was transferred to a microscope slide. The rest of the procedures were similar to those for the preparation of the poly(HEMA) membrane. The entire process was very rapid and took less than five minutes to complete. It is believed that poly(vinyl alcohol) does not deactive

or block off the micropores on the polymer microspheres before polymerization because the PVA molecule is too large to enter the micropores on the polymer.

Table 4-3 The basic formula for the preparation of PVA membranes

Ingredients	Name	Amount
Water soluble polymer	PVA	2 mL
Crosslinker	glutaraldehyde[a]	100 μL
Initiator	HCl (4M)	25 μL
Sensing element	Nitrated PHS beads[b]	1wt %

[a] The amount of glutaraldehyde varies from 50 ~ 200 μL; [b] The amount of beads varies from 0.1 to 2 wt % to the monomer.

4.4.4 Turbidity Measurement Using a Spectrophotometer

Measurements of pH were performed by pipetting 1.5 ml of solution into a 1.0 cm x 1.0 cm cuvette. A Teflon holder was designed for the turbidity measurements. The holder has a window of 5 mm diameter such that 99% of the incident light can pass through the membrane. The membrane in the special Teflon holder was immersed in the cell in a fixed, reproducible position. The turbidity was measured in absorbance units with a Cary 5 Spectrophotometer. An identical Teflon holder placed in a cuvette containing deionized water was used as the reference cell.

4.5 Results and Discussion

4.5.1 Hydration of Hydrogel Membranes

The optical properties of hydrogel membranes with embedded polymer microspheres depend on both the refractive index of the particles as well as the degree of

hydration of the hydrogel matrix. A high degree of hydration or water content of the hydrogel can not only decrease the refractive index of the membrane matrix but also enhance the diffusion of analyte ions from the aqueous phase to the membrane. Therefore, a high degree of hydration of hydrogel is desirable. This depends on the degree of hydrogel crosslinking. Because the membrane response depends on the difference in refractive index between the membrane matrix and the polymer particles, the lower the degree of crosslinking, the higher the water content, and the larger the difference in the refractive indices.

The degree of hydration of a membrane was determined by subtracting the weight of a completely dehydrated membrane from the weight of a completely hydrated membrane and then dividing by the weight of the dry membrane. Figure 4.3 shows the water percentage vs. the degree of crosslinking. It can be seen that the water percentage decreases as the membrane crosslinking increases. Poly(HEMA) membranes are mechanically stable both with and without crosslinking. In contrast, PVA membranes are mechanically fragile. Table 4-4 shows the membranes with different amounts of crosslinker and HCl. The formulation with 100 μL crosslinker and 25 μL HCl gave the most mechanically stable membrane. The water content was not significantly affected by the volumes of crosslinker. The average water content was approximately 90%.

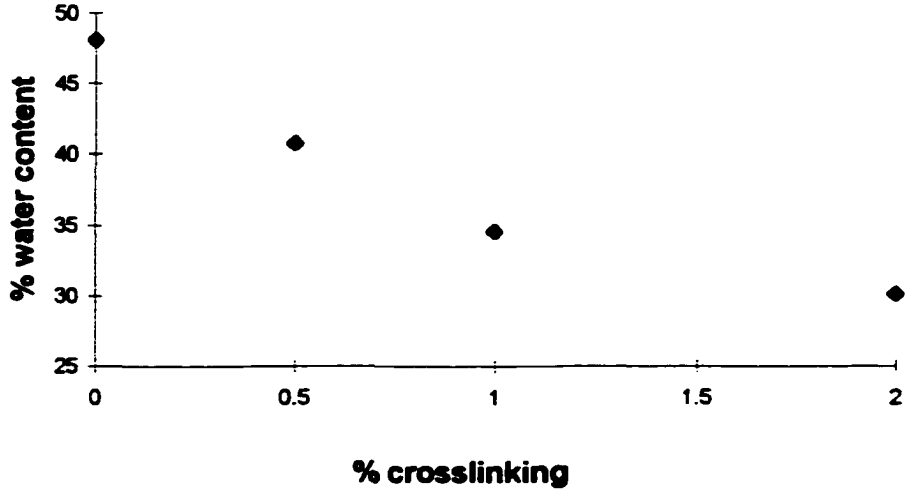

Figure 4.3 Water content of poly(HEMA) vs. percentage of crosslinking

Table 4-4 Effect of PVA membranes with different formulas

Ingredients	1	2	3	4
PVA	2 mL	2 mL	2 mL	2 mL
Glutaraldehyde	10 μL	25 μL	50 μL	100 μL
HCl	25μL	25 μL	25 μL	25 μL
water %	91.8	90.6	91.3	89.4
Mechanical stability	very fragile	fragile	good	very good

4.5.2 Characterization of Nitrated Poly(4-hydroxystyrene) Microspheres Immobilized in Poly(HEMA) Membranes

4.5.2.1 Turbidity Spectra

Poly(HEMA) membranes with embedded nitrated poly(4-hydroxystyrene) were characterized with a Cary 5, a conventional UV/VIS spectrophotometer. The measured "absorbance" is actually a combination of absorbance and turbidity. At long wavelengths where the nitrated poly(4-hydroxystyrene) structure does not absorb, the response is due only to turbidity.

Figure 4.4 shows the turbidity spectra of a poly(HEMA) membranes containing immobilized nitrated poly(4-hydroxystyrene) microspheres with diameters of approximately 0.68 μm prepared by dispersion polymerization and having a nitrogen content of 8.69 %. The bead concentration was 3 wt % (to the monomer), the concentration of the buffers was 0.1M and the ionic strength is 0.1M. As can be seen, the turbidity decreases with increasing wavelength. Unlike the membranes with embedded aminated VBC microspheres, at shorter wavelengths there is an increase in the absorption band at ~ 450 nm with increasing pH. This is due to the deprotonation of the nitro-phenol group on the polymer backbone. The decrease of turbidity with increasing wavelength at 600 nm and beyond is more gradual especially in the near-IR region.

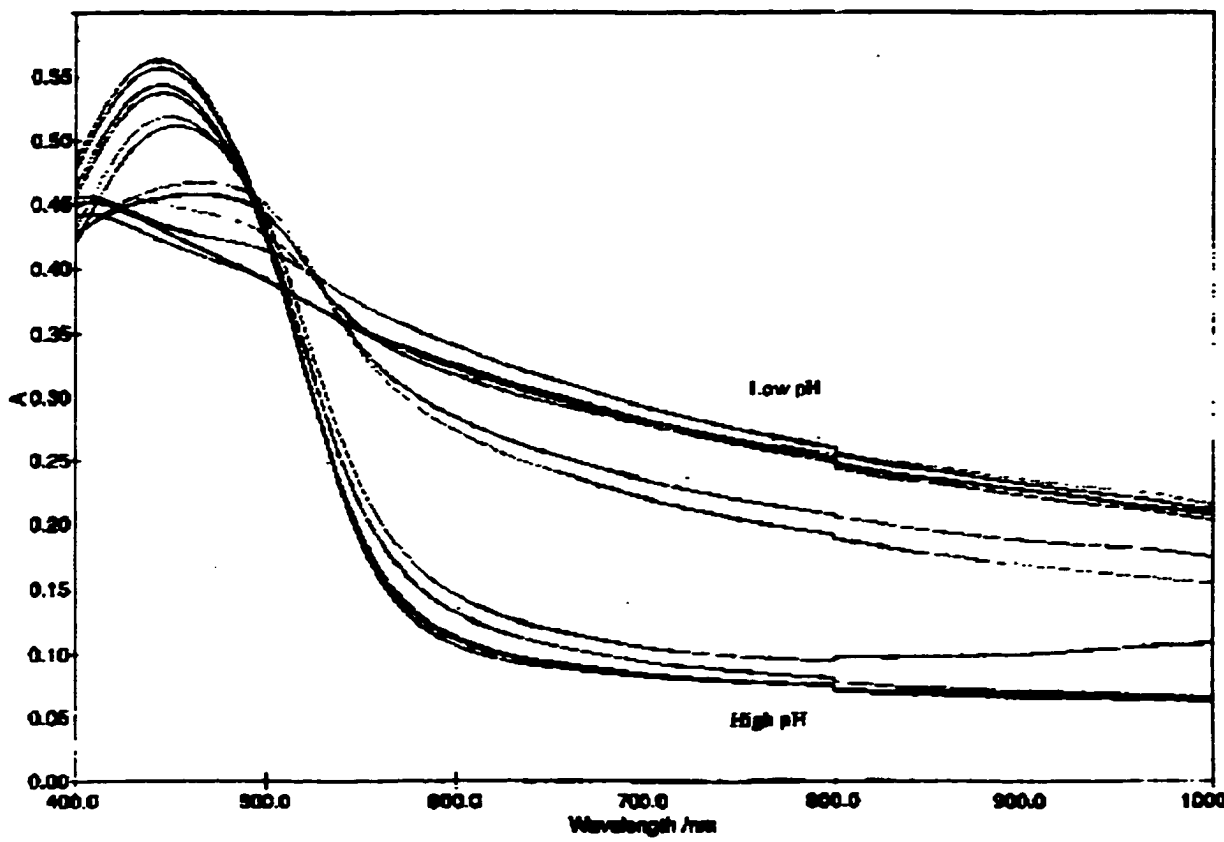

Figure 4.4 Turbidity spectra (measured as absorbance) of poly(HEMA) membrane with embedded 3 wt % nitrated poly(4-hydroxystyrene) microspheres in pH buffers (0.1M, IS 0.1M)

The spectra shown in Figure 4.5 also indicate that the turbidity of the membrane decreases as the pH increases due to the decrease in the refractive index of the microspheres that accompanies the particle swelling. The swelling as a function of pH is reflected in the spectrum as a decrease in the membrane turbidity in the visible and near-IR region. Figure 4.5 shows the change in the membrane turbidity as a function of pH at five different wavelengths. It can be seen that the tubidity levels are lower at longer wavelengths but the shape of the curves of turbidity vs. pH are similar at all wavelengths.

4.5.2.2 Turbidity Ratio

The relative change in turbidity with respect to wavelength is somewhat larger for the swollen form of the microspheres than for the shrunken form. This can be seen by plotting the turbidity ratio (see Figure 4.6), i.e. the ratio of turbidity for the shrunken and swollen forms of the microspheres vs. wavelength. As shown in Figure 4.6, the turbidity ratio increases from 2.9 to 3.5 as the wavelength increases from 600 to 800 nm. Beyond 800 nm the ratio changes only slightly. Similar results were observed by Rooney.[I-25]

We don't understand why the turbidity ratio shows the observed variation in response. The data suggest that the relative decrease in turbidty with the wavelength is larger for the swollen microspheres than for the shrunken microspheres. However, the turbidity of larger particles is usually less dependent on wavelength than the turbidity of smaller particles when particle diameters are similar in magnitude of the wavelength. Perhaps, the observed variation in turbidity ratio is due to the differences in the wavelength dependence of the refractive index for swollen and unswollen particles.

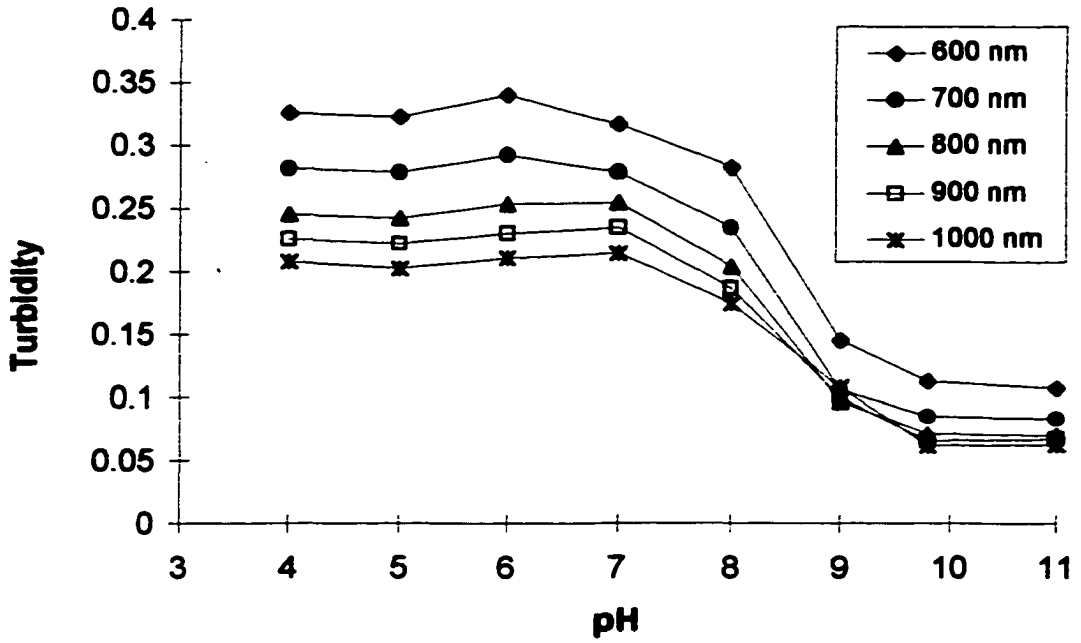

Figure 4.5 The turbidity change as a function of pH at five different wavelengths for the membrane shown in Figure 4.4

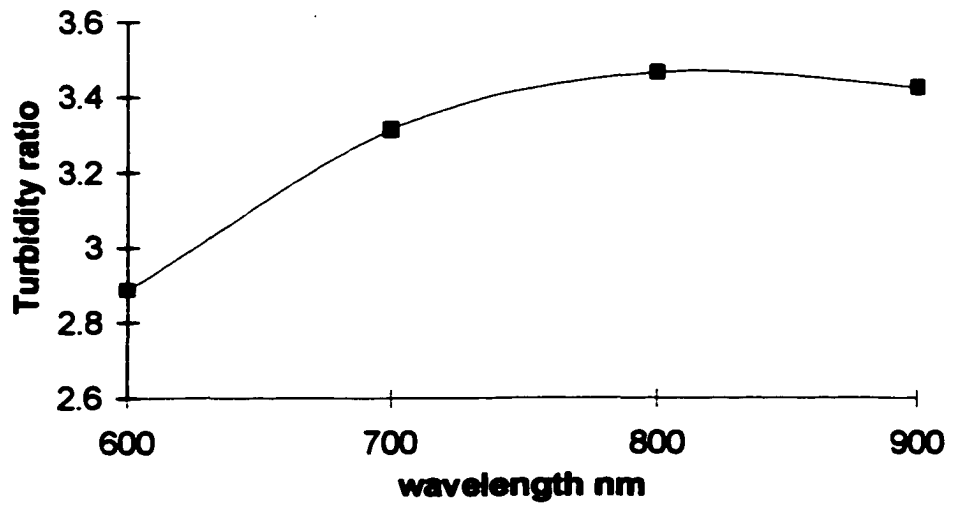

Figure 4.6 Turbidity ratio for the membrane shown in Figures 4.4

4.5.2.3 Apparent pK_a

Nitrophenols, such as 2-nitrophenol, 3-nitrophenol, 4-nitropenol, 2,4-dinitrophenol, and 2,6-dinitrophenol have all been used as pH.indicators. Table 4-5 lists the pK_a values for the nitrophenols.

Table 4-5 pK_a values for nitrophenols

Components	pK_a
2-nitrophenol	7.21
3-nitrophenol	8.39
4-nitrophenol	7.15
2,4-dinitrophenol	4.11
2,6-dinitrophenol	3.86

The pK_a values of polymers with nitrophenol functional groups are related to the percentage of nitrogen. Theoretically the nitrogen content of nitrophenol polymers can be calculated based on the polymer repeating units. For example, poly(3-nitro-4-hydroxystyrene) (PNHS) contains 8.48 % N and poly(3,5-dinitro-4-hydroxystyrene) (PDNHS) contains 13.3 % N as shown in Table 4-6. The determination of apparent pK_a values of polynitrophenol microspheres immobilized in a hydrogel can be made by measuring the pH from the graph of turbidity vs. pH, e.g. from Figure 4.6, at the point where the response is half-way between the maximum and minimum membrane tubidity change. These values are called "apparent pK_a's" because the turbidity vs. pH curves have not been described theoretically in a way that allows us to know how to calculate the pK_a from the observed data. The average pK_a value of the membrane shown in Figure 4.5 with five different wavelengths is approximate 8.45. Because the observed nitrogen content of the polymer microspheres, 8.69 %, is close to the calculated value of 8.48 for a single

hydrogen, it is likely that predominantly mono-polynitrophenol was obtained for this specific membrane. The apparent pK_a value is more than one pH unit higher than for 2-nitrophenol, which has a structure similar to that of the polymer. The shift is due to the fact that the polymer backbone is more hydrophobic than water which reduces the activity of water in the polymer. The sensitive range of the membrane is approximately from pH 7 to pH 9 and the response time was about 1 ~ 2 minutes.

Table 4-6. Calculated N% for poly-mono- and di-nitrohydroxystyrene

Polymers	N%
Poly(3-nitro-4-hydroxystyrene) (PNHS)	8.48
Poly(3,5-dinitro-4-hydroxystyrene) (PDNHS)	13.3

4.5.3 Characterization of Nitrated Poly(4-hydroxystyrene) Microspheres Immobilized in PVA Membranes

For a membrane with immobilized particles, the scattered light at the interface between the particles and the membrane medium is proportional to the squared difference of the refractive index of the two media. The larger the difference of the refractive index between the two media, the greater the reflected light. The PVA membranes in this work possess two advantages. One is that hydrated PVA has a refractive index of 1.34 which is much lower than that of poly(HEMA), 1.42. The other one is that the degree of hydration of PVA is approximate 90 % which is much higher than that of the poly(HEMA) membrane, ~ 48 %. The high water content should enhance the rate of diffusion for hydrogen ions from the aqueous solution through the hydrogel and into the microparticles

and this should lead to a decrease in the response time. The only disadvantage of using the PVA membrane is that it is not mechanically strong and has to be stored in water.

Polymer microspheres prepared by seeded emulsion polymerization were used in this part of study. There are two important advantages using these beads. One is that microspheres prepared by seeded emulsion polymerization are likely to swell more than the microspheres prepared by dispersion polymerization. The reason for this is the presence of porogenic solvent in the seeded emulsion microspheres. When the porogenic solvent is present, the polymer chains are less tangled and more swelling is possible. The second reason is that because there are larger and a greater number of pores, ions can diffuse into the polymer more quickly. As can be seen in the following sections, the PVA membranes with embedded microspheres prepared by seeded emulsion polymerization showed greatly improved response and reduced response times with a smaller amount of the microspheres.

4.5.3.1 Turbidity Spectra

Typical turbidity spectra of PVA membranes containing nitrated poly(4-hydroxystyrene) microspheres, with diameters of approximately 1.1 μm and nitrogen content of 10.52 %, are shown in Figure 4.7. The bead concentration was 0.1 wt % (based on monomer), the buffer concentration was 0.1M and the ionic strength was 0.1M. The spectral features are similar to those of the polymers in a poly(HEMA) hydrogel. The turbidity decreases gradually with increasing wavelength, from approximately 600 to 900 nm, for each spectrum which corresponds to a different pH buffer. The turbidity also decreases with increasing pH when the solution in which the membrane is immersed is

changed from a low pH to a high pH. This is caused by the decrease of the refractive index of the polymer accompanying swelling and results in less light being scattered from the membrane. Again at shorter wavelengths, ~ 480 nm, there is an absorption band which increases with increasing pH and is due to the deprotonation of the nitro-phenol group on the polymer backbone. The small feature at 800 nm is due to the change of the instrument detector and is not related to the membrane.

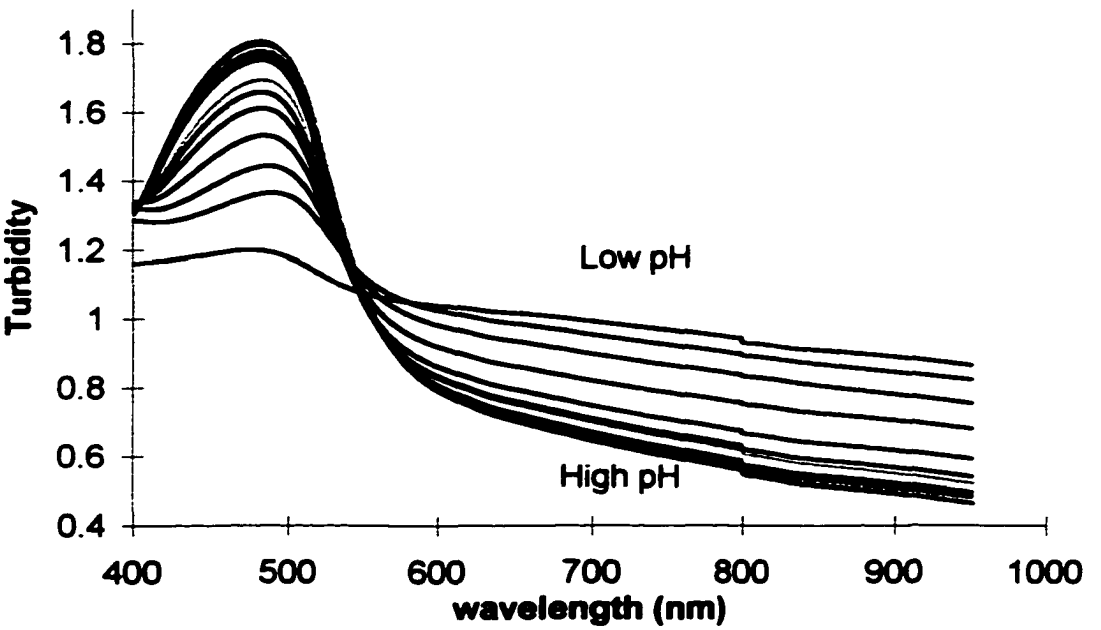

Figure 4.7 Turbidity spectra (measured as absorbance) of PVA membrane with embedded 0.1 wt % nitrated poly(4-hydroxystyrene) microspheres in pH buffers (0.1M, IS 0.1M)

4.5.3.2 pH response

Figure 4.8 shows the membrane turbidity change as a function of pH at three different wavelengths. As can be seen the average apparent pK_a at three different wavelengths is approximately 5.6 in which the microspheres have a nitrogen content of 10.52%. Again the experimentally observed pK_a was determined based on the turbidity measurement at the point where the intensity of the turbidity is half-way between the maximum and the minimum values. This corresponds to the point at which there are approximately equal amounts of the protonated and deprotonated forms of the polymer.

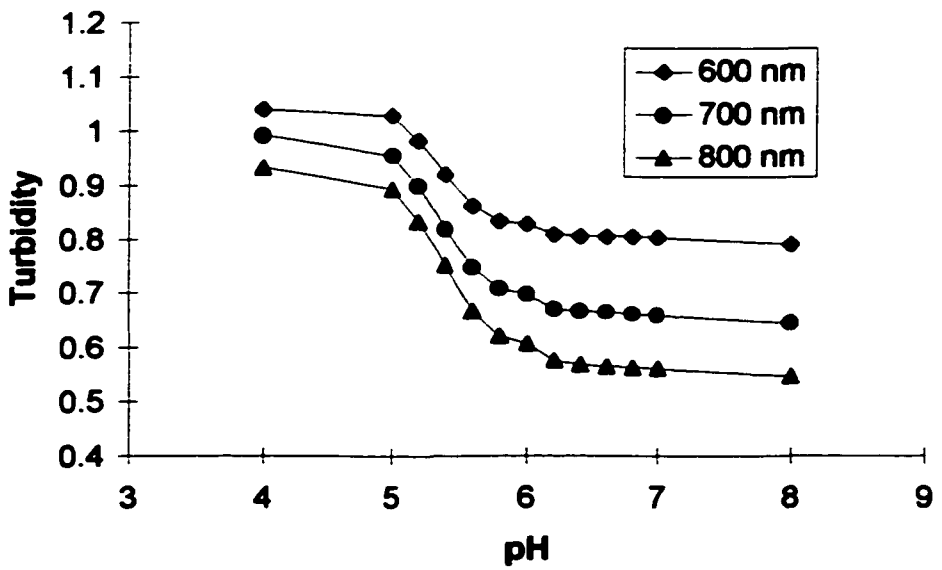

Figure 4.8 The turbidity change as a function of pH at three different wavelengths with the membrane shown in Figure 4.7

4.5.3.3 Turbidity Ratio

The turbidity ratio of the unswollen nitrated poly(4-hydroxystyrene) microspheres (pH 4) and the swollen microspheres (pH 10) immobilized in a PVA membrane is shown in Figure 4.9. The turbidity ratio increases gradually with wavelength from approximately 1.3 at 600 nm to about 1.7 at 800 nm. Also, it can be noted that the turbidity ratio change with wavelength is not so large as in the poly(HEMA) membrane. The turbidity ratio change with wavelength is caused by the different wavelength dependence of the refractive index between the swollen and the shrunken microspheres. When a polymer particle swells, its size changes and this opposes the refractive index effect. Perhaps the size change effect is wavelength dependent when the particle diameters are in a certain range relative to the wavelength. The effective wavelength range will be different for particles with diameters of 0.67 μm compare to those with diameters of 1.1 μm. In the example shown in Figure 4.10, the particles diameter is approximately 1.1 μm and the effective wavelength region is longer compared to that of the poly(HEMA) membrane in Figure 4.4. This explains why the turbidity ratio increases with wavelength especially at longer wavelength. The turbidity ratio is higher in poly(HEMA) than in PVA because the refractive index for PVA is further from the microsphere refractive index. According to the Fresnel equation, when the refractive index of the microsphere, n_1, stays the same, a smaller value of the refractive index of the hydrogel matrix, n_2, results in larger turbidity. However, the change in turbidity is smaller. Further investigation would be needed in order to explore how the size, refractive index, and the membrane matrix affect the membrane response.

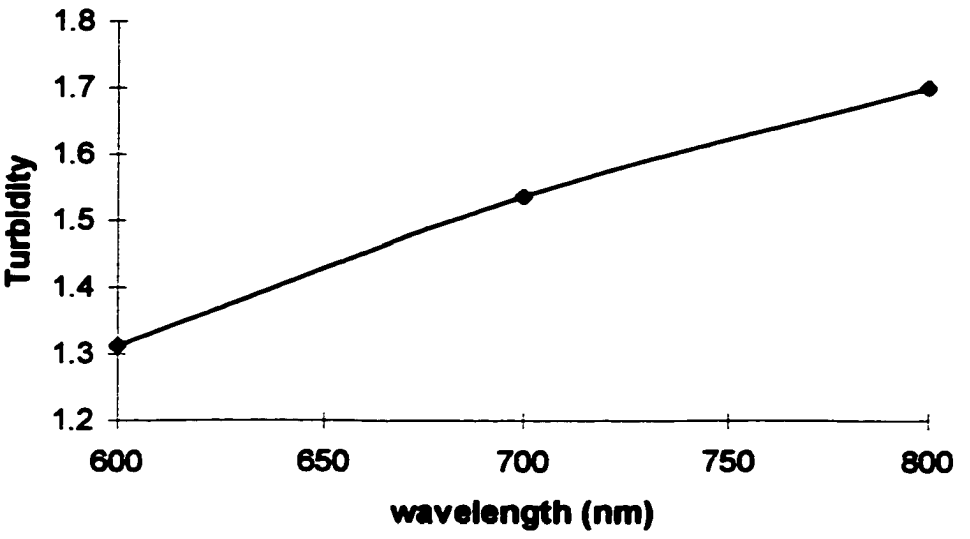

Figure 4.9 Turbidity ratio for the membrane shown in Figures 4.7

4.5.3.4 Percentage of Microspheres

As noted from Figures 4.4 and 4.7, the bead concentration is much less for the PVA membrane than for the poly(HEMA) membrane. This is further evidence that polymer microspheres prepared by seeded emulsion polymerization with larger diameters can swell to a greater extent and much more efficiently than those microspheres prepared by dispersion polymerization. The bead concentration of the poly(HEMA) membrane shown in Figures 4.4 and 4.5 was 3 wt % to the monomer. As shown in Figure 4.10 the turbidity per percentage of microspheres at 700 nm is 0.094 for the shrunken state and 0.0283 for the swollen state. The bead concentration of the PVA membrane shown in Figures 4.7 and 4.8 was 0.1 wt % to the monomer. As can be seen in Figure 4.11 the turbidity per percentage of microspheres at 700 nm is 9.93 for the shrunken state and 6.46 for the swollen state. It is obvious that the turbidity per percentage of microspheres is much higher in the PVA membrane with particles prepared by seeded emulsion

polymerization than in the poly(HEMA) membrane with particles prepared by dispersion polymerization.

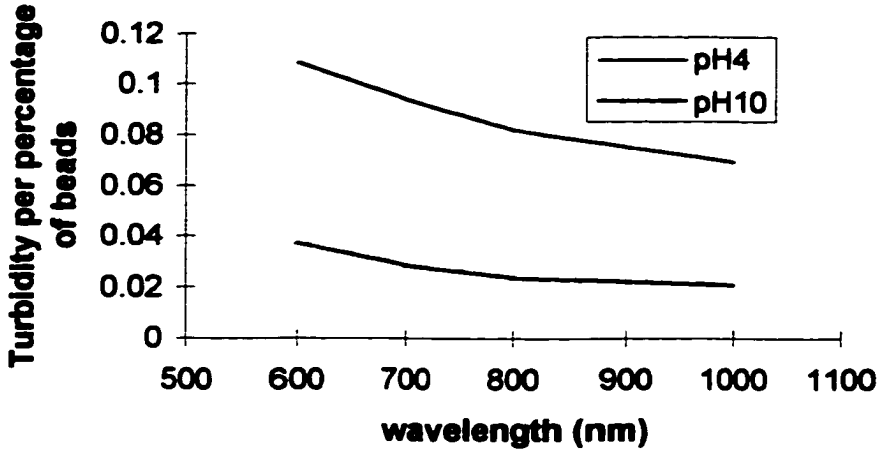

Figure 4.10 Turbidity per percentage of beads vs. wavelength for poly(HEMA) membrane as shown in Figures 4.4

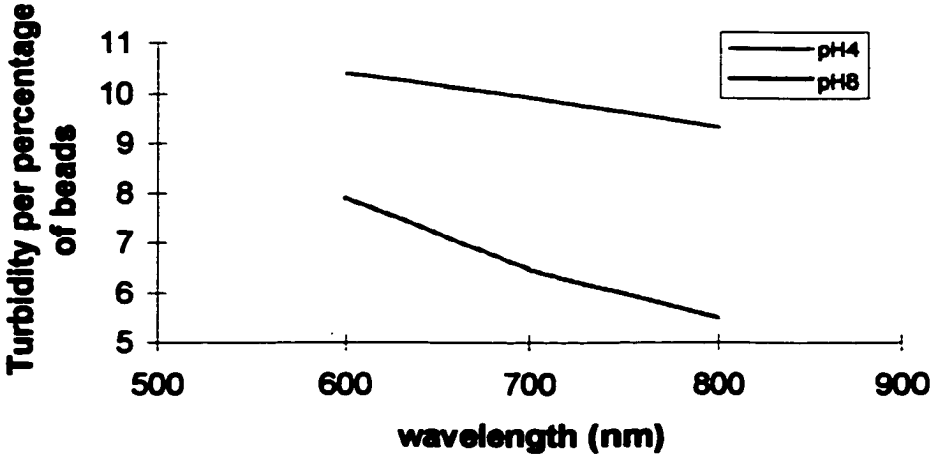

Figure 4.11 Turbidity per percentage of beads vs. wavelength for PVA membrane as shown in Figures 4.7

4.5.3.5 Tunable pK_a Values

Note that the percentage of nitrogen in nitrated poly(4-hydroxystyrene) polymers can be varied based on the conditions of the nitration reaction as described in Chapter III. Nitrated poly(4-hydroxystyrene) microspheres synthesized by dispersion polymerization can react with different concentrations of nitric acid at different temperatures to prepare polymers with different N % in order to tune the pK_a values for a large dynamic range for pH sensing. As shown in Figure 4.4 and Figure 4.5, the nitrogen content was found to be 8.69 % with an apparent pK_a value of 8.48 which is approximately 1 unit higher than the value of 7.2 for 2-nitrophenol in aqueous solution. From the data in Table 4-7, Figure 4.12, and Figure 4.13, it is found that the apparent pK_a values are approximately linearly related to the nitrogen content. Ideally it can be adjusted easily from 5 to 10, or perhaps even wider, by varying the number of nitro-functional groups. It is apparent that a mixture of mono-nitrophenol, poly(3-nitro-4-hydroxystyrene) (PNHS), and poly(3,5-dinitro-4-hydroxystyrene) (PDNHS) was obtained although it was not possible to prepare the pure di-nitro polymer. The pH sensitive regions can be easily adjusted through the experimental conditions without a major change in the polymer itself. The higher the nitrogen content, the lower is the pK_a value. Table 4-7 shows the apparent pK_a values versus the nitrogen content and Figure 4.10 and Figure 4.11 show the turbidity of four different PVA membranes with different N % and the apparent pK_a values vs. the N %. The ability to tune the pK_a value by varying the degree of nitration of the polymer is a major step in the improvement of pH sensors of this type. Table 4-7 shows the observed pKa value of 10.2 when the nitrogen percentage is 7.01 % and this means that pure mono-nitrophenol, PNHS, was obtained with a single pK_a value. In other cases, a mixture of

PNHS and PDNHS was probably obtained with two pK_a values. For the polymer with a pK_a of 5.46, the PDNHS is in the predominate form.

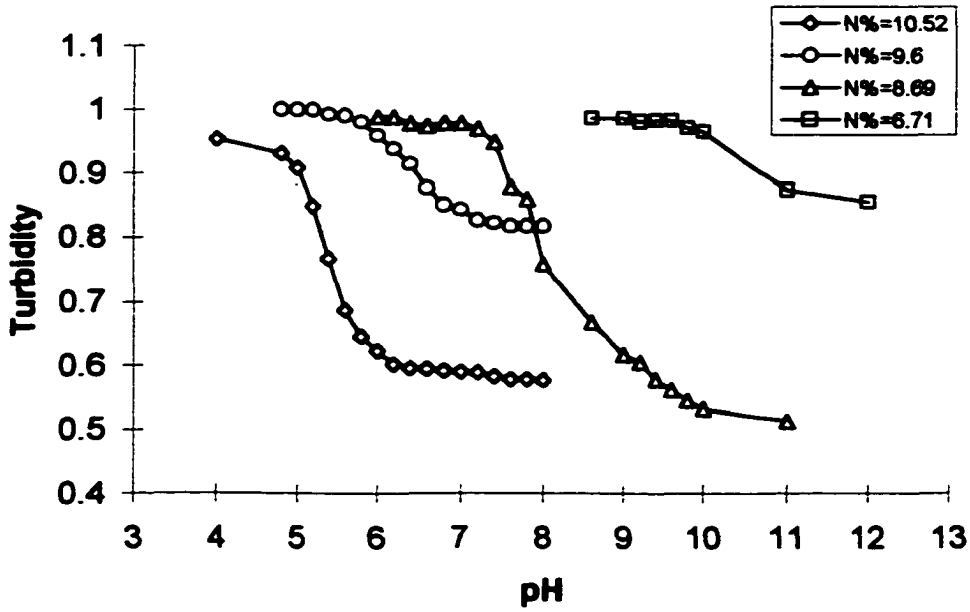

Figure 4.12 Turbidity of four different PVA membranes with different N% (the ordinate values have been adjusted in order to fit all the spectra in one graph)

Table 4-7 Observed pK_a values vs. N%

N%	pK_a
7.01	~10.2
8.69	~8.02
9.60	~6.61
10.52	~5.46

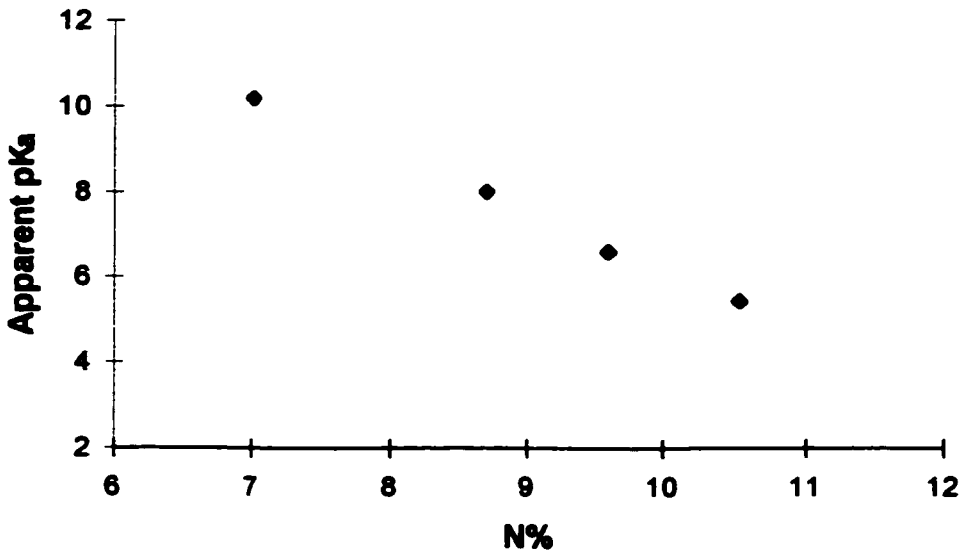

Figure 4.13 The apparent pKa values vs. the N%

4.5.3.6 Ionic Strength Effect

Figures 4.14, 4.15, and 4.16 show the membrane turbidity versus pH with buffer concentration of 0.1M at three different ionic strengths at 780 nm. The magnitude of the membrane turbidity decreases as the ionic strength of the solution increases. The increased ionic strength can reduce the extent of swelling of the deprotonated polymer by shielding adjacent negative charges which results in a reduced repulsive effect. Alternatively, the ionic strength effect can also be explained as an osmotic pressure effect. Swelling arises from the difference between the charge density on the polymer backbone and the ionic strength in solution. The higher the ionic strength in the solution, the smaller

the difference between the two media, the less the swelling and the lower the turbidity of the membrane. This is an undesirable effect for any pH sensor. One way to solve it is to reduce the charge density on the polymer backbone to ensure that swelling depends only on the affinity of the backbone for the solvent rather than interaction between adjacent charges.

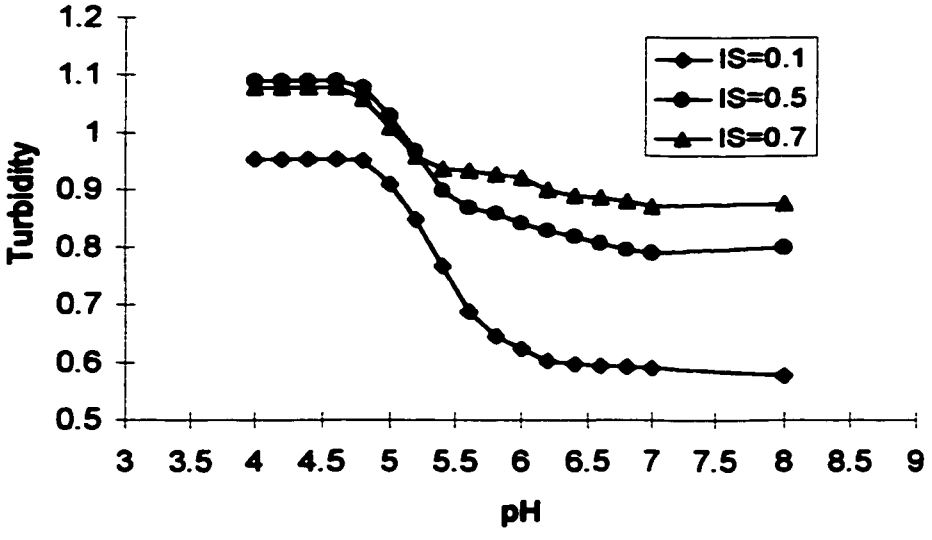

Figure 4-14 Ionic strength effect on membrane response with nitrated poly(4-hydroxystyrene) microspheres containing 10.52 % N, 0.1 % beads embedded in a PVA membrane at 780 nm

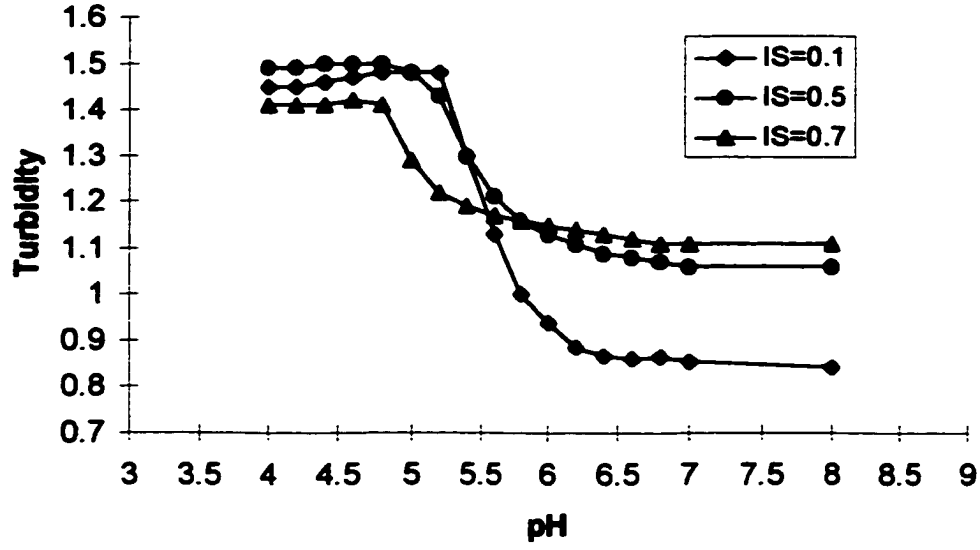

Figure 4-15 Ionic strength effect on membrane response with nitrated poly(4-hydroxystyrene) microspheres containing 10.52 % N, 0.3 % beads embedded in a PVA membrane at 780 nm

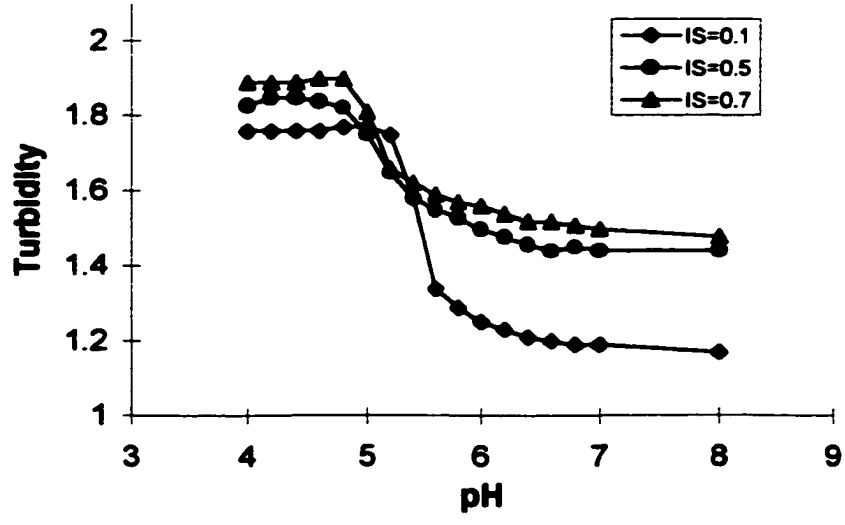

Figure 4-16 Ionic strength effect on membrane response with nitrated poly(4-hydroxystyrene) microspheres containing 10.52 % N, 0.6 % beads embedded in a PVA membrane at 780 nm

4.5.3.7 Loading Effect

Figures 4-17a, 4-17b, and 4-17c show the loading effect on membrane response. Different weight percentages of microspheres in the PVA membrane matrix were studied. The membranes were 127 μm thick and the measurements were made in different pH buffer solutions with total concentration of 0.1M. The magnitude of the change in turbidity should be proportional to the bead concentration. However, experimentally this might not always be the case, especially when the bead concentration is relatively high. As described in earlier sections, membranes are prepared by uniformly suspending particles in the membrane solution before polymerization. Since we are dealing with such small particles, bead aggregation can occur as the membrane forms even if the microspheres are initially fully dispersed. As shown in Table 4-8, the magnitude change of the change in membrane turbidity with 0.3 wt % beads is larger than in the membrane with 0.1 wt % beads which is expected. However, the magnitude of the change with 0.6 wt % beads is slightly smaller than that of the membrane with 0.3 wt %. This is probably due to the bead aggregation as the membrane forms. There are two effects on the membrane response due to aggregated beads. One is that aggregation can reduce the degree of swelling by reducing the hydrated environment surrounding the bead; and two, aggregation can change the shape of the spherical particles which also can affect the swelling.

The concentration of buffers used in these experiments was 0.1M for all the measurements. That means the available OH^- or H^+ density in the solution is approximately 0.1M or 1×10^{-4} moles per cc.. The calculated reagent density on the membrane with 0.3 wt % loading is 0.0082 M (moles nitrophenol per cc. of membrane) or 8.2×10^{-6} moles per cc. of membrane. As can be seen, the solution OH^- / H^+

concentrations are much higher than the membrane phenol concentration and a much smaller OH^- / H^+ is needed to completely deprotonate or protonate the polymer than for those membranes having much higher reagent density. The reason why such low reagent densities can give such a large response is because the polymer microspheres prepared by seeded emulsion polymerization have larger size and more pores than the beads prepared by dispersion polymerization. This also explains why the response time is faster. This is another advantage of using microspheres instead of the pure membrane (the membrane itself is the sensing polymer) because for a pure polymer membrane many more protons would be needed in order to completely protonate the polymer. As noted in Table 4-8, the PVA membrane with higher bead concentration shows a slower response. This is a further indication that reducing the density of reagent on the membrane would be the direction to go in order to improve the membrane response and reduce the response time.

The overall effects of loading, ionic strength, and response time are summarized in Table 4-8. The concentration of particles in the membranes in this study is within the range of 0.1 - 0.6 wt % and is much lower than in the membranes in the previous work which was in the range of 2 - 8 wt %.[28] This means that using microspheres synthesized by the seeded emulsion polymerization which have larger size and greater porosity has greatly improved the membrane response and response time.

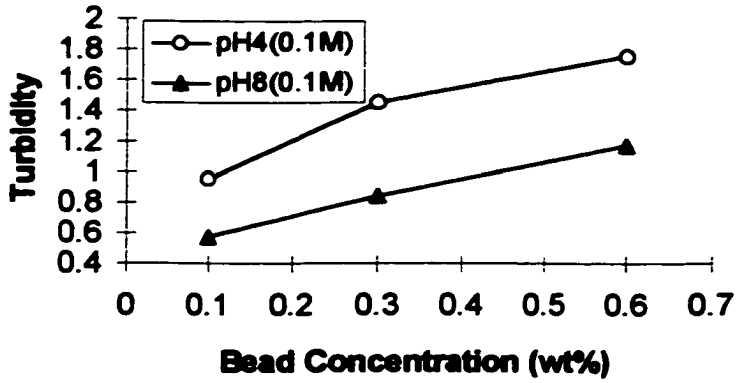

(a)

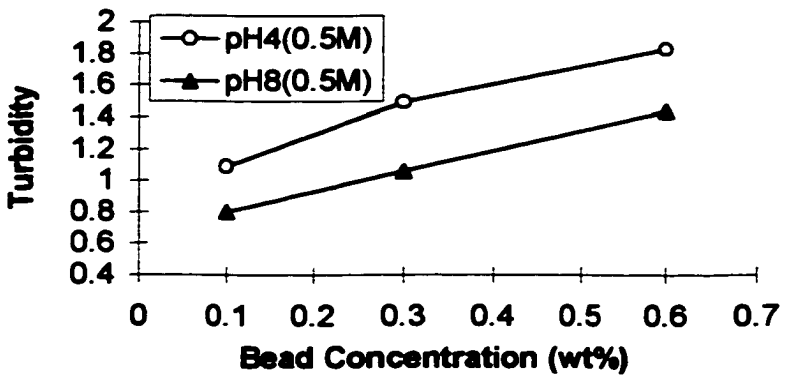

(b)

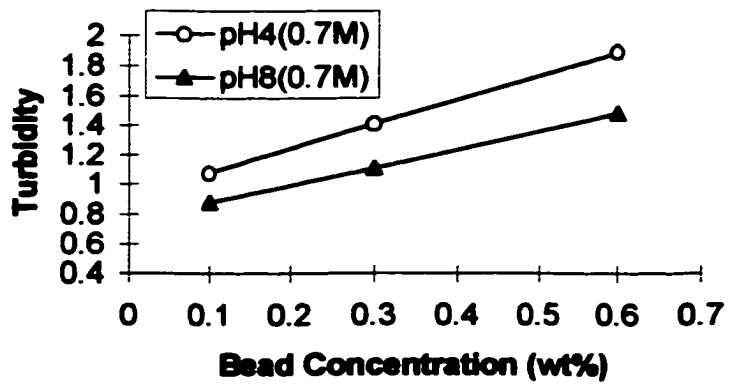

(c)

Figure 4-17 Plot of membrane turbidity as a function of bead concentration for PVA membranes containing nitrated poly(4-hydroxystyrene) microspheres with 10.52 % N at 780 nm; a) ionic strength of 0.1 M; b) ionic strength of 0.5 M; c) ionic strength of 0.7 M

Table 4-8. Loading effect on the magnitude of membrane response and response time

Bead concentration (wt%)	PVA membrane	poly(HEMA) membrane	Response time (sec)
0.1	0.377[a]		~10
0.3	0.608[a]		~15
0.6	0.581[a]		~15
1.0		0.211[b]	~30
6		0.178[c]	~90

[a] N%=10.52; [b] N%=8.69; [c] N%=7.01

4.5.4 Estimation of the Relative Reflectance Using the Theory of Optical Sensing Based on Swellable Polymer Embedded in a Hydrogel

In Chapter II we introduced the theory of estimating relative reflectance based on swellable polymer microspheres embedded in a hydrogel. Recalling equations (7) to (10) from Chapter II:

$$R_r = (d_{ps}/ d_{pu})^m \times (n_{ps} - n_h)^2 / (n_{pu} - n_h)^2 \quad (7)$$

$$n_{ps} = n_{pu} \times (1 - f_{H2O}) + n_{H2O} \times f_{H2O} \quad (8)$$

$$f_{H2O} = (V_{ps} - V_{pu}) / V_{ps} = [(d_{ps}/d_{pu})^3 - 1] / (d_{ps}/d_{pu})^3 = (d_r^3 - 1) / d_r^3 \quad (9)$$

$$R_r = d_r^m \times [(n_{pu} \times (1/ d_r^3) + n_{H2O} \times (d_r^3 - 1) / d_r^3 - n_h]^2 / (n_{pu} - n_h)^2 \quad (10)$$

we can calculate the relative reflectance based on estimated values of the parameters. Some of these estimations may be extremely rough due to the uncertainty in the values for the parameters. In equation (10), m is wavelength dependent and the value of m=1 is estimated based on the spectra in Figure 4.9 which shows the turbidity decrease is about

the same ratio as the wavelength increase (Table 4-9). The values of 1.555 and 1.564 for n_{pu} are based on the refractive indices for PNHS and PDNHS calculated from group contributions, assuming a water content of 25 % by volume for the protonated form. The diameter ratio, d_r=1.3, is estimated from the value in the reference[20] increased by 20 % to account for the fact that particles prepared by seeded emulsion polymerization have a greater porosity and larger pores and thus can swell much more than those prepared by dispersion polymerization. The rest of the parameters are n_{H20}=1.333 and n_h=1.340, respectively. The refractive index for the hydrogel is based on the refractive index of PVA and its water content which has been discussed in Chapter III. The calculated values of the relative reflectance from equation (10) are listed in Table 4-10.

The refractive indices for the swollen particles can also be calculated from equation (8). As shown in Table 4-10 the values are very close to those calculated from the group contributions and this confirms that the estimated diameter ratio is consistent with the water content which was determined experimentally. In contrast, the relative reflectance calculated from equation (7) using the refractive indices estimated from group contributions are in less satisfactory agreement with those calculated from equation (10) which uses the value of n_{ps} calculated from equation (8). This is because different values of n_{ps} are used in both equations, which means a small difference in the refractive index can result in a magnified difference in the relative reflectance.

Table 4-9 Turbidity ratio between two wavelengths

pH	Turbidity Ratio (600 nm / 700 nm)	Turbidity Ratio (700 nm / 800 nm)
4	1.0473	1.0654
5	1.0785	1.0682
6	1.1859	1.1497
7	1.2179	1.1762

Table 4-10 Estimated parameters for equation (10) based on the PVA memabrane with embedded PNHS/PDNHS microspheres

Polymer	n_{pu}	n_{ps}	R_r[b]	n_{ps}[c]	R_r[d]
PNHS	1.555	1.450	0.3403	1.434	0.2502
PDNHS	1.564	1.456	0.3486	1.438	0.2495
PNHS/PDNHS[a]	1.557	1.451	0.3401	1.435	0.2487

[a]The N% of the mixture is 10.52. The estimates are based on 80.6 % PNHS and 19.4 % PDNHS; [b] calculated from equation (7); [c] calculated from equation (8); [d] calculated from equation (10).

Table 4-11 lists the reflectance values and the reflectance ratios between the swollen and unswollen stages based on the spectra shown in Figure 4.9. In the table, it is assumed that the optical measurement of the membrane only involves transmitted and scattered (reflected) light and there is no absorption. As can be seen, the calculated reflectance ratios from both equations (7) and (10) are closer to the observed reflectance ratios at the longer wavelengths which is consistent with the results that Rooney and Seitz reported.

Table 4-11 Observed reflectance and reflectance ratios from Figure 4.9

	Turbidity	Transmission	Reflectance
Unswollen (600 nm)	1.04	0.0912	0.9088
Swollen (600 nm)	0.792	0.1614	0.8386
Ratio	1.313[a]		0.9227[b]
Unswollen (700 nm)	0.993	0.1016	0.8983
Swollen (700 nm)	0.646	0.2259	0.7740
Ratio	1.537[a]		0.8616[b]
Unswollen (800 nm)	0.932	0.1169	0.8830
Swollen (800 nm)	0.548	0.2831	0.7169
Ratio	1.700[a]		0.8119[b]

[a] The ratio is unswollen vs. swollen; [b]the ratio is swollen vs. unswollen according to equations (7) to (10)

4.5.5 Stability Test

These studies were designed to test the stability of nitrated poly(4-hydroxystyrene) microspheres prepared by seeded emulsion polymerization with an average diameter of 1.1 μm and 10.52 % N, immobilized in poly(HEMA) membranes in different environments. The membranes were stored in four different ways under three conditions. The first group of membranes was stored in pH 4 buffer at room temperature, 80 ^{0}C, and in direct sunlight at ambient temperature for approximately one month. The second group was stored in pH 10 buffer under the same three conditions. The third group was stored in deionized water, and the fourth group were stored dry under the same three condition.

As shown in Figure 4.18, after 25 days in pH 4 buffer, the intensity of the membrane turbidity remained very close to the initial value under room temperature, 80 ^{0}C and sunlight, respectively. Figure 4.19 shows the intensity of the membrane turbidity in pH 10 buffer for 25 days under room temperature, 80 ^{0}C, and sunlight, respectively. Figure 4.20 and Figure 4.21 show the turbidity of membranes stored in deionized water and dry under the same three conditions of room temperature, 80 ^{0}C, and sunlight.

Figures 4.22, 4.23, and 4.24 summarize the turbidity changes under the three conditions for membranes stored in four different ways. Table 4-9 and Figure 4.25 summarize the standard deviations of the measurements made on the membranes stored under these different conditions.

Figure 4.18 shows that membranes stored in pH 4 at room temperature and 80°C are more stable than in sunlight. It means that both nitrated poly(4-hydroxystyrene) and poly(HEMA) are stable up to 80 °C. After few days in sunlight photodecomposition of nitrated poly(4-hydroxystyrene) may start and cause the turbidity to decrease. When the nitrophenol absorbs light and decomposes, it may cause polymer refractive index to decrease. Membranes stored in pH 10 are less stable than in pH 4 especially at high temperature and in sunlight as shown in Figure 4.19. The deprotonated state of the nitrated poly(4-hydroxystyrene) is less stable than the protonated state. At pH 10 ionic interaction between the charged polymer backbone and the external solution and water solvation may also influence the function of the polymer microspheres. It is not clear that why the turbidity intensity increased with time under these conditions. As shown in Figure 4.20, the turbidity started to decrease in the membranes stored in deionized water for two days under all three conditions. After about 12 days the turbidity decreased to the level of the completely deprotonated form as shown in Figure 4.19. Membranes stored dry gave the highest standard deviation as shown in Figure 4.21.

Table 4-12 Standard deviations of measured turbidity under different conditions

	pH 4	pH 10	Deionized water	Dry
Room Temp	1.3	2.1	5.7	8.1
80 degree C	1.7	3.9	5.0	6.5
Sunlight	3.2	2.8	8.2	3.3

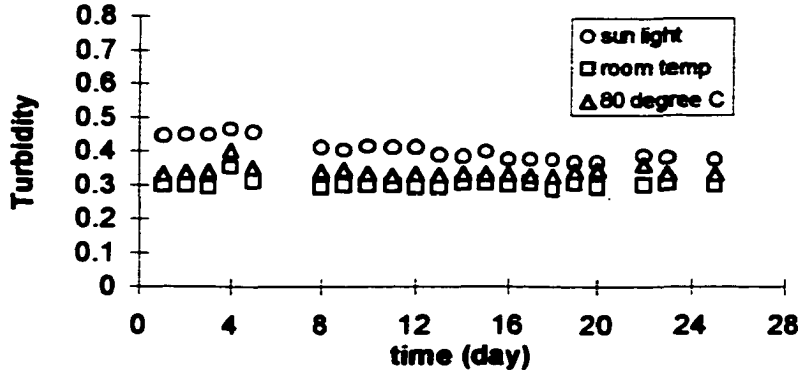

Figure 4.18 Membrane turbidity vs. time for storage for 25 days in pH 4 buffer at room temp, 80 ^{0}C, and in sunlight

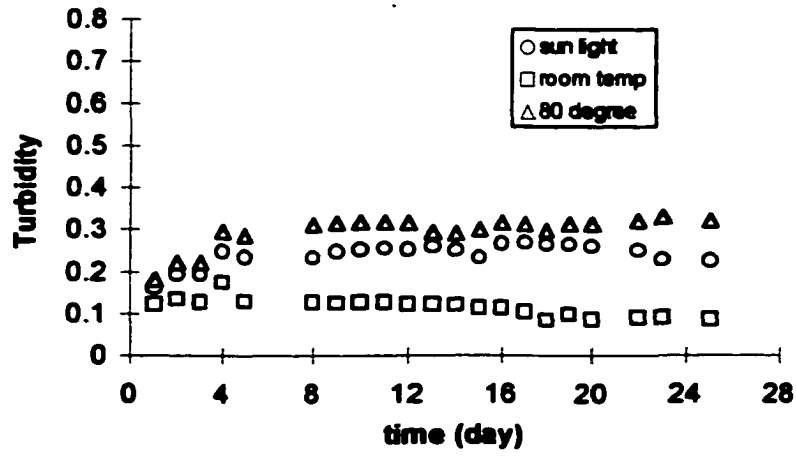

Figure 4.19 Membrane turbidity vs. time for storage for 25 days in pH 10 buffer at room temp, 80 ^{0}C, and in sunlight

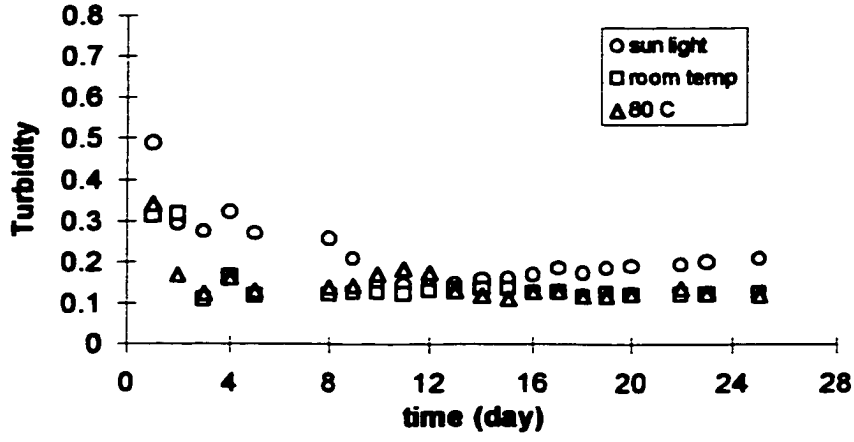

Figure 4.20 Membrane turbidity vs. time for storage for 25 days in deionized water at room temp, 80 ^{0}C, and in sunlight

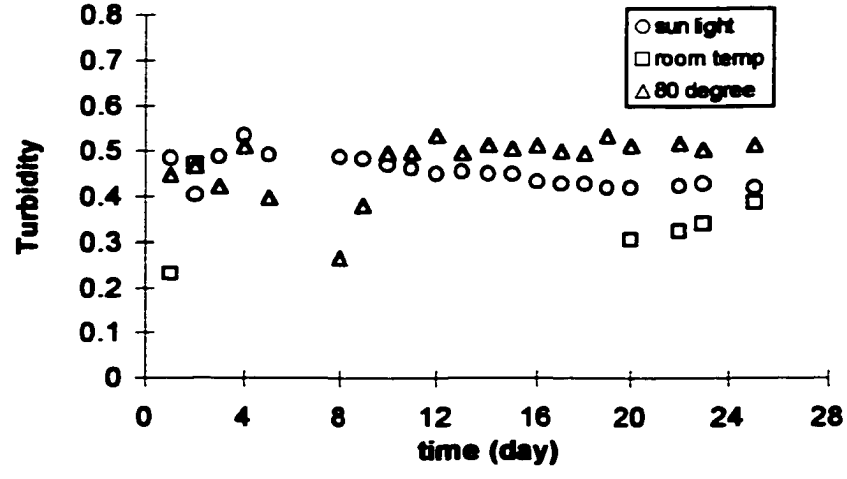

Figure 4.21 Membrane turbidity vs. time for storage for 25 days dry at room temp, 80 ^{0}C, and in sunlight

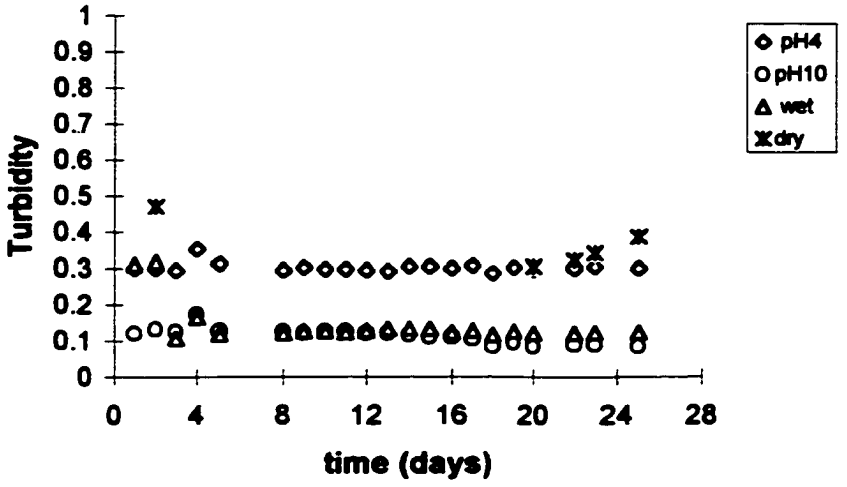

Figure 4.22 Membrane turbidity vs. time for storage for 25 days in pH 4, pH 10, deionized water, and dry at room temperature

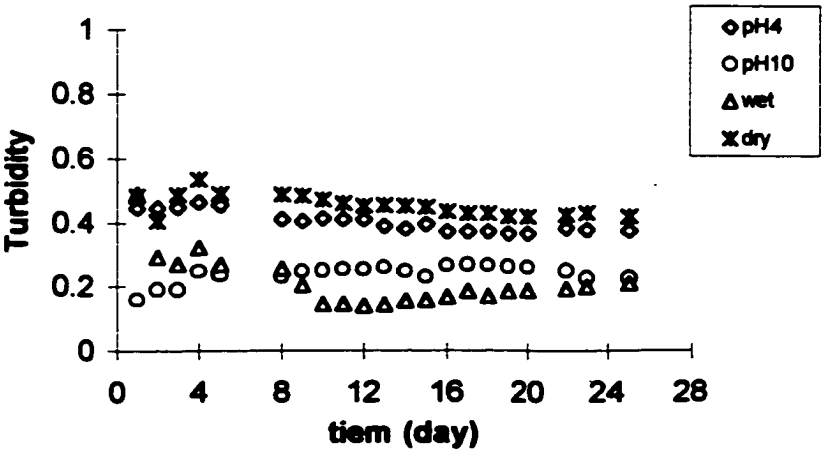

Figure 4.23 Membrane turbidity vs. time for storage for 25 days in pH 4, pH 10, deionized water, and dry in sunlight

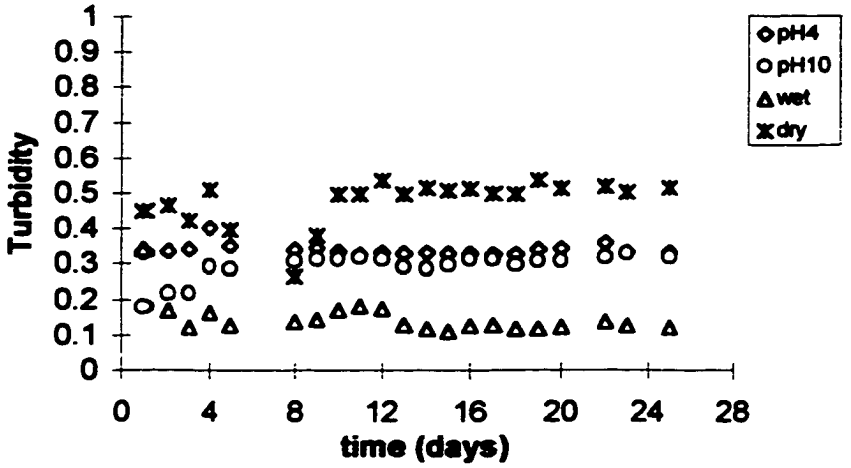

Figure 4.24 Membrane turbidity vs. time for storage for 25 days in pH 4, pH 10, deionized water, and dry at 80 ^{0}C

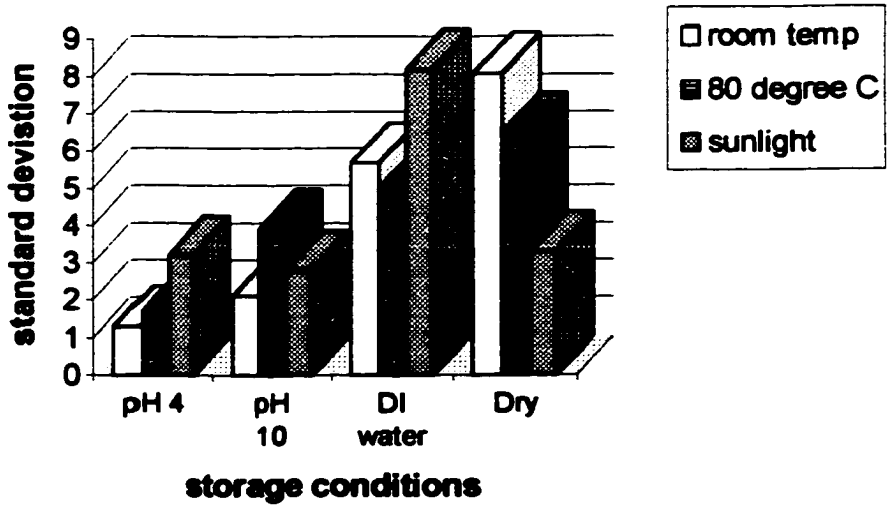

Figure 4.25 Summarize of standard deviations for the stability test

The membranes which were stored in pH 4 buffer under the three conditions were re-tested after about four months and the results are shown in Table 4-13. The turbidity was measured by immersing the membrane in pH 10 buffer and then in pH 4 buffer. The turbidities listed in Table 4-13 are the average turbidity after three cycles. It is clear that the membranes can be used for many cycles for about four months with the relative error of < 10% under three conditions.

Table 4-13 Stability test for pH response

Under sunlight	**pH 4**	**pH 10**
Initial value	0.446	0.169
Value after 4 months (average)[a]	0.421	0.181
Relative Error (%)	5.61	-7.10
At room temp	**pH 4**	**pH 10**
Initial value	0.301	0.121
Value after 4 months (average)[a]	0.291	0.116
Relative Error (%)	3.32	4.13
At 80 °C	**pH 4**	**pH 10**
Initial value	0.341	0.180
Value after 4 months (average)[a]	0.333	0.197
Relative Error (%)	2.64	-9.44

[a] Average of three measurements

Although the turbidity of the membranes varys in different conditions with time, the poly(HEMA) membrane matrix are mechanically stable under all the conditions including dry membranes. This is the important advantage of using this kind of hydrogel as the substrate for sensing elements especially for the application of biomedical samples.

4.6 Conclusions

The major improvement of this work is that the available range for pH sensing has been markedly increased by varying the nitrogen percentage. The observed pK_a value can be as low as pH 5.6 or as high as pH 10.2. The results presented in this work show that PNHS / PDNHS microspheres may be used to sense hydrogen concentration over a wide range of pH. The response time of the membrane with microspheres prepared by seeded emulsion polymerization has been significant decreased by utilizing PVA as the membrane matrix comparing to the poly(HEMA) matrix with microspheres synthesized by dispersion polymerization. This is due to larger and more porous polymer particles and the use of the hydrogel membranes with a higher degree of hydration. The magnitude of the membrane response also increased with a very low percentage of beads in PVA matrix. A small amount of particles were needed to obtain significant of changes in turbidity. Based on the direct evidence presented in this work, particles made by seeded emulsion polymerization have larger and more pores and can swell and shrink very rapidly. Diffusion of hydrogen ions from aqueous phase through the membrane matrix to the polymer microspheres might be enhanced in the 90 % hydrated PVA environment. Particle sizes may also play an important role in the membrane response. When the particles are closer or slightly larger than the incident radiation scattering will be increased. Swelling also increases the particle size but is not as significant as the decrease in refractive index. The turbidity ratio of the PVA membrane gradually increased with the wavelength. The stability test showed that the poly(HEMA) hydrogel membranes are mechanically stable when they are stored in pH 4, pH 10, deionized water, and dry at room temperature, 80 ^{0}C, and in sunlight. The turbidity intensity of nitrated poly(4-

hydroxystyrene) microspheres embedded in poly(HEMA) was more stable in pH 4 and pH 10 than in deionized water and dry after 25 days storage.

CHAPTER V

IONOPHORE-DOPED NITRATED POLY(4-HYDROXYSTYRENE) MICROSPHERES EMBEDDED IN A HYDROGEL FOR POTASSIUM SENSING

5.1 Introduction

This chapter covers a new approach for potassium ion selective membranes based on polymer swelling utilizing ionophore modified swellable polymer microspheres embedded in a hydrogel. The microspheres described in the previous chapters are pH sensitive nitrated poly(4-hydroxystyrene). With an ionophore incorporated into the polymer, the membrane can also be used as an ion sensor. In this study the ionophores dibenzo-18-crown-6 (DB18C6) or valinomycin have been immobilized on a lightly crosslinked polystyrene copolymer system. The polymer backbone is designed to be partially hydrophilic so that it allows ions to penetrate into its interior when it swells. Ion binding between the ionophore and the potassium ion is accompanied by deprotonation of the hydroxy group on the polymer backbone and causes it to swell. Swelling lowers the turbidity of the membrane because the refractive index of the swollen particles is closer to the refractive index of the hydrogel membranes. The change in the optical properties of the membrane varies continuously with ion concentration and can be detected remotely through fiber optics.

5.2 Principle of Operation

Optical membranes based on swellable nitrated poly(4-hydroxystyrene) microspheres can be used as a sensing material for ions other than hydrogen, such as potassium, by taking advantage of the large number of neutral ionophores developed for ion-selective electrodes.[84-91] The ionophore modified nitrated poly(4-hydroxystyrene) ion-selective membrane can be modeled as a cation-exchange membrane. In such a membrane, the pH sensitive, nitrated poly(4-hydroxystyrene) acts as an acid-base indicator, (HIn) and the ionophore (L) acts as a cation complex reagent for the metal ion. Figure 5.1 shows the ion-extraction system for the potassium ion sensing membrane where nitrated poly(4-hydroxystyrene) microspheres with immobilized ionophore are suspended in a hydrogel matrix.

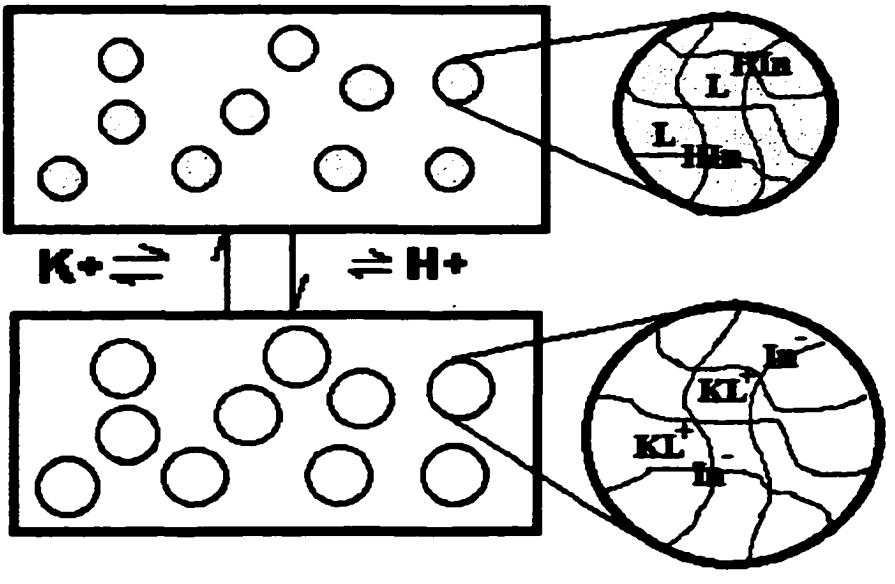

Figure 5.1 The model of the ionophore modified nitrated poly(4-hydroxystyrene) ion-selective cation-exchange membrane

When the membrane is immersed in a solution of potassium ions, the neutral ionophore L in the polymer will selectively bind K^+ to form KL^+. This ion binding is accompanied by deprotonation of the hydroxy group of HIn to form an anion In^-. This introduces charged sites to the polymer causing it to swell. The overall process is :

$$K^+(aq) + HIn(poly) + L(poly) \rightleftharpoons KL^+(poly) + In^-(poly) + H^+(aq) \quad (1)$$

Because the KL^+ complex on the polymer is essentially a hydrophobic cation, it forms an ion-pair with the anion on the polymer backbone. Swelling results in a decrease in refractive index as the water content increases. The feasibility of this analytical approach has been demonstrated by measuring spectral changes caused by the resultant polymer swelling in the presence of potassium ions. The pH of the analyte solution is held constant by the buffer so that the swelling process can be related to the concentration of potassium in solution. Although the ions are combined in an ion pair, they still have a high affinity for water. Observations obtained in the testing of microsphere membrane, with DB18C6 and valinomycin confirm that the ion pairing chemistry can be implemented to sense potassium ion. The turbidity change of the membrane, which is due to the ratio of hydrogen and potassium ion concentrations, can be measured by interrogating the sensing membrane with a light beam of any desired wavelength in the visible or near-infrared regions.

5.3 Experimental

5.3.1 Immobilization of Ionophores onto the Polymer

There are two ways to incorporate the ionophore onto the polymer. The first approach is to bind ionophore covalently to the polymer. This offers the important advantage that the ionophore will not slowly leach out of the polymer with time. However, to avoid complicated syntheses, we decided on the second approach which is to add the ionophore to the solution of monomer, crosslinker, porogenic solvent, etc. so that the ionophore is mechanically incorporated into the polymer during the polymerization process. This is much easier and the degree of loading can be easily controlled. Another noncovalent approach is to immobilize the ionophore by soaking the polymer microspheres or the membrane with embedded microspheres in an ionophore solution. In this work, only noncovalent methods were used for the immobilization.

5.3.1.1 Preliminary Study

This experiment was conducted to the demonstrate the feasibility of forming ion pairs on the polymer substrate.[89] The immobilized neutral potassium ionophore (DB18C6 or L) in the polymer phase extracts potassium ion from an aqueous solution of KCl to form a cation complex. The anionic fluorophor, 8-anilino-1-naphthalenesulfonate (ANS) in aqueous solution is then co-extracted onto the polymer beads to form an ion pair. The excitation and emission wavelengths for ANS^--KL^+ are approximately 380 and 460 nm. After the polymer beads were separated from the solution and transferred to a test tube, a detectable fluorescence intensity could be observed under room light or by using a conventional UV mini detector. In the absence of KCl, there was a significant decrease in the fluorescence intensity.

5.3.1.1.1 **Reagents**

The ammonium salt of 8-anilino-1-naphthalenesulfonic acid was purchased from Aldrich Chemical Company. Standard 2.0 M potassium ion solutions and 0.5 mM ANS were prepared by weighing reagent-grade potassium chloride and ANS respectively and dissolving in the appropriate amount of deionized water.

5.3.1.1.2 **Procedure**

The polymer beads with immobilized DB18C6 were prepared by suspension polymerization as described in Chapter III. They were soaked in a test tube with the solution of 2.0 M KCl and 0.5 mM ANS buffered at pH 9. For complete extraction, the beads were kept in the solution for 24 hours. The beads were separated from the solution and washed with distilled water before measuring fluorescence.

5.3.1.1.3 **Results and discussion**

Table 5-1 shows the change in the fluorescence excited by a mini UV lamp (365 ~ 400 nm) with the variation in the solution composition. The increase in intensity is due to the formation of ion-pairs accompanying two different extractions. One of the extractions is due to the potassium-DB18C6 cation complex formation and the other one is based on the charge-charge interaction between the complex cation and the anionic fluorophor. The blank test gives the base line. In the absence of potassium ion, the intensity is probably due to the non-specific adsorption of ANS onto the polymer phase. The significant increase in the intensity is due to ion-pair extraction. The fluorescence is based

on the formation of the potassium ion - ionophore complex and the formation of the ion-pair.

Table 5-1. Preliminary results based on the ion-pair extraction and fluorescence

Ingredient	Test tube #1	Test tube #2	Test tube #3
Polymer	TCPA-Styrene beads	TCPA-Styrene beads	TCPA-Styrene beads
Buffer	pH 9	pH 9	pH 9
Fluorophor	-	ANS	ANS
potassium ion	-	-	2.0 M KCl
Fluorescence Intensity	No intensity (Very light blue)	Low (light yellow)	High (Very bright yellow)

5.3.1.1.4 Conclusion

The preliminary ion selective binding test showed two important observations. One is that the ionophore can be immobilized on a polymer substrate by incorporating an ionophore into a polymer solution before polymerization. The TCPA-styrene co-monomer system was chosen because the co-polymer can be derivatized to increase the hydrophilicity of the polymer substrate. DB18C6 was used for the binding test because it is inexpensive and readily available even though the selectivity is not very high for potassium ion over sodium ion. The second observation is that ionophores immobilized in a polymer can be used for the ion sensing element based on the ion-extraction process. Although this detection method was not very interesting for the ultimate goal of this work, the observations were very encouraging because the immobilization and ion-extraction techniques would be suitable for ion sensors based on polymer swelling which will be discussed in the following sections.

5.3.1.2 Incorporation into TCPA-Styrene Polymer Formulation

Initial ionophore immobilization experiments were undertaken with large beads prepared by suspension polymerization. In order to show that this approach can be implemented with polymer microspheres membranes, experiments were carried out to show that ionophore could be immobilized on microspheres prepared by dispersion polymerization. The TCPA-styrene copolymer system was chosen because TCPA can be derivatized with amines to increase backbone hydrophilicity.

The typical polymer formulation is listed in Table 5-2. The polymer microspheres were synthesized by dispersion polymerization as described in Chapter III. In all formulations DB18C6 was loaded at approximately 1 wt % to monomer.

Table 5-2. A basic recipe for polymer microspheres based on the styrene-TCPA co-polymer system by dispersion polymerization

Ingredient	Name	Amounts
Monomer I	Styrene	50 % mole to total monomer
Monomer II	TCPA	50 % mole to total monomer
Crosslinker	Divinylbenzene	2 wt % to monomer
Stabilizer	Polyvinylpyrrolidone	22 wt % to monomer
Inophore	DB18C6	1 wt % to monomer
Initiator	2,2'- azobisisobutyronitrile	2 wt % to monomer
Solvent I	Ethanol	85 mL
Solvent II	Water	5 mL
Porogenic Solvent	Toluene	10 mL

5.3.1.3 Incorporation into 4-acetoxystyrene-DVB polymer formulation

The TCPA-styrene copolymer system was useful for the investigating ionophore immobilization on the polymer. However, a hydrophobic counter ion had to be added to

solution to induce ion binding. Therefore, this system was not desirable for the ion sensing based on the polymer swelling, and a new system with improved response time and greater sensitivity was desired. The 4-acetoxystyrene-DVB copolymer system with immobilized ionophores was chosen for this purpose. This system was designed for ion sensing based on the ion-extraction and ion-exchange chemistry as described in section 5.2. The idea is that poly(4-acetoxystyrene) derivatized to form nitrated poly(4-hydroxystyrene) not only provides a more hydrophilic environment on the polymer backbone than styrene but also serves as the acid-base indicator in reaction (1). A typical polymer formulation is listed in Table 5-3. The polymer microspheres were synthesized by dispersion polymerization and then derivatized as described in Chapter III. In all formulations, DB18C6 was loaded at the ~1 wt % level.

Table 5-3. A basic recipe for polymer microspheres based on the 4-acetoxystyrene polymer system by dispersion polymerization

Ingredient	Name	Amounts
Monomer	4-acetoxystyrene	10 mL
Crosslinker	Divinylbenzene	2 wt % to monomer
Stabilizer	Polyvinylpyrrolidone	22 wt % to monomer
Ionphore	DB18C6	1 wt % to monomer
Initiator	2,2'- azobisisobutyronitrile	2 wt % to monomer
Solvent I	Ethanol	140 mL
Solvent II	Water	50 mL
Porogenic Solvent	Toluene	10 mL

5.3.2 Immobilizing Ionophores by Adsorption

5.3.2.1 Directly Adsorbing DB18C6 into Polymer

It was found that incorporation of ionophores into polymer formulations by

dispersion polymerization was efficient for the immobilization. However, as will be discussed later, the response time for potassium ion sensing was about 20 minutes and a high concentration of KCl was required in order to observe a measurable signal. One possible problem could be that the ionophore molecules do not or very small amount of them get incorporated into the polymer. Another is that ionophore could be trapped in a location in the polymer network where it is not accessible to potassium ion. It is also possible that the immobilized DB18C6 could have slowly leached out during the hydrolysis and nitration reactions. Therefore, a new technique of immobilizing the ionophore was evaluated by soaking the polymer microspheres or the microsphere membranes directly in a saturated ionophore solution.

There were two reasons why we started to immobilize ionophore by adsorption from aqueous solution as the cation complex: This way we would position the ionophore on the polymer where it would be available to complex with potassium ion and form the ion pair. It was expected that this approach would give faster response, since it would not require that the ionophore migrate within the polymer to bind potassium ion. The second reason was that we could monitor the immobilization process by conducting it at a pH slightly below the pK_a so that immobilization would be accompanied by the formation of the phenol anion which could be monitored by measuring the magnitude of the anion absorption band.

5.3.2.2. Principle and Procedure

Immobilization of an ionophore onto a polymer substrate was based on the adsorption of the ionophore-K^+ complex onto a hydrogel membrane containing the

nitrated poly(4-hydroxystyrene) microspheres. When the K^+ ions are subsequently removed from the polymer, the ionophore remained in the polymer. This is accomplished by placing the membrane in contact with a concentrated potassium ion solution saturated with the ionophore, DB18C6 or valinomycin, and buffered at a pH at which nitrated poly(4-hydroxystyrene) is predominantly in the neutral form. Potassium ion forms a cation complex with the ionophore in the solution before contacting the membrane. When the membrane is immersed in the solution, the cation complex is extracted into the polymer phase because the cation complex, LK^+, prefers the polymer phase. To maintain charge neutrality in the polymer phase, the hydroxy group on the polymer backbone loses a proton to the solution to maintain electroneutrality. The extraction is based on the hydrophobic interaction between LK^+ and the polymer as well as electrostatic interaction between the cation complex and the deprotonated anion on the polymer backbone. After this soaking process the potassium ions are removed from the polymer by repeatedly washing with a low pH buffer. This protonates the nitrophenol and pushes the complexation equilibrium toward dissociation.

5.3.2.3 Immobilization

Figure 5.2 shows the spectra monitoring the immobilization process with a PVA membrane containing nitrated poly(4-hydroxystyrene) microspheres buffered at pH 4 in the presence and absence of the DB18C6 / DB18C6-K^+ / K^+ solution. As can be seen, there is an absorbance band at ~500 nm, which is very similar to that of the pH sensitive polymer. This is due to the deprotonation of the nitro-phenol functional group and confirms that K^+ / H^+ ion exchange is accompanied by the K^+ ion binding. In a saturated

DB18C6-3M KCl mixture, the immobilization had taken place as indicated by the increase in the phenol anion absorption band at ~500 nm. When the membrane was washed with pH 4 buffer (0.1M, IS=0.1M) and the absorbance subsequently measured in the buffer, the absorbance decreased dramatically due to the protonation of the nitro-phenol group. The membrane absorbance was measured again after it had been continually washed with pH 4 buffer (0.1M, IS=0.01). The final measurement was taken after immersing the membrane in deionized water. The results showed that the immobilization was very effective and the process by which K^+ was removed was nearly complete. It is not surprising that the turbidity intensity of the membrane remains nearly the same for both the deprotonated and protonated forms in the wavelength region from 700 to 1000 nm. With such a high ionic strength, 3M KCl, the charges on the polymer backbone would be shielded by external ions and the osmotic pressure would be reduced significantly. As a result the polymer microspheres can not swell in such an environment.

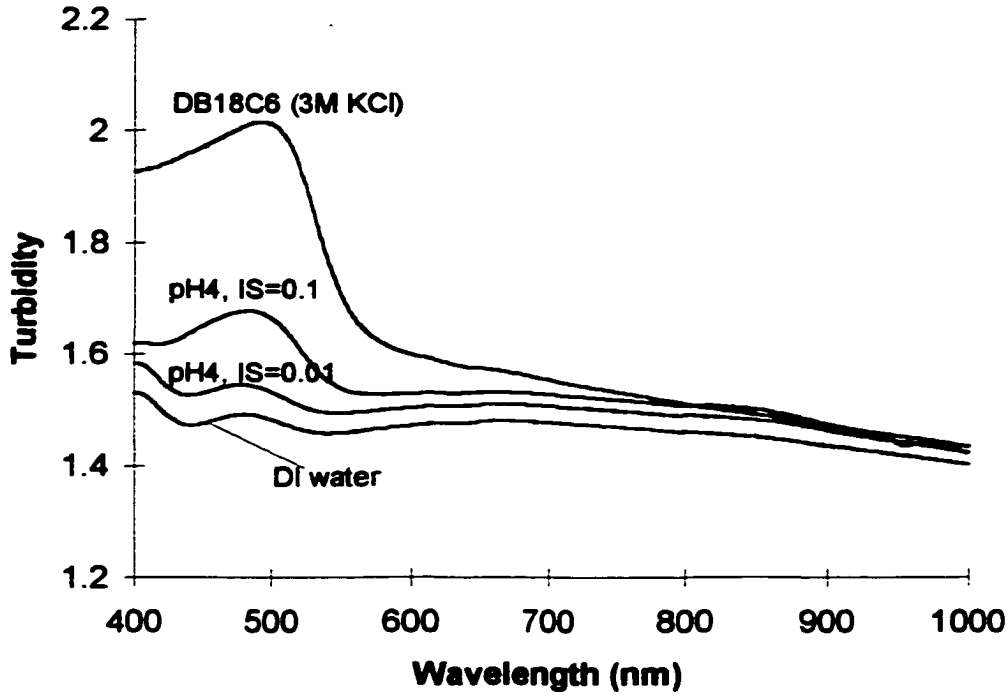

Figure 5.2 Spectra of the immobilizing process with PVA membrane incorporated with nitrated poly(4-hydroxystyrene) microspheres at pH 4 in the presence and absence of the DB18C6 / DB18C6-K^+ / K^+

Figure 5.3 shows the response time of the DB18C6 modified PVA membrane monitored as the absorption change at 490 nm in solutions of 0.1M KCl (buffered at pH 4) and just in the buffer. The potassium ion complexation and dissociation processes with DB18C6 is accompanied by deprotonation and protonation of the nitrophenol group. The measurements were carried out by immersing the membrane in the buffer, measuring the absorption, and then switching the membrane to the solution of 0.1M KCl and measuring the absorption. As can be seen, the ion binding, or deprotonation takes about 3 minutes to reach the 90 % final value and the dissociation, or protonation takes about 5 minutes to reach the 90 % final value.

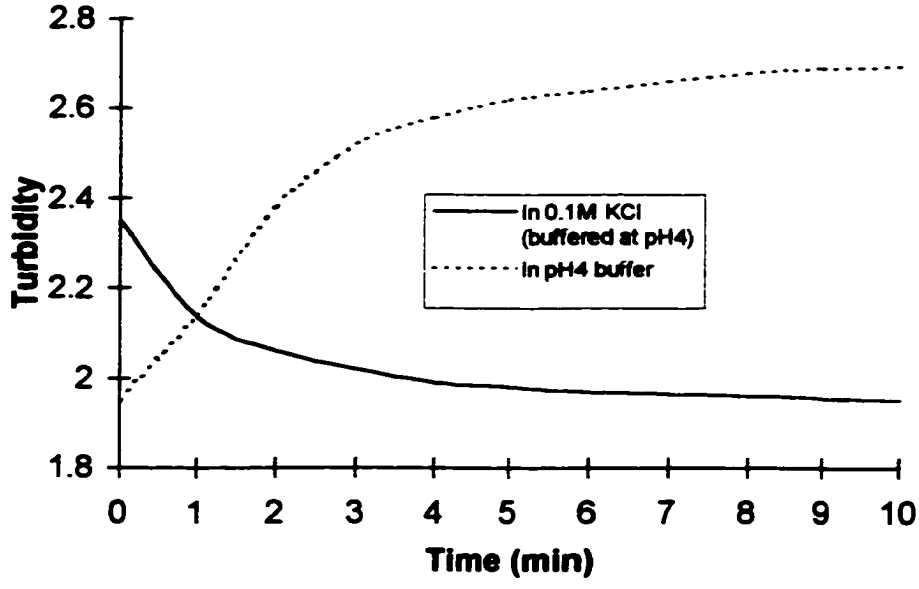

Figure 5.3 The response time of the DB18C6 modified PVA membrane monitored as the absorption change at 490 nm nitrophenol in solutions of 0.1M KCl (buffered at pH 4) and just in the buffer.

5.3.2.4 Conclusion

The immobilization is specific and efficient for the polymer and is not affected by the hydrogel matrix. The modified membrane can be used for many shrinking and swelling cycles. Although there may be residues of LK^+ or L adsorbed on the hydrogel, this does not affect the response of the membrane for the following two reasons: 1) the residues do not swell the polymer microspheres embedded in the hydrogel; and 2) they do not absorb light, especially in the near IR region. Immobilization by directly soaking polymer microspheres alone in the cation complex solution would be more efficient before making membranes. However, due to the size of the microspheres, washing and separation of the microspheres from the solution was a problem.

5.3.3 Potassium Ion Sensing Membranes

5.3.3.1 Poly(HEMA) Membrane

Poly(HEMA) membranes with ionophore immobilized nitrated poly(4-hydroxystyrene) microspheres are prepared in the same way as described in Chapter IV.

5.3.3.2 PVA Membrane

The PVA membrane with suspended nitrated poly(4-hydroxystyrene) microspheres was prepared as described for pH sensing in Chapter IV except that the microspheres are modified with the immobilized ionophore. PVA membranes with suspended nitrated poly(4-hydroxystyrene) microspheres as prepared for pH sensing was modified with ionophore by soaking the membranes in the ionophore-KCl solution for potassium ion sensing as described in 5.3.2.

5.4 Optical Properties of Ionophore Modified Membranes

5.4.1 Refractive Index

The optical properties of ionophore modified membranes for potassium ion sensing are basically similar to those for pH sensing. Ideally the refractive index of the hydrated hydrogel matrix should have the same value although the residue of L or KL^+ may have some slight effect. However, the changes should not be significant and besides, the effect should be constant. In the same way, the refractive index of the modified microspheres would be slightly affected by the immobilized ionophores but the change should be small compared to the unmodified polymer microspheres. The water content of the microspheres might be slightly reduced with an increase in the refractive index due to the

immobilized crown ether.

5.4.2 Turbidity Spectra

The principle of the potassium ion sensing membrane has been described in section 5.2. The turbidity change of the membrane as a function of K^+ concentration is based on the polymer swelling accompanying the deprotonation of the nitro-phenol group and the ion-pair interaction between the anion on the polymer backbone and the cationic complex, KL^+. Figure 5.4 shows turbidity spectra of the DB18C6 modified PVA membrane with embedded nitrated poly(4-hydroxystyrene) microspheres in potassium ion solutions. The polymer microspheres were prepared by seeded emulsion polymerization with an apparent pK_a of 5.2. The potassium ion solutions, from 10^{-2} to 10^{-4} M, were buffered at pH 4. The ionic strength of each solution was 0.01M which was adjusted with an appropriate amount of NH_4Cl. The spectra show that the turbidity decreases with an increase in KCl concentration. Also, there is an absorption band near 500 nm which is due to the deprotonation of the nitro-phenol group. As noted, the band shifts to longer wavelengths, from ~ 480 nm (as shown in Figure 4.8) to ~500 nm. This is likely due to the influence of the interaction of the ion-pair with the deprotonated anion.

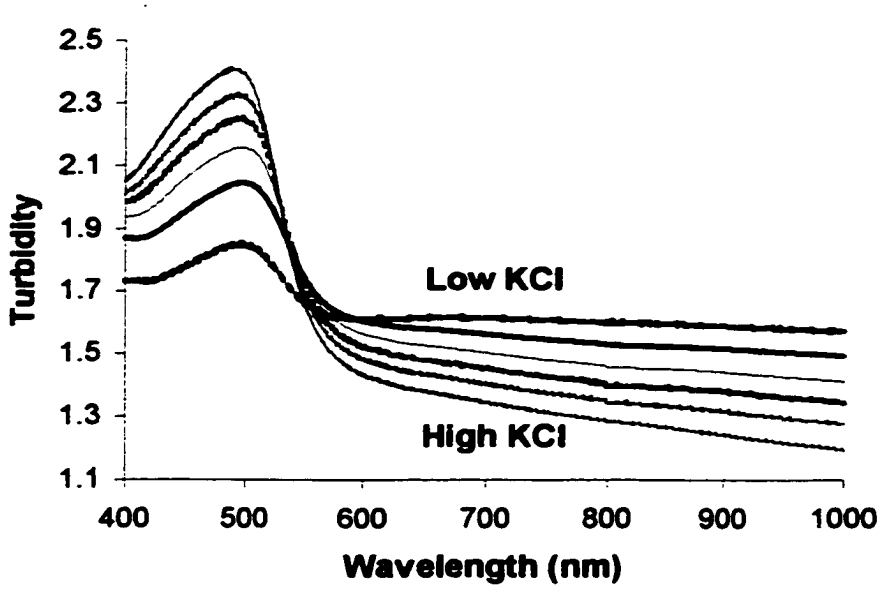

Figure 5.4 Turbidity spectra (measured as absorbance) of nitrated poly(4-hydroxystyrene) microspheres (0.3 wt %) with immobilized DB18C6 embedded in a PVA membrane (127 μm) in KCl solution at pH4 (IS=0.01M)

5.4.3 Turbidity Ratio

Figure 5.5 shows the graph of the turbidity ratio with wavelength region from 700 to 1000 nm between the most swollen and non-swollen forms shown in the spectra (Figure 5.4). The microspheres used for this membrane were prepared by seeded emulsion polymerization with an average diameter approximate 1.1 μm. As can be seen the turbidity ratio increases almost linearly over the wavelength region evaluated. This suggests that the refractive indices of the shrunken and swollen forms vary differently with wavelength.

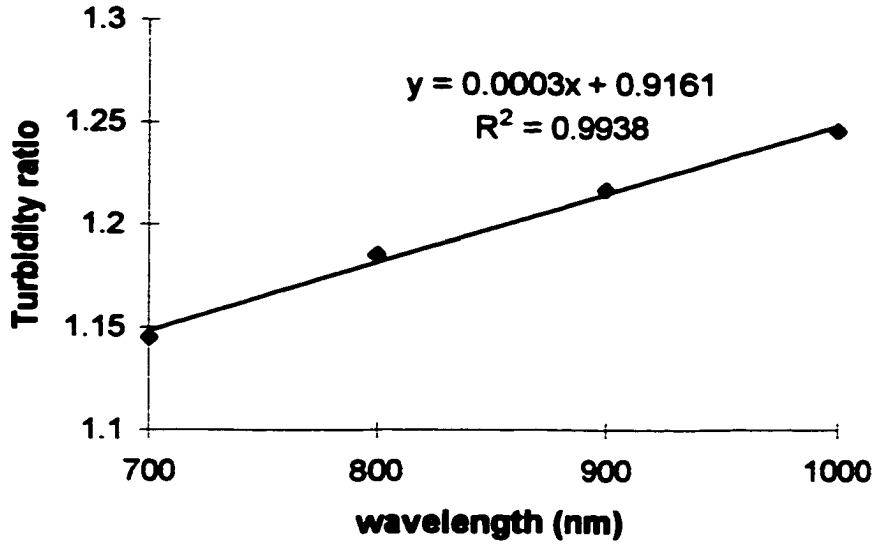

Figure 5.5 Turbidity ratio between the most shrunken form vs. the most swollen according to the spectra shown in Figure 5.4

5.5 Results and Discussion

5.5.1 Response based on the Different Methods of Ionophore Immobilization

Table 5-4 shows how the membrane response is affected by the method of ionophore immobilization. The response time is the time for the intensity to reach 90 % of the maximum reading. The response time of the last case in Table 5-4, PVA membrane modified with DB18C6 by soaking the entire membrane, was ~ 2 minutes and is much faster than the other cases. The response time can be reduced further by preparing thinner membranes. The calculation of loading was the same as described in Chapter IV. As can be seen, a very small amount of the beads was needed for the PVA membrane. This is because the refractive index of hydrated PVA is much lower than the refractive index of the microspheres. The lowest concentration in Table 5-4 was defined as the value of the

potassium ion concentration giving a signal which is equal to the signal of the membrane itself before it was in contact with the KCl solution. Also indicated in the table for each entry are the method of preparing the microspheres and the method used to immobilize the ionophore. The overall membrane response showed that nitrated poly(4-hydroxystyrene) microspheres prepared by seeded emulsion polymerization embedded in a PVA membrane with the method of soaking the entire membrane gave the optimum response.

Table 5-4 Membrane response based on the methods of ionophore immobilization[a]

Membrane	Methods of immobilizing DB18C6)	Response time (min)	Loading (wt %)	Detection limit
Poly(HEMA)	TCPA-styrene formulation(dispersion)	~30	2.7	0.5 M
Poly(HEMA)	Derivatized TCPA-styrene beads (soaking) (dispersion)	10 ~30	2.3	0.1 M
Poly(HEMA)	4-Acetoxystyrene formulation(dispersion)	~20	1	10^{-2}M
Poly(HEMA)	Nitrated poly(4-acetoxystyrene) beads (soaking) (dispersion)	10~20	6	10^{-3}M
PVA	Nitrated poly(4-acetoxystyrene) membrane[b] (soaking)(seeded emulsion)	~2	0.3	10^{-4}M

[a] Poly(HEMA) membrane thickness was 127 μm for all the cases. [b] PVA membrane was 127 μm

5.5.2 Turbidity of Poly(HEMA) Membrane

As shown in Table 5-4, the method of adsorbing DB18C6 into nitrated poly(4-hydroxystyrene) microspheres, prepared by dispersion polymerization, gave better response compared to others. The detailed data to be discussed in this section are based on this method. Figure 5.6 shows the membrane turbidity spectra as a function of

potassium ion concentration and Figure 5.7 shows the turbidity ratio. The turbidity vs. KCl concentration is shown in Figure 5.8.

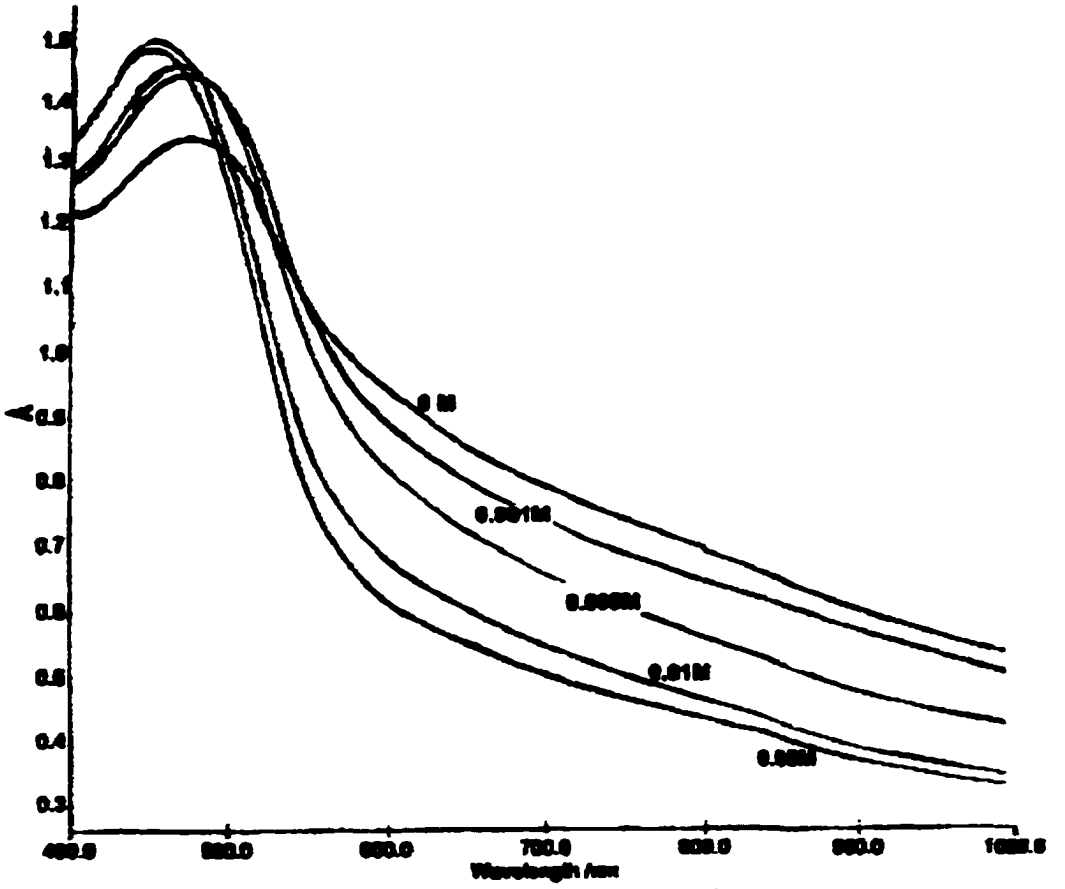

Figure 5.6 Turbidity spectra (measured as absorbance) for DB18C6 modified nitrated poly(4-hydroxystyrene) microspheres, prepared by dispersion polymerization, suspended in poly(HEMA) in KCl solution buffered at pH7, IS=0.1M with 6 wt % loading of beads

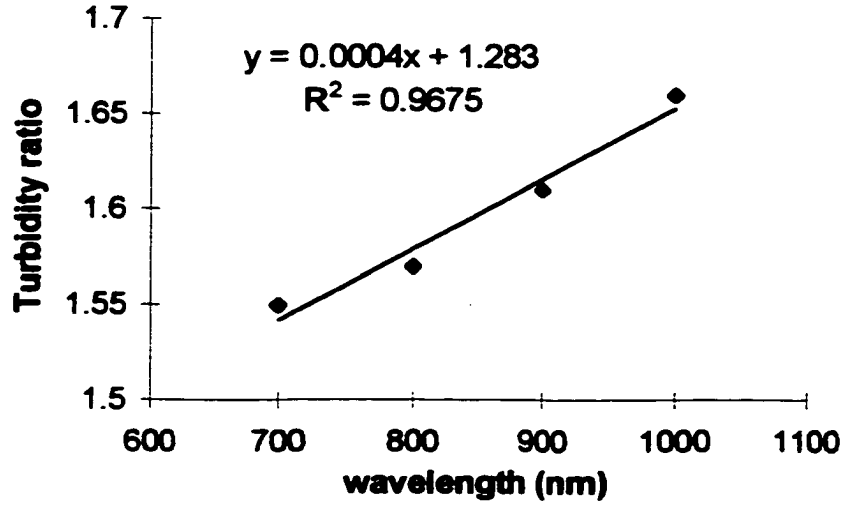

Figure 5.7 Turbidity ratio between the most shrunken form vs. the most swollen form according to the spectra shown in Figure 5.6

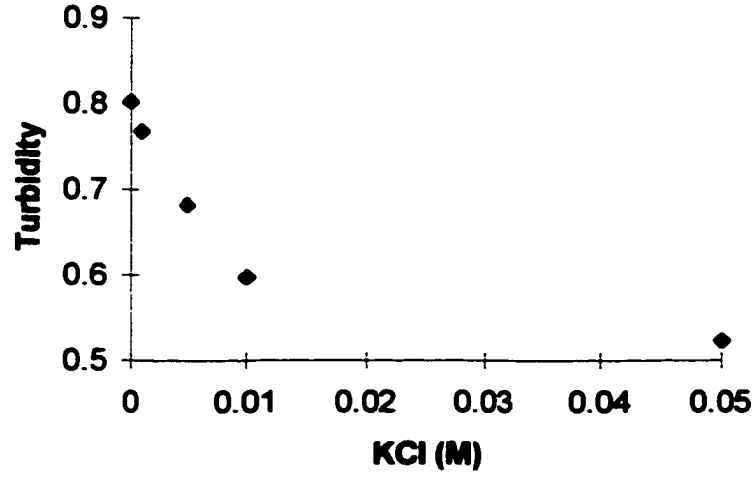

Figure 5.8 Turbidity vs. KCl concentration for the poly(HEMA) membrane with immobilized DB18C6

5.5.3 Turbidity of PVA Membrane

PVA hydrogel matrix with suspended polymer microspheres prepared by seeded emulsion polymerization was primarily studied in this part of the thesis work. The ionophore was immobilized into the polymer by soaking the PVA membranes with embedded nitrated poly(4-hydroxystyrene) microspheres in KCl solution saturated with DB18C6 or valinomycin.

5.5.3.1 DB18C6 Modified Membrane

The spectra of DB18C6 modified PVA membrane with the suspended nitrated poly(4-hydroxystyrene) was shown in Figure 5.4 (pH 4, IS 0.01, membrane thickness 127 μm) and the turbidity ratio corresponding to the spectra is shown in Figure 5.5. The membrane turbidity vs. KCl concentration is shown in Figure 5.9. It can be seen that the membrane response is more sensitive at lower concentrations of KCl.

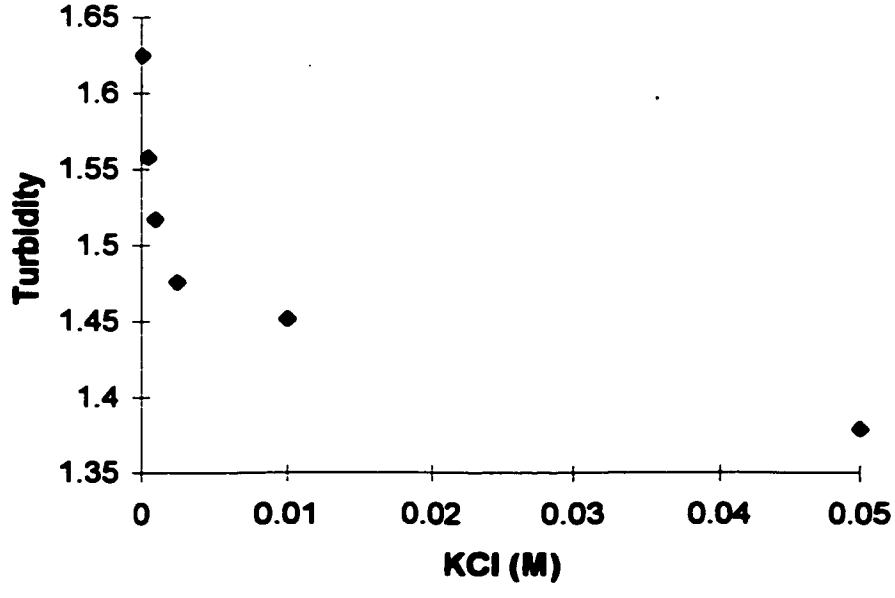

Figure 5.9 Turbidity vs. KCl concentration for the PVA membrane with immobilized DB18C6

5.5.3.2 Valinomycin Modified

Figure 5.10 shows the spectra obtained for a valinomycin modified PVA membrane contenting the suspended nitrated poly(4-hydroxystyrene) microspheres which was prepared the same way as the DB18C6 modified membrane. The apparent pK_a of the polymer is 5.2 and the loading of the microspheres in the membrane is 0.1 wt %. The KCl solutions were buffered at pH 4 with an ionic strength of 0.01M which was adjusted by NH_4Cl. The membrane thickness was 127 μm. The membrane turbidity change as KCl concentration is shown in Figure 5.11.

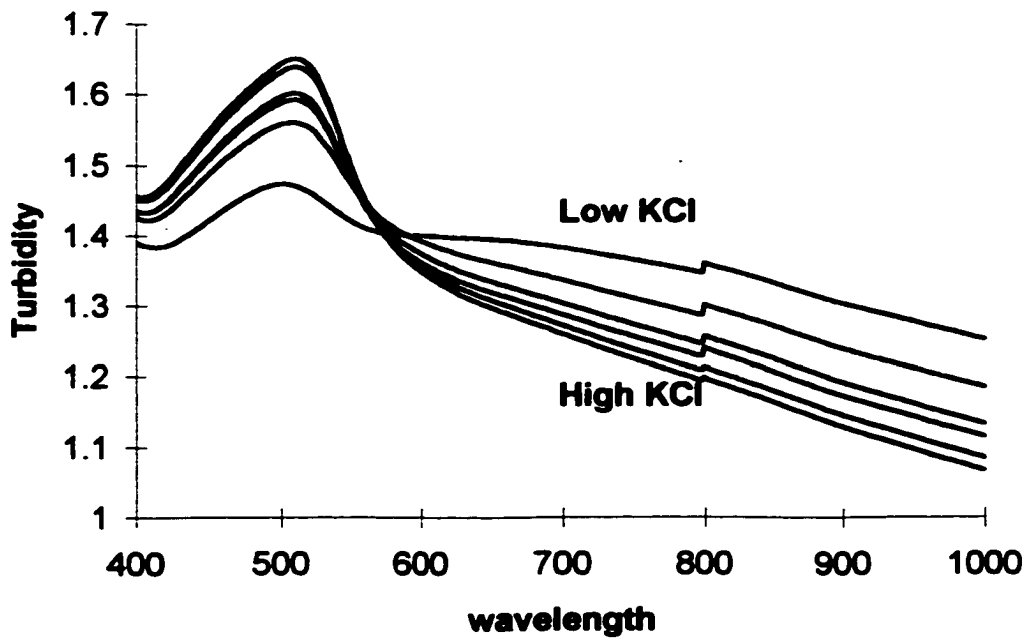

Figure 5.10 Turbidity spectra (measured as absorbance) of nitrated poly(4-hydroxystyrene) microspheres (0.1 wt %) with immobilized valinomycin embedded in a PVA membrane (127 μm) in KCl solution at pH4 (IS=0.01M)

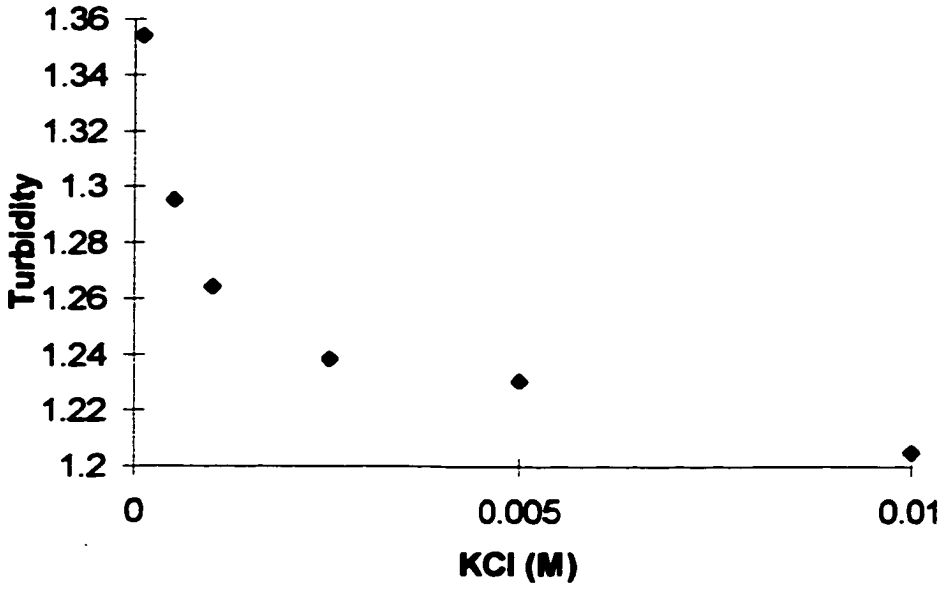

Figure 5.11 Turbidity vs. KCl concentration for the PVA membrane with immobilized valinomycin

5.5.4 Absorption versus Turbidimetry

As discussed in section 5.2, the potassium ion sensing system is indeed a cation exchange system and involves the competition between the complexation and deprotonation processes. Therefore, both the turbidity intensity change, which is due to the change of the refractive index, in the wavelength region 700 ~ 1000 nm and the absorbance intensity change, which is due to the deprotonation of the nitrophenol, at approximately 480 ~ 500 nm, are based on the ratio of hydrogen and potassium ion concentrations. As shown in Figure 5.12, the tubidity change at 780 nm and the absorbance change at 500 nm of the PVA membrane, previously shown in Figure 5.5, give a perfectly symmetric response. This indicates that both absorption and turbidimetry methods can be used for the potassium ion sensing.

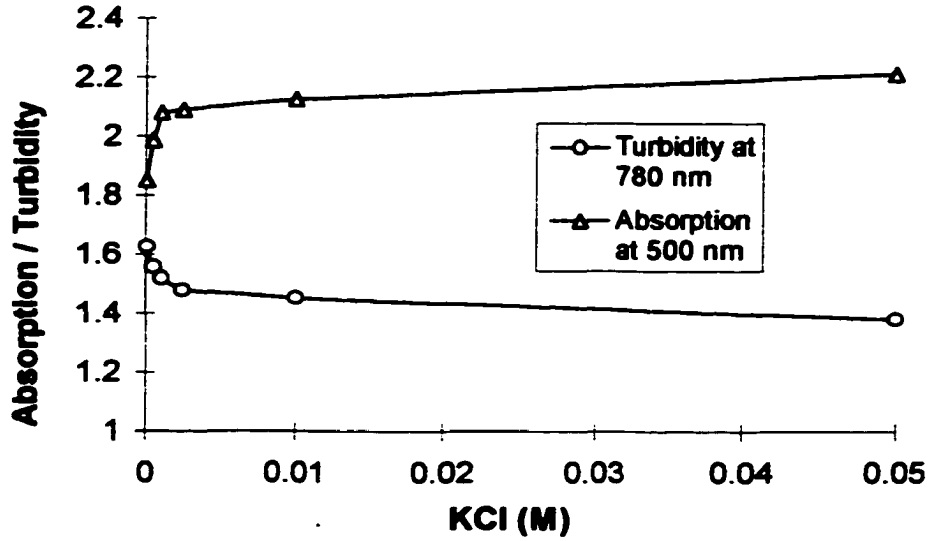

Figure 5.12 Response of PVA membrane shown in Figure 5.5 at 780 and 500 nm

5.6 Conclusions

The important accomplishment of this work is that the chemistry for the potassium ion sensing system works. The membrane can be used to sense K^+ concentrations as low as 10^{-4} M. Although it is not as sensitive as the traditional ion-selective electrode, this sensing approach would be suitable for many types of fiber optic chemical sensors. The response time of the PVA membrane with microspheres prepared by seeded emulsion polymerization has been significantly decreased compared to that of the poly(HEMA) matrix with microspheres prepared by dispersion polymerization. This is further evidence confirming that larger and more porous polymer particles were observed.

Chapter VI

CONCLUSIONS

Poly(4-acetoxystyrene) microspheres, with diameters > 1 μm synthesized by seeded emulsion polymerization have more and larger pores than those synthesized by other methods. Nitrated poly(4-hydroxystyrene) with varying nitrogen content can be obtained by controlling the nitration reaction conditions. These microspheres are highly sensitive to pH and strongly colored. They can swell and shrink reversibly and this is associated with the deprotonation / protonation of the hydroxy functional group.

Hydrogel membranes with embedded nitrated poly(4-hydroxystyrene) microspheres can be used for pH sensing based on turbidity changes. Decreased turbidity is caused by the decrease in the scattered light at the interface of the hydrated polymer and the hydrogel membrane which is accompanied by the decrease in the refractive index of the polymer while the refractive index of the hydrogel remains the same. The available dynamic range for pH sensing can be increased by varying the nitrogen percentage of the microspheres between that of the mono- and di-nitro substituted polymers. The observed pK_a for the polymers obtained in this study was from 5.6 to10.2. The response time has been significantly decreased by utilizing PVA as the membrane matrix and by preparing porous microspheres by seeded emulsion polymerization. The magnitude of the membrane turbidity is affected by both ionic strength and the loading. The stability test showed that the poly(HEMA) hydrogel membranes are mechanically stable when they are

stored in pH 4, pH 10, deionized water, and dry under room temperature, at 80 ^{0}C, and in sunlight.

Ionophore modified nitrated poly(4-hydroxystyrene) microspheres embedded in a hydrogel can be used for potassium ion sensing. The model of the sensing membrane is a cation-exchange system. Noncovalent immobilization of the ionophore can be accomplished by either incorporating the ionophore into the polymer formulations or by adsorbing the ionophore into polymer microspheres directly or through the hydrogel matrix. Ion binding is accompanied by deprotonation of the hydroxy group of nitrated poly(4-hydroxystyrene) to form an anion and this causes the polymer to swell due to the electrostatic repulsion between the charged sites on the polymer backbone. Swelling results in a decrease in refractive index as the water content increases which leads to a measurable membrane turbidity change which is related to the change of the ratio of hydrogen and potassium ion concentrations. DB18C6 and valinomycin have been used as the ionophores for potassium ion sensing. The lowest concentration of K^+ tested with an ionophore modified PVA membrane was 10^{-4} M. The lowest K^+ concentration observed with the ionophore modified poly(HEMA) membrane was 10^{-3} M. The response time of the PVA membrane with microspheres prepared by seeded emulsion polymerization was ~2 minutes which is significantly shorter than that for the poly(HEMA) matrix with microspheres synthesized by dispersion polymerization.

REFERENCES

[1] *Technology Vision* 2020

[2] *Design News* July 6, 1998

[3] G. Boisde, F. Blanc, and J-J. Perez, *Talanta*, **1988**, 35, 75-82

[4] J. E. Freeman, et al., *Analytical Chemistry*, **1985**, 56, 2246-2249

[5] J. I. Peterson, et al., *Analytical Chemistry*, **1980**, 52, 864

[6] M. Monici, et al., *Proc. SPIE*, **1987**, 798, 294

[7] L. A. Saari and W. Rudolf Seitz, *Analytical Chemistry*, **1982**, 54, 821-823

[8] Z. Zhang, and W. R. Seitz, *Anal. Chim. Acta*, **1984**, 160, 47

[9] H. Offenbacher, O. S. Wolfbeis, and E. Furlinger, *Sens. Actuators*, **1986**, 9, 73

[10] O. S. Wolfbeis and H. Offenbacher, *Sens. Actuators*, **1986**, 9, 85

[11] M. J. P. Leiner and P. Hartmann, *Sensors & Actuators*, **1993**, B11, 281

[12] Arnold, Mark A., *Anal. Chem.* **1992**, 64, 1015A

[13] Beer, P. D. "Molecular and Ionic Recognition by Chemical Methods", in: Edmonds, T. F. (Ed.), Chemical Sensor, Blackie, London, 1987

[14] S. C. Charlton et al. *US Pat.* 4,645,744, **1987**

[15] R. H. Ng, K. M. Sparks, and B. E. Statland, *Clin. Chem.* **1992**, 38, 1371

[16] I. Gibb, *Clin. Pathol.*, **1987**, 40, 298

[17] S. C. Charlton, R. L. Fleming, and A. Zipp, *Clin. Chem.*, **1982**, 28, 1857

[18] A. Kumar, et al., *Clin. Chem.*, **1988**, 34, 1709

[19] Lerchi, M., Reitter, E., Simon, W., and Pretsch, E., *Anal. Chem.* **1994**, 66, 1713

[20] Bakker, E., Rosatzin T., and Simon W., Anal. Chim. Acta, **1993**, 278, 211

[21] W. Rudolf Seitz, *Journal of Molecular Structure*, **1993**, 292, 105-114

[22] Marian F. McCurley and W. Rudolf Seitz, *Analytica Chimica Acta*, **1991**, 249, 373-380

[23] Sizhong Pan, Vicki Conway, Ziad Shakhsher, Susan Emerson, Mingqi Bai, and W. Rudolf Seitz, *Analytica Chimica Acta*, **1993**, 279, 195-202

[24] Ziad Shakhsher and W. Rudolf Seitz, *Anal. Chem.*, **1994**, 66, 1731-1735

[25] Michael T. Rooney, Ph.D. Thesis, University of New Hampshire, **1996**

[26] Eric W. Miele, PhD. Thesis, , University of New Hampshire, **1999**

[27] Necati Kaval, M.S. Thesis, , University of New Hampshire, **1998**

[28] Li Zhang, Ph.D. Thesis, University of New Hampshire, **1998**

[29] W. L. Sederel and G. J. Dejong, *J. of Applied Polymer Science*, **1973**, 17, 2835-2846

[30] Li Zhang, Margeret E. Langmuir, Mingqi Bai, and W. Rudolf Seitz, *Talanta*, 44, **1997**, 1691-1698

[31] Mingqi Bai and W. Rudolf Seitz, in press.

[32] Z. Zhang, J. L. Mullin, W. R. Seitz, *Anal. Chem. Acta*, **1986**, 184, 251

[33] W. R. Seitz, *Anal. Chem.* **1984**, 56, 16A

[34] Ziad Shakhsher, W. R. Seitz, *Anal. Chem.* **1994**, 66, 1731

[35] D.C. Sherrington. Preparation, *Functionalization, and Characteristics of polymer support*. John Wiley & Sons, **1980**

[36] P. Hodge and D.C. Sherrington. *Polymer Reactions in Organic synthesis*. John Wiley & Sons, **1980**

[37] Peter A. Lovell and Mohamed S. El-Aasser., *Emultion Polymerization and Emulsion Polymers*. John Wiley & Sons, **1997**

[38] John Ugelstad, Kari Herder Kaggerud, Finn Kunt Hansen, and Arvid Berge. *Makromol. Chem.* **1979**, 180, 737-744

[39] J. Ugelstad and P. C. Mork. *Advances in Colloid and Interface Science*. **1980**, 13, 101-140

[40] H. R. Sheu, M. S. El-Aasser, and J. W. Vanderhoff. *J. of Polymer Science: Part A: Polymer Chemistry*. **1990**, 28, 653-667

[41] C. M. Cheng, F. I. Micale, J. W. Vanderhoff, and M. S. El-Aasser. *J. of Polymer Science: Part A: Polymer Chemistry*. **1992**, 30, 235-244

[42] C. M. Cheng, J. W. Vanderhoff, and M. S. El-Aasser. *J. of Polymer Science: Part A: Polymer Chemistry*. **1992**, 30, 245-256

[43] K. Kobayashi and M. Senna. *J. of Applied Polymer Science*. **1992**, 46, 27-40

[44] Q. Ching Wang, Ken Hosoya, Frantisek Svec, and Jean M. J. Frechet. *Anal. Chem.* **1992**, 64, 1232-1238

[45] Jean-Pierre Montheard, Amar Zerroukhi, and Morad Quaisse. *Macromolecular Reports*. **1994**, A31(Suppl. 5), 471-480

[46] V. Smigol, F. Svec, K. Hosoya, Q. Wang, J. M. J. Frechet, *Angew. Makromol. Chem.*, **1992**, 195, 151

[47] M. Okubo, M. Shiozaki, M. Tsujihiro, Y. Tsukuda, *Colloid Polym. Sci.*, **1991**, 269, 383

[48] M. Okubo, T. Nakagawa, *Colloid Polym. Sci.*, **1992**, 270, 853.

[49] K. Ogino, H. Sato, K. Tsuchiya, H. Suzuki, S. Moriguchi, *J. Chromatogr. A*, **1995**, 699, 59

[50] K. Ogino, H. Sato, Y. Aihara, H. Suzuki, S. Moriguchi, J. *Chromatogr. A*, **1995**, 699, 67

[51] A. Paine, Y. Deslandes, P. Gerroir, B. Henrissat, *J. Colloid Interface Sci.*, **1990**, 138, 170

[52] P. J. Flory, Principles of Polymer Science, Cornell University Press: Ithaca, NY, **1953**

[53] H. A. Strobel and W. R. Heineman, *Chemical Instrumentation: A Systematic Approach*, 3rd Ed. Wiley: New York, **1989**

[54] Michael T. V. Rooney and W. Rudolf Seitz, *Anal. Commun.* **1999**, 36, 267-270

[55] A. Ledwith, M. Rahnema, and P. K. Sen Gupta. *Journal of Polymer Science*. **1980**, 18, 2239-2246

[56] R. Arshady, G. W. Kenner and A. Ledwith. *Journal of Polymer Science*. **1974**, 12, 2017-2025

[57] Herve Deleuze and David C. Sherrington. *J. Chem. Soc. Perkin Trans*. **1995**, 2, 2217-2221

[58] Jean M. J. Frechet, Eva Eichler, Hiroshi Ito and C. Grant Willson. *Polymer*. **1983**, 24, 995-1000

[59] Vladimir Smigol, Frantisek Svec, and Jean M. J. Frechet. *Journal of Liquid Chromatography*. **1994**, 17(2), 259-276

[60] E. G. Lezcano, M. G. Prolongo and C. Salom Coll. *Polymer*. **1995**, 36(3), 565-573

[61] Kevin Lewandowski, Frantisek Svec, and Jean M. J. Frechet. *J. Liq. Chrom & Rel. Technol*. **1997**, 20(2), 227-243

[62] D.C. Sherrington and P. Hodge (eds), *Synthesis and Separations using Functional Polymers*, Wiley, New York, **1988**

[63] Shizuo Arichi, and Shozo Himuro. *Polymer*. **1989**, 30, 686-692.

[64] Shozo Himuro, Noriyuki Sakamoto, and Shizuo Arichi. *Polymer Journal*. **1992**, 24(12), 1371-1376

[65] David L. Trumbo. *Polymer Bulletin*, **1996**, 37, 617-623

[66] Bo Gao, Xianyi Chen, Bela Ivan, Jorgen Kops and Walther Batsberg. *Macromol. Rapid Commun*. **1997**, 18, 1095-1100

[67] R. Arshady, G. W. Kenner and A. Ledwith, *J. Polym. Sci., Polym. Chem*. **1974**, 12, 2017

[68] A. Ledwith, M. Rahnema and P. K. Sen Gupta. *J. Polym. Sci., Polym. Chem*. **1980**, 17, 2239

[69] K. J. Zhu, W. Liqun, W. Ji and Y. Shikn. *Macromol. Chem. Phys*. **1994**, 195, 1965

[70] Vicki Lynn Conway, Ph.D. Thesis, University of New Hampshire, **1994**

[71] Kenneth P. Hassen, M.S. Thesis, University of New Hampshire, **1993**

[72] D. I. Packham. *J. Chem. Soc*. **1964**, 8, 2617-2624

[73] W.-H. Li, K. Li, H. D. H. Stover, and A. E. Hamielec. *J. Polymer Science: Part A: Polymer Chemistry*, **1994**, 32, 2023-2027

[74] R. H. Wiley and G. L. Mayberry. *J. Polym. Sci.* A. **1963**, 1, 217

[75] H. A. Mizes, et al., *Appl. Phys. Lett.*, **1991**, 59 (22), 2901-2903

[76] Zhujun Zhang, Ziad Shakhsher and W. Rudolf Seitz, *Mikrochim. Acta*, **1995**, 121, 41-50

[77] Vicki L. Conway, Kenneth P. Hassen, Li Zhang, W. Rudolf Seitz, and T. S. Gross, *Sensors and Actuators: B. Chemical*, **1997**, 45, 1-9

[78] W.Rudolf Seitz, M. T. V. Rooney, E. W. Miele, H. Wang, N. Kaval, L. Zhang, S. Doherty, S. P. Milde and J. Lenda, *Anal. Chim. Acta*, in press

[79] S. Pan, V.L. Conway, Z. Shakhsher, S. Emerson, M. Bai, W.R. Seitz and K.D. Legg, *Anal. Chim. Acta*, **1993**, 279, 74

[80] Z. Zhang, Z. Shakhsher and W.R. Seitz, *Mikrochim. Acta*, in press

[81] W.R. Seitz, K.P. Hassen, V.L. Conway and S. Pan, Proc. *Symposium on Chemical Sensors, Electrochem. Soc.* **1993**, 74

[82] Mike Civillo, MS Thesis, University of New Hampshire. **1997**

[83] D. W. VAN Krevelen, "Properties of Polymers", **1990**

[84] Mark A. Arnold, *Anal. Chem.* **1992**, 64, 1015A

[85] M. Lerchi, E. Reitter, W. Simon, and E. Pretsch, *Anal. Chem.* **1994**, 66, 1713

[86] E. Bakker, T. Rosatzin, and W. Simon, *Anal. Chim. Acta*, **1993**, 278, 211

[87] J. F. Alder, D. C. Ashworth, R. N. Narayanaswamy, R. E. Moss, and I. O. Sutherland, *Analyst*, **1987**, 112, 1191

[88] J. N. Roe, F. C. Szoke, and A. S. Verkman, *Analyst*, **1990**, 115, 353

[89] Z. Zhang, J. L. Mullin, W. R. Seitz, *Anal. Chem. Acta*, **1986**, 184, 251

[90] K. Suzuki, H. Ohzora, *Anal. Chem. Acta*, **1990**, 237, 155

[91] D. I. Packham, *J. Chem. Soc.*, **1964**, 8, 2617

APPENDIX 1

THE ESTIMATION OF POLYMER REFRACTIVE INDEX

This estimation is based on the theory of Lorentz and Lorenz.[R] The refractive index can be calculated according to the following equation at $\lambda = 589$ nm:

$$n = \left(\frac{1+2\frac{R_{LL}}{V}}{1-\frac{R_{LL}}{V}} \right)^{1/2}$$

where R_{LL} is the molar refraction and V is the molar volume, cm^3 / mol, at 298K. The V and R_{LL} values are based on the group contribution which is listed in Table 1-A.

Table 1-A R_{LL} and V values from Table IX

Groups	R_{LL} (λ = 589 nm)	V (298K)
$-CH_3$	5.64	23
$-CH_2-$	4.65	16.37
	3.62	10.8
	2.58	5.32
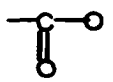	6.71	21
—OH	2.45	8.0
$-NO_2$	6.66	16.8
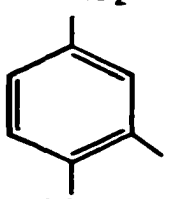	24.4	65.5

The estimate refractive indices for the following four polymers are listed in Table 1-B

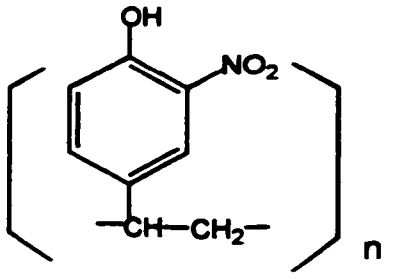

MW = 165 g /mol

Poly(3-nitro-4-hydroxystyrene) (PNHS)

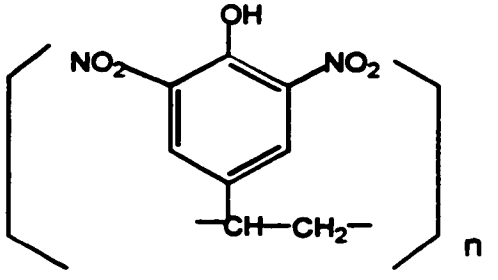

MW = 210 g/mol

Poly(3,5-dinitro-hydroxystyrene) (PDNHS)

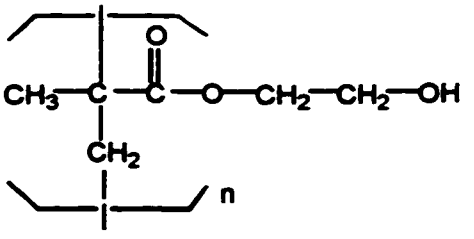

MW = 130.14 g/mol

Poly(2-hydroxyethylmethacrylate) (poly(HEMA))

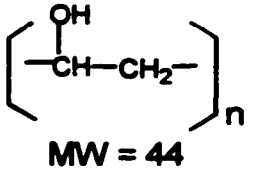

MW = 44

Poly(vinyl alcohol) (PVA)

Table 1-B Calculated refractive indices for four polymers

Polymer	$R_{LL}(\lambda = 589\ nm)$	V (298K), cm_3 / mol	n
PNHS	41.78	117.47	1.630
PDNHS	48.44	134.27	1.641
Poly(HEMA)	31.33	106.43	1.500
PVA	10.72	35.17	1.522